EnSTaR

Environmental Sensing Technologies and Research

Eramurra mapping
Mangrove - Remote Sensing

Technical report for:
Leichhardt
A7/436 Roberts Road
Subiaco, WA 6008

EnSTaR
ABN: 79 861 342 089
41 Hilltop Place, Kelmscott, WA, 6111, AUSTRALIA

Document Information

Report No.	RL004b
Title	Eramurra Mapping Mangrove - Remote Sensing
Date	January 2024
Job Reference	LEI-PO-0029 PO from Leichhardt Salt Pty Ltd
Job Description	Process Sentinel satellite data to produce maps of environmental regions as defined by Leichhardt.
Leichhardt Doc. No.	ESSP-EN-14-TRPT-0016

Version 1 submitted.	November 2022
Addendum produced. Project development envelopes changed slightly, requiring recalculation of some parameters.	July 2023
Final version. Changes in response to EPA feedback. Removal of project envelopes data after discussion with Leichhardt.	February 2024

1. Background

We report here methods to produce maps showing the Mangrove extent along the northwest coast of Western Australia using satellite remote sensing data from Sentinel-2 A/B, plus a demonstration of the potential for high spatial resolution mapping and Pléiades Neo. The mangrove maps and data derived from this feasibility study are to support studies of current environmental state, and change from recent times, with relevance to potential industrial development in the region.

There are many approaches to mapping mangroves that use Light Detection and Ranging (LiDAR) and optical remote sensing data combined with machine learning or conventional targeted image-based processing. Conventional image-based mangrove identification is useful in identifying mangrove in a small region, but it is ineffective in large area of observations. The machine learning approaches, such as Support Vector Machine (SVM) and Random Forest (RF) classification in mapping mangrove, have gained momentum in the last decade (Jiang et al. 2021). The rapid adoption of machine learning approaches is mainly due to much improved access to large processing/compute power readily available via various cloud compute providers such as Amazon Web Services and Google Earth Engine (Diniz et al. 2019), and increasing recognition that machine learning approaches are efficient in mining and using spatial information (Dennis et al 2012).

In this study, we used the SVM model for mangrove classification with aims to:

1. study the feasibility of satellite remote sensing data from Sentinel-2 A/B in mapping mangrove extent in the study area shown in Figure 1.
2. develop a methodology, and assess limitations, to identify mangrove from Sentinel satellite data and generate a mangrove map to inform the extent of mangrove in the study region.

2. Study Sites

The region of interest, shown in Figure 1, extends from the southern extent of Exmouth Gulf to approximately 118 degrees east. A localised region representing the focus of proposed development is indicated in Figure 1 by a magenta rectangle (Eramurra AOI). A larger project area is indicated by a cyan boundary (Horseflats AOI). The project also has an interest in the broader regional area bounded by green in Figure 1 (Regional AOI).

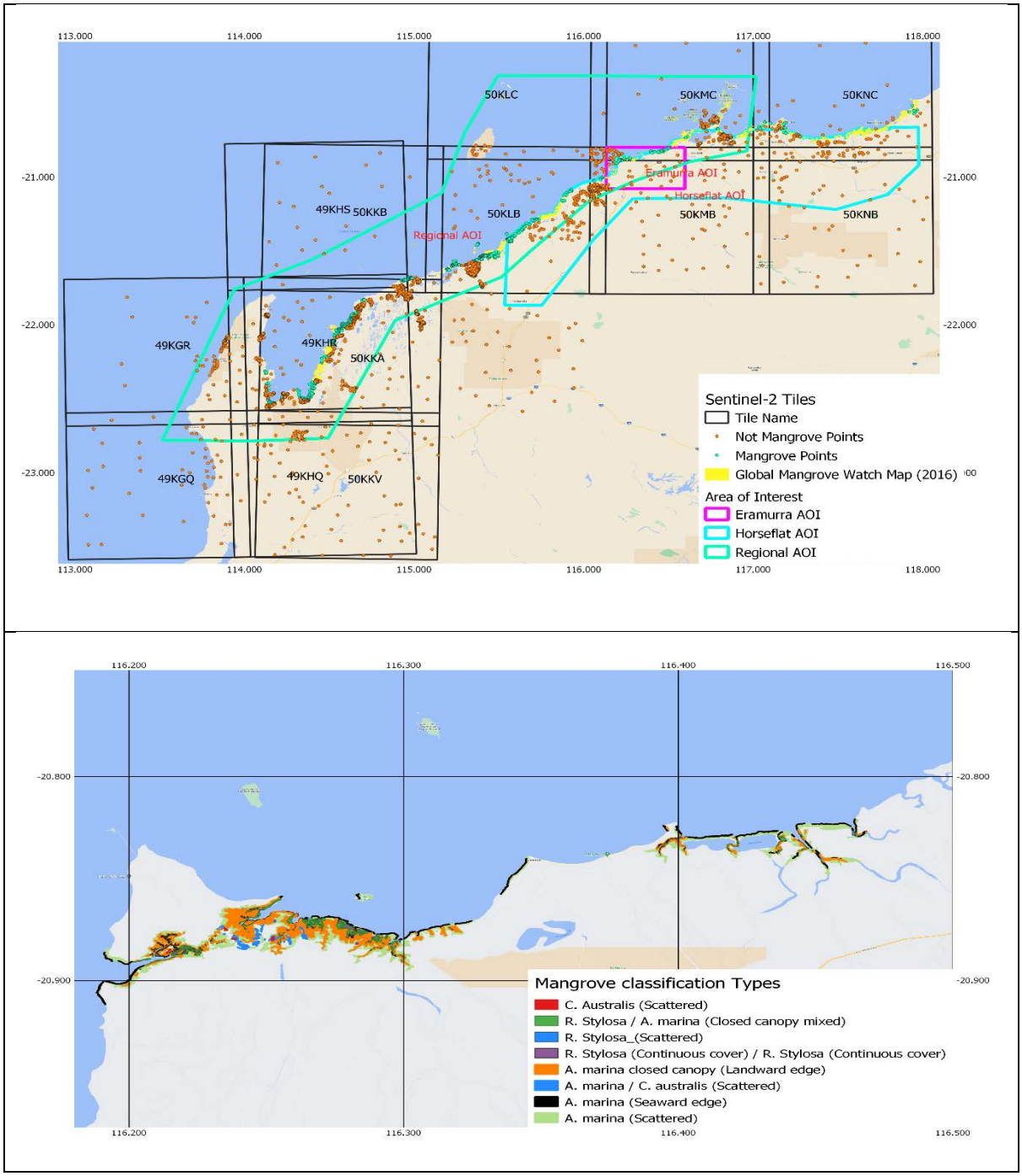

Figure 1. Top: Region of interest for remote sensing-based mapping comprises areas bounded by green, cyan and magenta. Bottom: The in-situ mangrove classification sites provided by Leichhardt Salt Pty Ltd over the Eramurra AOI.

3. Data

Optical satellite data from Sentinel-2 A/B (See Section 3.1 for details) and Synthetic Aperture Radar (SAR) data from Sentinel-1 A/B from the European Space Agency were used in this study. The SAR dataset used comprised a composite of normalized backscatter data in VV polarization collected in 2016 (Bauer et al. 2021). The 1 second STRM Digital Elevation Model (DEM) from Geoscience Australia and previously classified map data of mangrove

produced by Global Mangrove Watch (Bunting et al., 2018) were also used. In addition, a vector data set originally created and produced by O2Marine (2022) in 2021 showing ground coverage of mangroves in the study area was made available by Leichhardt and was used in validating the results.

3.1 *In-situ Data*

The pre-identified mangrove land features vector data provided by Leichhardt were used in this study to validate the classification results. In total, 1321 polygons were provided with different mangrove classification types as listed in Table 1. There were 21 polygons with missing class attributes which were removed from the analysis. The final in-situ sites contained 1320 features, of which 865 were from the year 2020 and 455 from the year 2021. All the sites were located within the area identified as Eramurra AOI (see Figure 1-bottom). The mangrove classes 1-4 in Table 1 represent regions which had low density mangrove cover mixed with other land surface types. The mangrove classes 5-8 represent regions that had high densities of mangrove cover.

Table 1. The mangrove classification types and number of features identified in each class.

Number	**Mangrove Density**	**Mangrove Class**	**No of polygons**	
			2020	**2021**
1	Low	*Avicennia marina* (Scattered)	194	294
2		*A. marina* / *Ceriops australis* (Scattered)	31	9
3		*Rhizophora stylosa* (Scattered)	10	0
4		*C. australis* (Scattered)	6	1
5	High	*R. stylosa* / *A. marina* (Closed canopy mixed)	143	33
6		*A. marina* closed canopy (Landward edge)	146	23
7		*R. stylosa* (Continuous cover) / *R. stylosa* (Continuous cover)	171	0
8		*A. marina* (Seaward edge)	164	75

3.2 *Satellite Remote Sensing Data*

The Sentinel-2A and 2B each provide 10 day repeat views of the globe, interleaved to provide views of the earth at intervals of 5 days. Sentinel 2A began operation in June 2015 and Sentinel 2B in March 2017. Spatial resolution varies from 10 m to 60 m across 13 visible and infrared

spectral bands (see Table 2). For this work we used the Sentinel-2 data from 1st January 2018 to 31st of December 2021 for mapping. The Normalized Bottom of Atmosphere Reflectance and Terrain corrected (NBART) product from Sentinel-2 A/B and cloud mask generated using a python implementation of the `fmask` algorithm by Zu and Woodcock (2012) and Zhu et al (2015). The NBART products are preferred over the top of the atmosphere reflectance because NBART products have the atmospheric and terrain effects corrected to account for atmospheric, sun and satellite angles. The NBART product allows for accurate comparison of imagery at different product locations and seasons because inconsistencies can arise between the satellite images at different time periods because of variation in atmospheric conditions, sun and satellite angles and terrain slope and aspects (Li et al, 2010).

Table 2. Sentinel-2 Multi-spectral Instrument (MSI) band information.

	wavelength	resolution (m)
Band 1 – Coastal aerosol	443	60
Band 2 – Blue	492	10
Band 3 – Green	560	10
Band 4 – Red	665	10
Band 5 – Vegetation red edge	704	20
Band 6 – Vegetation red edge	740	20
Band 7 – Vegetation red edge	783	20
Band 8 – NIR	833	10
Band 8A – Narrow NIR	865	20
Band 9 – Water vapour	945	60
Band 10 – SWIR – Cirrus	1373	60
Band 11 – SWIR	1614	20
Band 12 – SWIR	2202	20

4. Methodology and Results:

4.1 *Time Series Analysis of Sentinel-2 Derived Indices*

In the preliminary investigation, Leichhardt showed that the ratio of Sentinel-2 bands 4 and 2 highlights the Horseflat land system, which is a significant clay dominated land system in our study region. The ratio Band4/Band2 has been assigned the name “Red Soil Index“ (RSI) in this study, because higher RSI index values highlight the predominantly red coloured land system more prominently. In addition to the RSI, we also investigated the Normalised

Difference Vegetation Index (NDVI), Enhanced Vegetation Index (EVI) and Normalised Difference Water Index (NDWI), derived from Sentinel-2 NBART data. Vegetation, and in this case in particular, mangrove, is identified by a high NDVI values throughout the year. Mangrove typically grow in intertidal zones and are therefore adjacent to water which may be identified using the NDWI.

Table 3. Sentinel-2 indices that were explored as input into SVM Model.

Enhanced Vegetation Index (EVI)	$EVI = 2.5 * \frac{Band8 - Band4}{(Band8 + 6.0 * Band4 - 7.5 * Band2) + 1}$	Huete et al. (2002)
Normalised Difference Vegetation Index (NDVI)	$NDVI = \frac{Band4 - Band8}{Band4 + Band8}$	Rouse et al. (1974)
Normalised Difference Water Index (NDWI)	$NDWI = \frac{Band3 - Band8}{Band3 + Band8}$	Gao (1996)
Red Soil Index (RSI)	$RSI = \frac{Band4}{Band2}$	

The indices listed in Table 2 were computed for each satellite pass individually after masking the clouds. For the two selected mangrove sites, which had dense mangrove (labelled as Mangrove in Figures 2-5) and scattered mangroves (labelled as Mangrove_Sparse_Mud in Figures 2-5), the median of 3 x 3 pixels was extracted from the index data to analyse the temporal pattern. The median of 3 x 3 pixels was selected to account for the fact that the pixels are affected by some degree of spatial variability as well as pixel adjacency issues. Time series plots of the median index values are shown in Figures 2- 5 respectively.

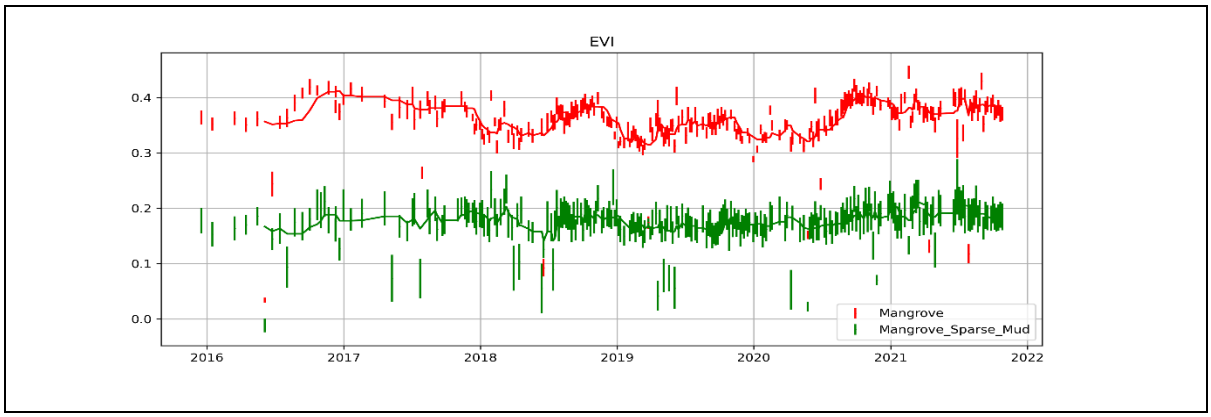

Figure 2. Time series plot of EVI for the mangrove dense and sparse mangrove sites.

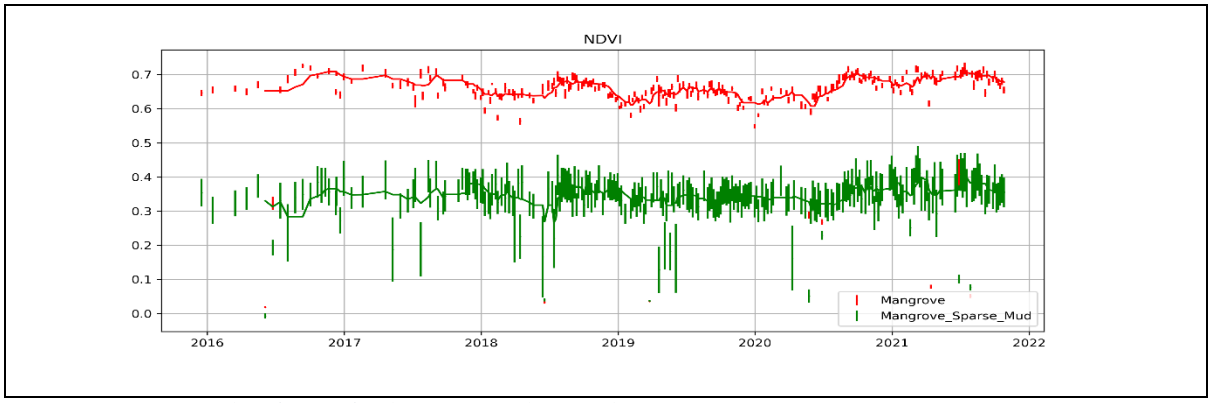

Figure 3. Time series plot of NDVI for the mangrove dense and sparse mangrove sites.

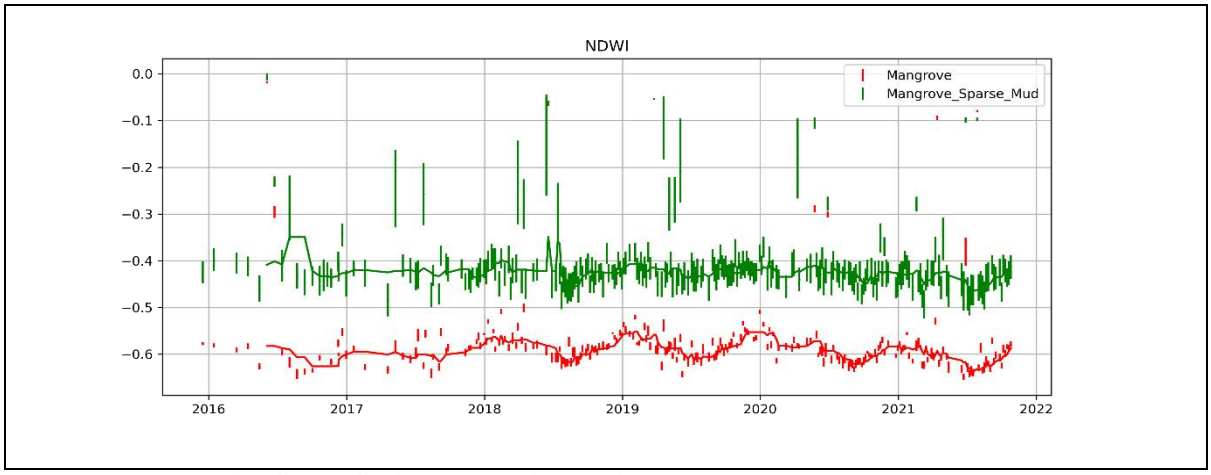

Figure 4. Time series plot of NDWI for the mangrove dense and sparse mangrove sites.

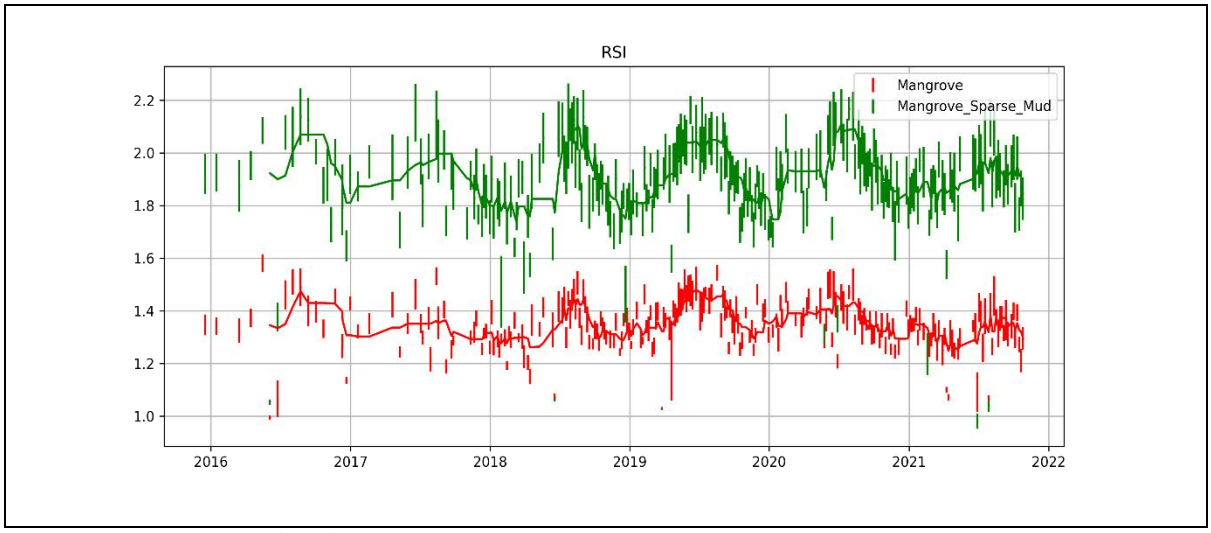

Figure 5. Time series plot of RSI for the mangrove dense and sparse mangrove sites.

From the time series analysis of vegetation indices, EVI (Figure 2) and NDVI (Figure 3), there are similarities between the two indices. Both EVI and NDVI show variability across different years, but consistently similar patterns between the two vegetation indices is observed. Because of similar temporal attributes of NDVI and EVI, the EVI was omitted from further analysis. The average value of NDWI throughout different years was approximately -0.4 and -0.6 for

sparse mangrove and dense mangrove sites indicating that for these selected locations the surfaces types are not likely to be dominated by water. The RSI time series showed that the dense mangrove type was not showing a strong red soil index, as may be expected from a dense vegetative canopy. The sparse mangrove site displayed a higher RSI, which is possibly indicative of a more visible red soil surface type being visible between the sparse canopy cover. The apparent seasonal cycle evident, most notable in the RSI signal, is interesting but as yet difficult to interpret.

4.2 *Monthly Statistics of Different Land Surfaces*

To decrease the impact of missing data due to clouds, monthly median composites of indices were generated, effectively producing composites without, or at least with a much-reduced frequency of, missing data. To assess variability in the NDVI, NDWI and RSI values for different dominant land surface types in the study region, we visually identified and selected a range of land surface types using a high-resolution Google Earth satellite image and generated monthly statistics for each land type using the 2018-2021 index datasets. The land surface types identified included blue mud, grey mud, mudflat at higher ground, sandbar, PEC (proxy for the red soil) and mangrove. The monthly NDVI, RSI and NDWI box-plots for the different land types are presented in Appendices 1 to 3 respectively. For each plot in the Appendices the data for each month represents data across all years from 2018 to 2021 inclusive.

From the monthly index statistics for different surface types represented in the Appendix 1, we observe that the NDVI of mangrove is consistently higher than the other land surface types. The NDVI median values of mangrove sites across all the months were all greater than 0.54, while the median value for other land surfaces were all less than 0.21. The difference and separability of the NDVI values between mangrove and other land surface types shows that the NDVI can be used with confidence in distinguishing the mangrove from the other land systems sampled. For the mangrove, the monthly median RSI values were all less than 1.41 while other land systems were greater than 1.5, except for the sandbar which was highly variable (see Appendix 2 for details). Further, in Appendix 3, we observe that the mangrove is characterised by NDWI less than -0.57 while other land systems were greater than -0.52. The distinct differences between mangrove and all other land surface types suggests that we can use NDWI, NDVI and RSI to classify satellite image pixels as mangrove.

4.3 *Support Vector Machine Model*

Support vector machine (SVM), a binary classification algorithm, is efficient at solving both linear and non-linear classification problems (Wang et al, 2018). The SVM model is a supervised learning method that uses a set of training data with labelled feature classes to build a model that categorizes new data into one or other feature based on the training dataset. Based on previous studies (Lien and Lars, 2017) and preliminary experimental results, we chose the SVM module available at https://scikit-learn.org/stable/modules/svm.html with radial basis function (RBF) kernel.

4.4 *SVM Model*

From Sections 4.1 and 4.2 we observe that there was no clear temporal trend that was obvious and useful in aiding the classification of mangrove data. Thus, we aggregated the monthly median indices data from 2018 to 2021 and generated one median dataset for each of the NDVI, NDWI and RSI. The all-temporal aggregated median values of each index across 4 years were used in extracting training and validation datasets. Further, to help provide some context for including classification of inland/dryland vegetation, man-made green surfaces (golf course, green parks, etc) and mangrove, we included the DEM and Sentinel-1 backscatter data in VV polarization described in Section 3.

The training and validation datasets for the SVM model were collected after overlaying the mangrove extents from the 2016 Global Mangrove Watch (GMW) datasets (Lucas et al. 2014, Bunting et al.2018). A total of 728 mangrove points (See Figure 1, blue points) were extracted from the regions inside the mangrove extents indicated by the 2016 GMW and visual interpretation of high-resolution Google Earth imagery. Further, 2287 points were selected from other regions that were representative of other surface types (See Figure 1, orange points). In training the SVM model, we used 70% of the datasets, while 30% were retained for validation of the model. The validation results of the SVM model had an accuracy of 99.1% and kappa coefficient of 99.71% with a precision of 98.07 % and recall rate of 98% with an F1-score of 98.07%.

4.5 *SVM Classified In-Situ Validation results and Mangrove Map*

The SVM Model was used in classifying mangrove using the yearly (2018-2021) median composites of NDVI, RSI, NDWI, DEM and Sentinel-1 VV backscatter datasets. Only the Sentinel-2 indices—NDVI, RSI and NDWI were aggregated for yearly median data. The DEM and Sentinel-1 backscatter datasets were kept the same for all the years because DEM is not

expected to change across different years, likewise, the Sentinel-1 backscatter which correlates with surface roughness was assumed to be relatively constant across years.

Since our SVM Model is only trained to assess two features, mangrove and not-mangrove, we were not able to validate different mangrove classification types available in Table 1. However, results do give an indication of the success of the Sentinel-based SVM mangrove mapping with respect to the O2Marine maps of both low- and high-density mangrove systems. We combined the two groups, low- and high-density mangrove features, identified in Table 1. The validation results, which present the number of pixels identified as mangrove in the high- and low-density mangrove features/polygons and the total number of pixels identified as mangrove by the SVM model within the features is presented in Table 4.

Table 4. Total number of pixels in the validation features (Low- and High-density mangrove coverage types) and the number identified by the SVM model as mangrove within the ground validation features shown.

Mangrove Density	2020		2021	
	Total Mangrove Pixels Count	SVM Model Count	Total Mangrove Pixels Count	SVM Model Count
Low Density	62,911	28,397	9,230	5,966
High Density	65,348	62,469	3,331	2,980

The classification maps over the validation sites are presented in Figures 6-9. Figures 6 and 7 represent low-density mangrove coverage for the years 2020 and 2021 respectively. The green regions represent only those areas classed as low-density mangrove by the O2Marine survey. The red regions are the regions classed as mangrove by the SVM process within the bounds of the low-density survey map. We observe that the total number of pixels identified as mangrove by the SVM model is relatively low when compared with pixels identified as low-density mangrove by the survey, only 45.14% in 2020 and 64.63% in 2021. This is largely due to the presence of other land surface types in the features/polygons of the low-density mangrove type. The SVM model results were identifying pixels that were only mangrove type while the low-density survey features contained pixels from other land types combined with mangrove. Figures 8 and 9 show high-density mangrove as identified by the survey, shown as green, and the pixels within this region identified as mangrove by the SVM model for the year 2020 and 2021 respectively. The commonly classified pixel results were high, with 95.59% in 2020 and 89.46% in 2021 identified as mangrove by the SVM model.

Figures 10 to 13 show the SVM model classified mangrove maps for the years 2018 to 2021 respectively.

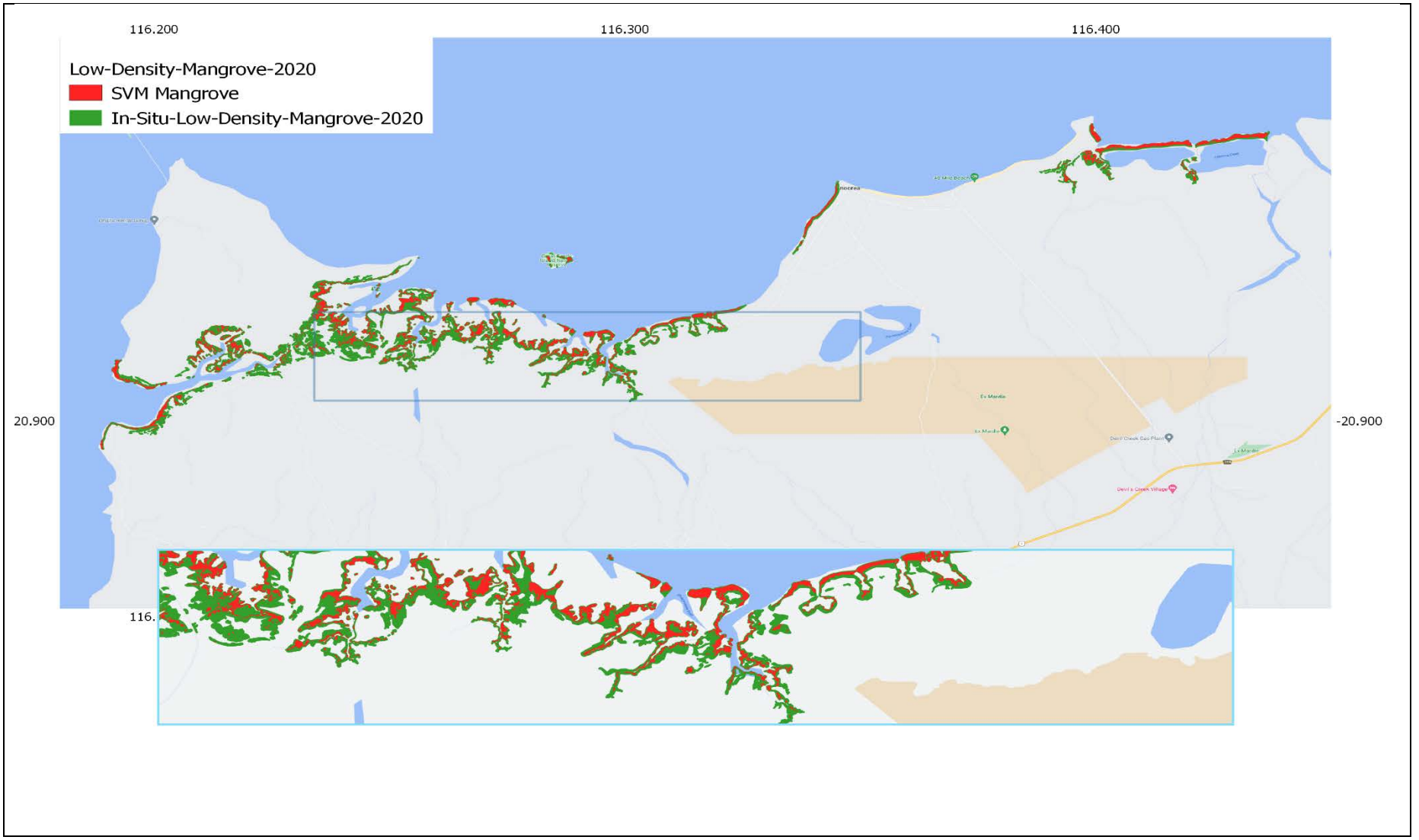

Figure 6. Low Density Mangrove validation results for the year 2020. The green colour represents the Ground-truth mangrove map and the red colour represents the mangrove map generated using the SVM Model. Note: The SVM results (red) are overlaid over the green.

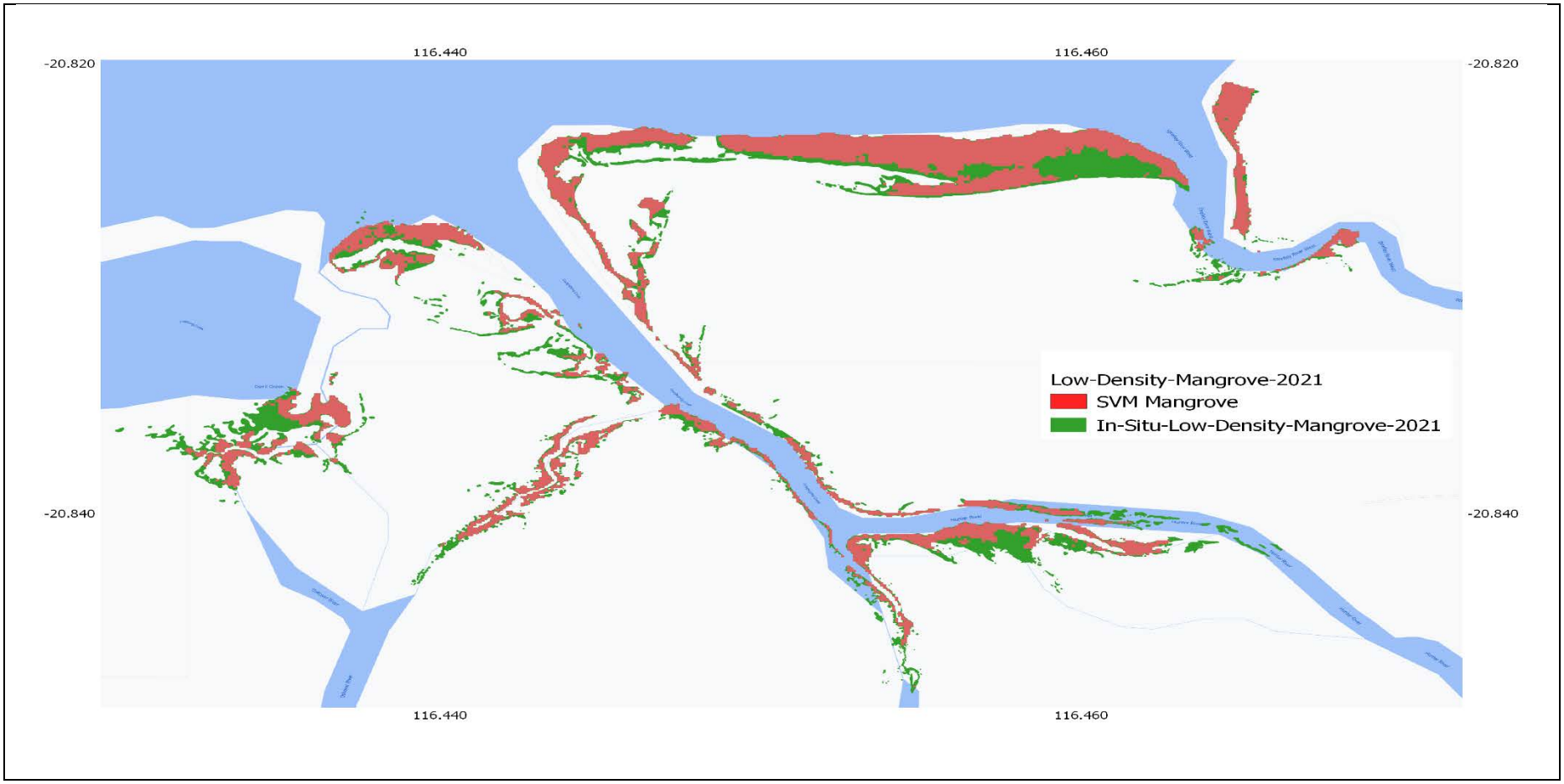

Figure 7. Low Density Mangrove validation results for the year 2021. The green colour represents the Ground-truth mangrove map and the red colour represents the mangrove map generated using the SVM Model.

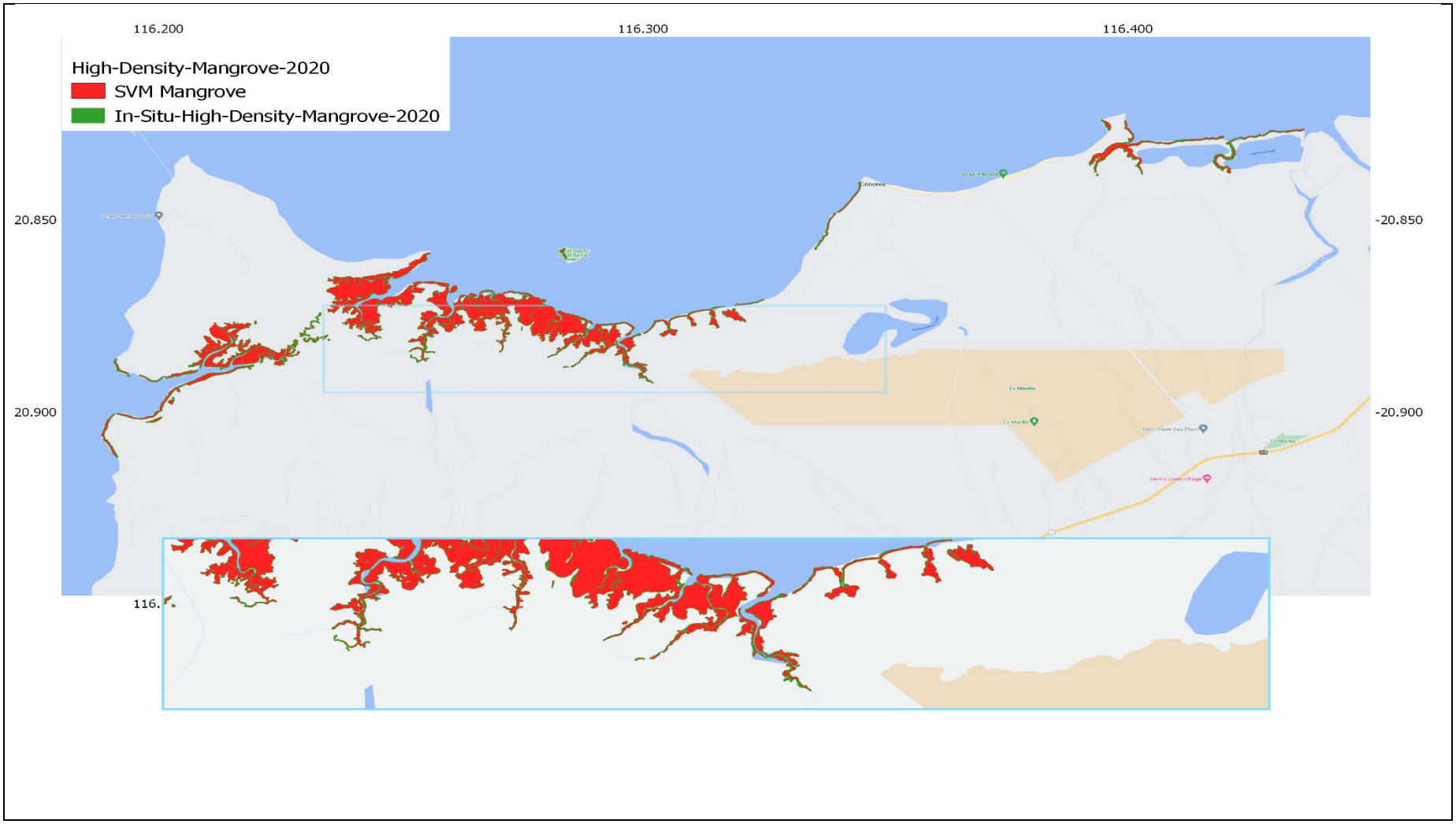

Figure 8. High Density Mangrove validation results for the year 2020. The green colour represents the Ground-truth mangrove map and the red colour represents the mangrove map generated using the SVM Model.

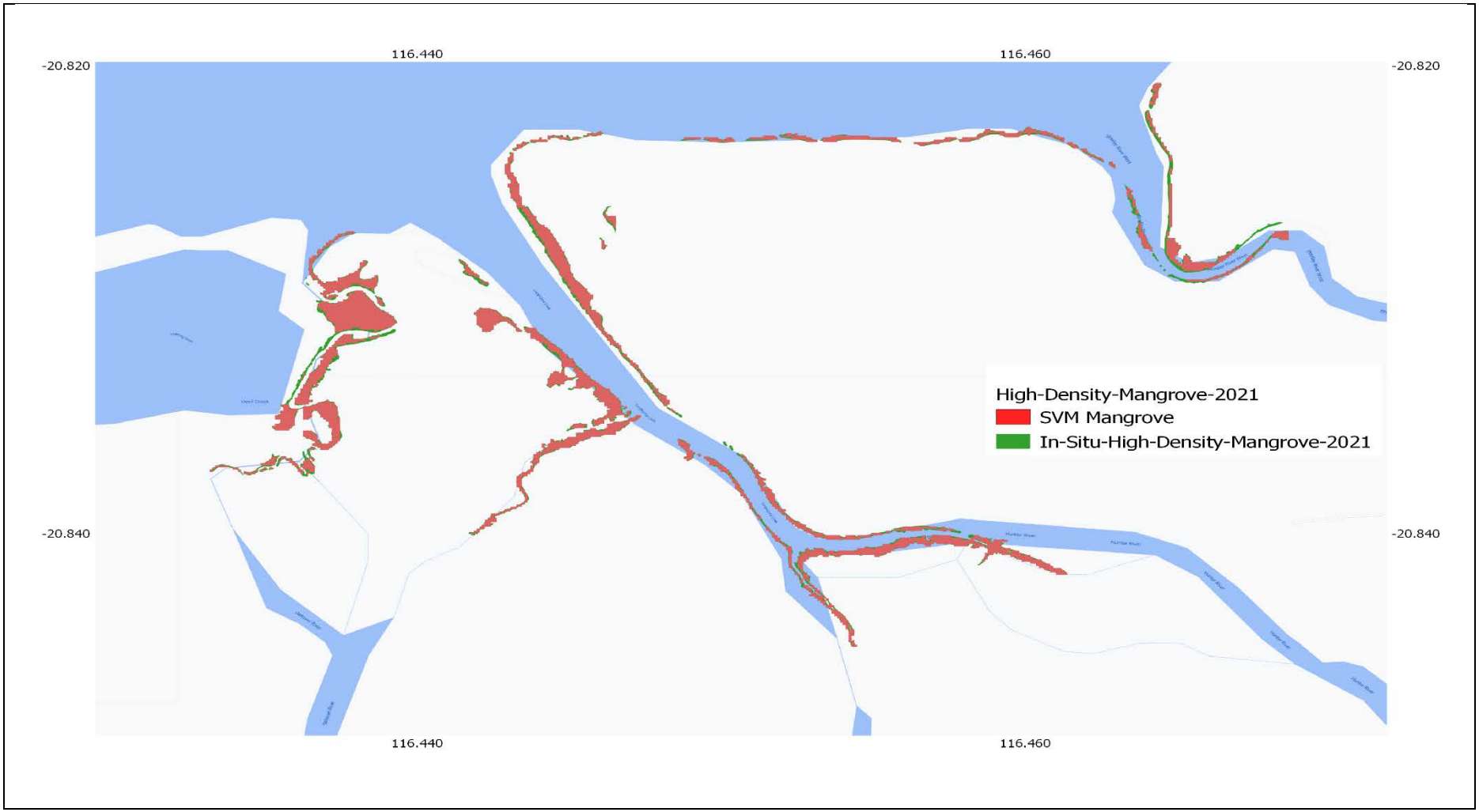

Figure 9. High Density Mangrove validation results for the year 2021. The green colour represents the Ground-truth mangrove map and the red colour represents the mangrove map generated using the SVM Model.

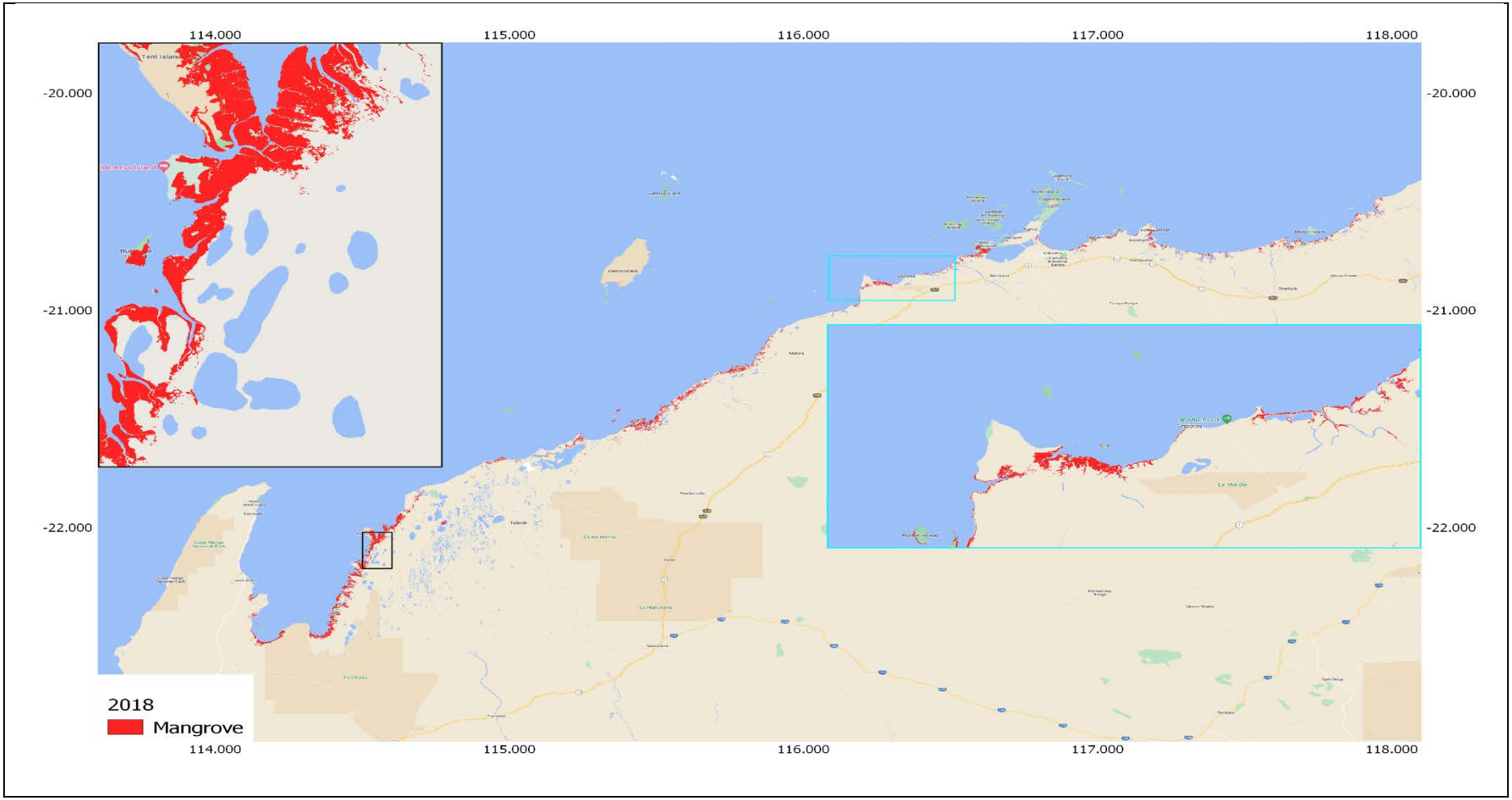

Figure 10. 2018 Mangrove Map generated from the SVM model.

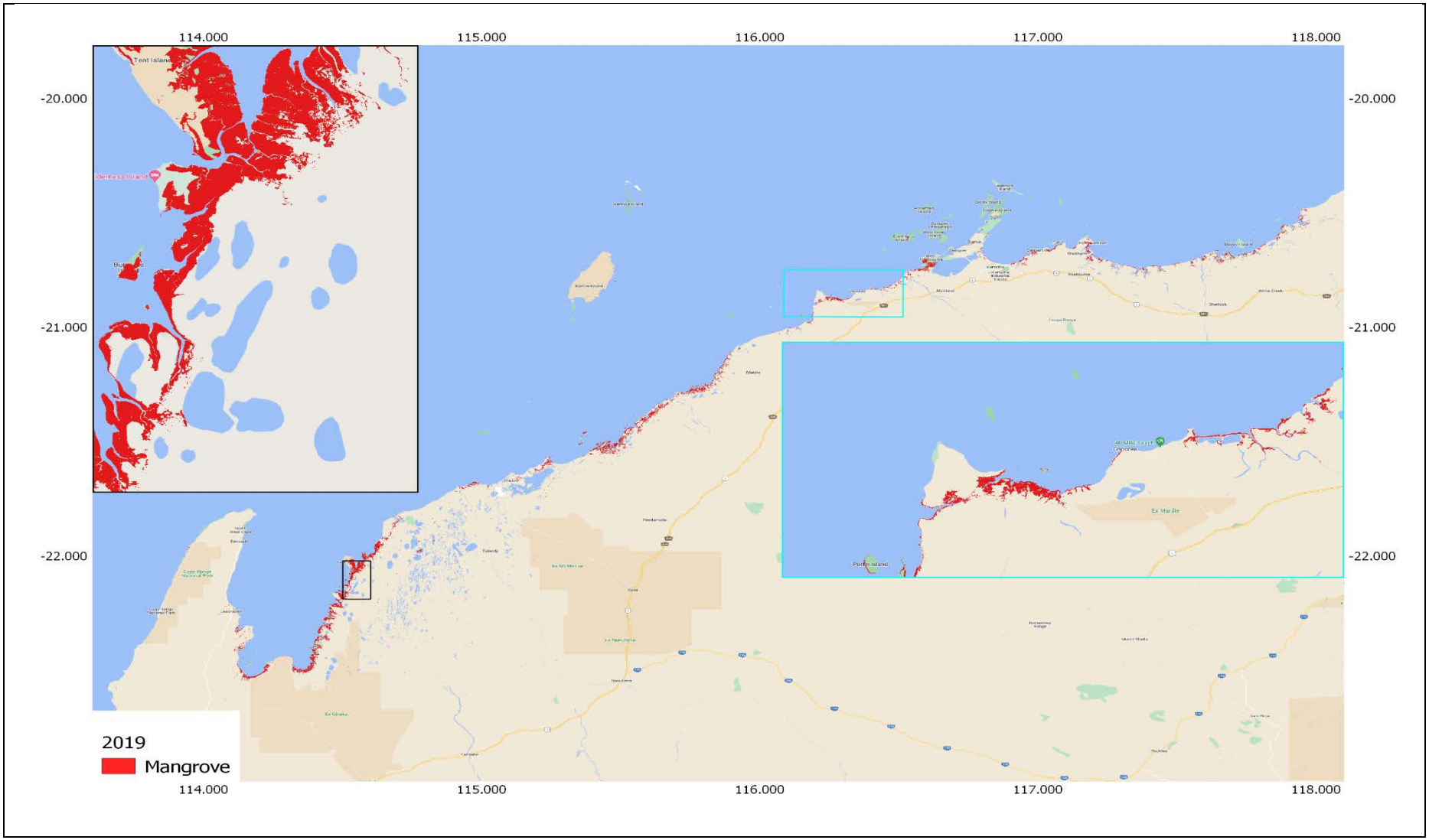

Figure 11. 2019 Mangrove Map generated from the SVM model.

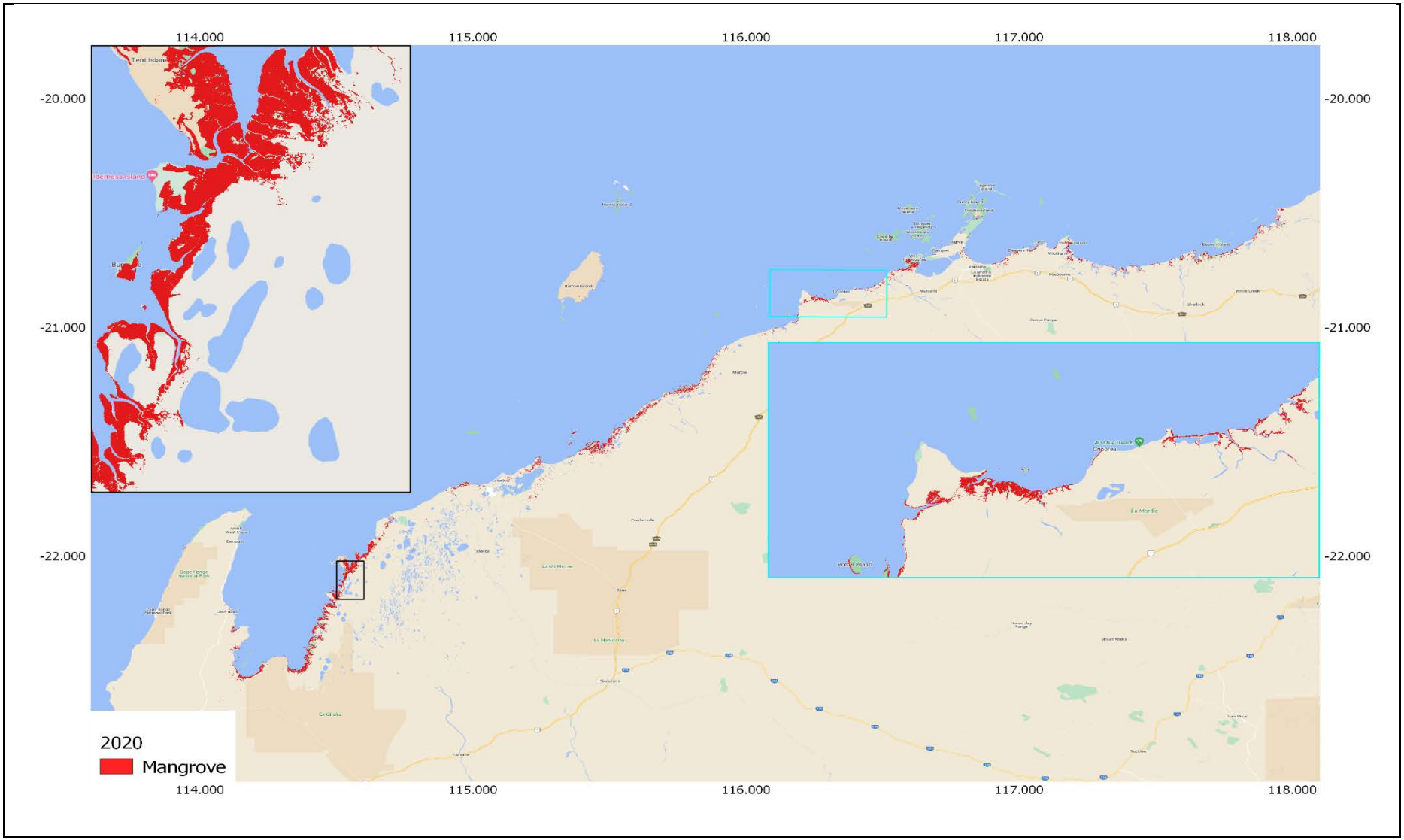

Figure 12. 2020 Mangrove Map generated from the SVM model.

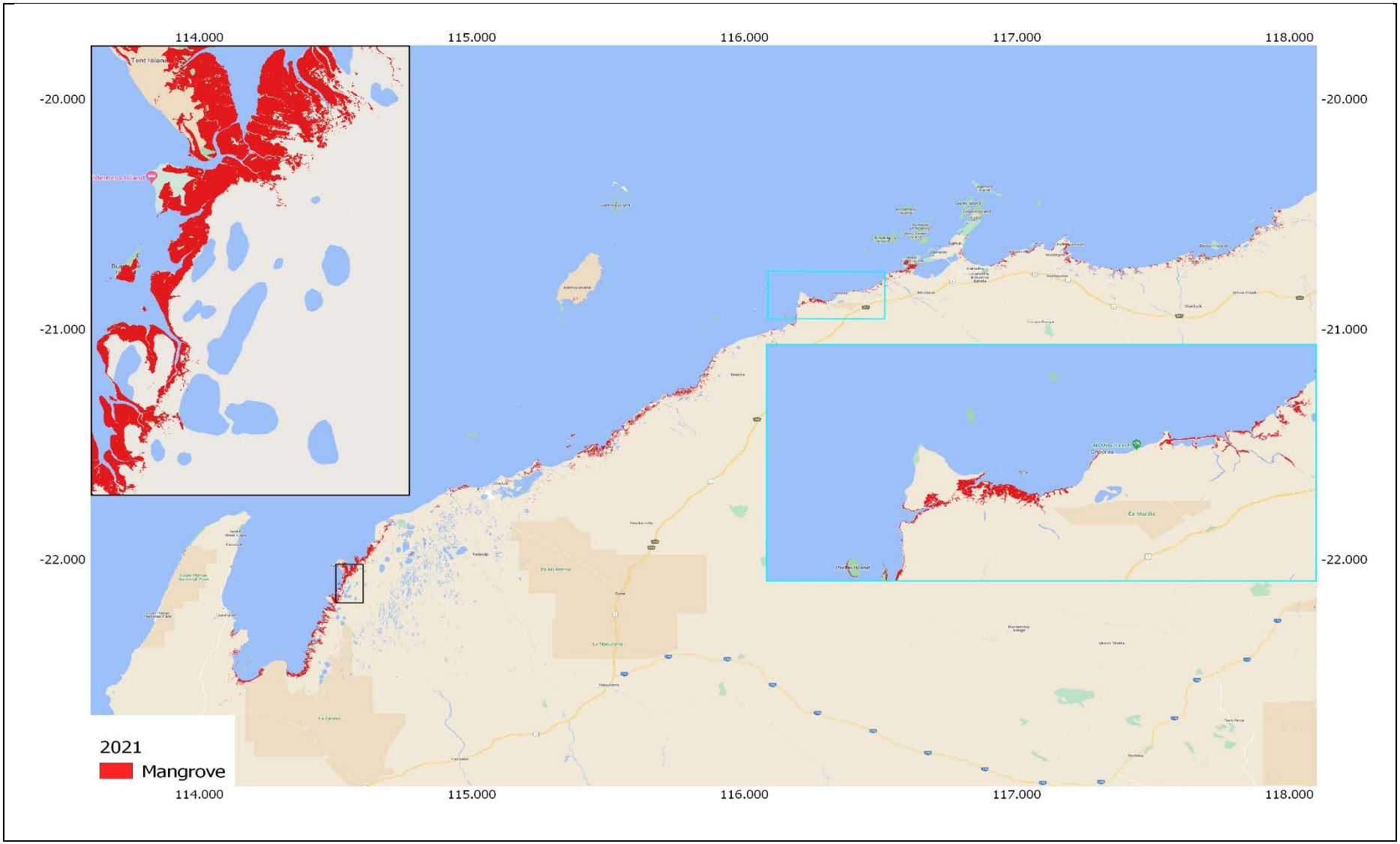

Figure 13. 2021 Mangrove Map generated from the SVM model.

4.6 *Selected details of SVM Mangrove Maps*

Figure 14 shows a sample region depicted by a Google Earth image dated November 2018, the most recent available in Google Earth Pro. Mangroves are easily discerned by eye and show a gradation in density from full canopy cover to very sparse. Figure 15 shows the same image with the O2Marine mangrove boundaries overlaid. Note, the O2Marine survey included classes ranging from full canopy cover to sparse. Figure 16 shows the same as Figure 15 with an overlay of mangrove classification pixels sourced from Digital Earth Australia (DEA) Mangrove Canopy Cover (Lymburner et al. 2020), which is a derivation of the Global Mangrove Watch (Lucas et al. 2014, Bunting et al.2018) data. The DEA data are displayed as black, grey and white shades which represent 20%-50%, 50%-80% and 80%-100% canopy cover. Figure 17 shows the SVM mangrove extent overlaid in green on the O2Marine survey boundaries. Figure 18 shows the DEA data overlaid on the SVM and O2Marine boundaries. A feature to note across all images is the river course running south to north through the middle of the image. The O2Marine and SVM maps do not include the river as mangrove cover however the DEA map does. The coverage of the SVM pixels is larger and more aligned with the O2Marine survey boundary, which in turn is strongly aligned with the underlying extent of mangroves shown in the Google Earth image. Of note are the regions located at the western side of the scene where the DEA data fails to detect any mangrove cover. An important issue depicted in these images is the classification of very sparse mangrove density as mangrove by the O2Marine survey, in contrast to the remote sensing methods where very sparse mangrove is not detected in a per-pixel method. There are some pixels within the O2Marine boundary that have no mangrove cover at all, however they are still classed as mangrove cover. It appears as though the O2Marine boundary is drawn to encompass full extent of mangroves by spanning some areas with no mangroves. This point is not made to highlight an error or misclassification, rather to highlight the distinction between terms such as canopy cover, canopy density and mangrove extent.

Figure 14. Google Earth Image. November 2018. Note the regions of mangrove cover ranging from dense to very sparse. Also note the appearance of the river course running south-north through the scene.

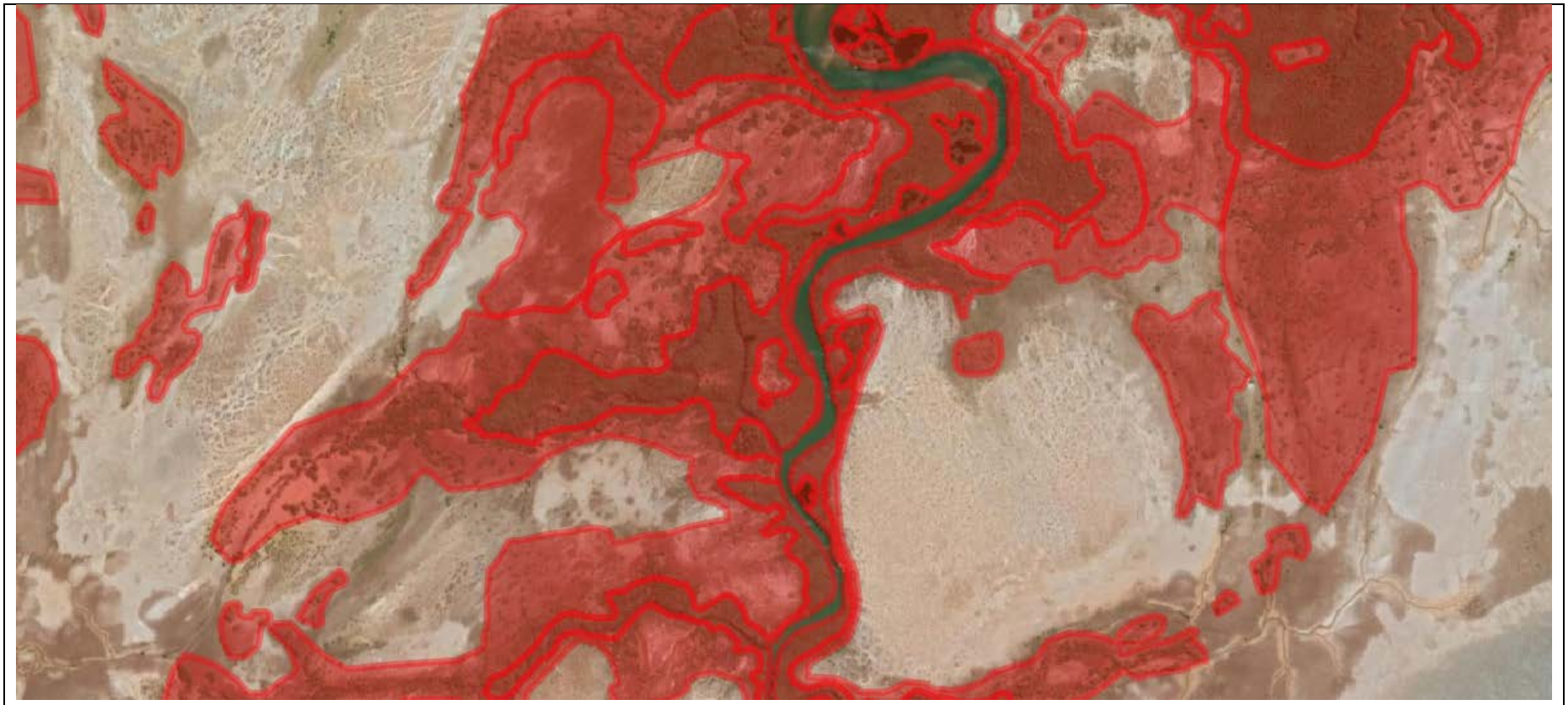

Figure 15. Google Earth Image with O2Marine (2021) survey mangrove boundaries.

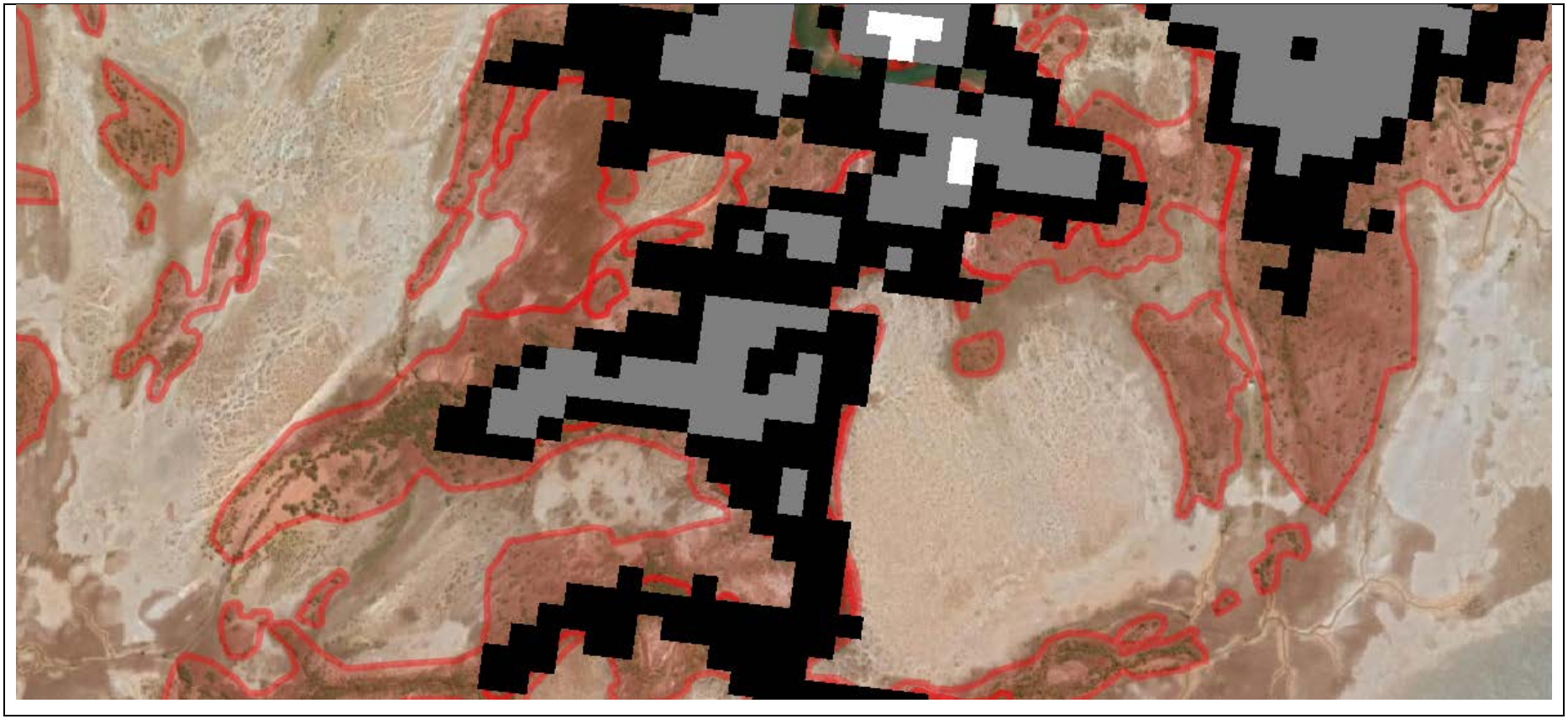

Figure 16. Google Earth Image with O2Marine (2021) survey mangrove boundaries (red) and DEA 2019 data. Black/Grey/White represent mangrove density from low to high.

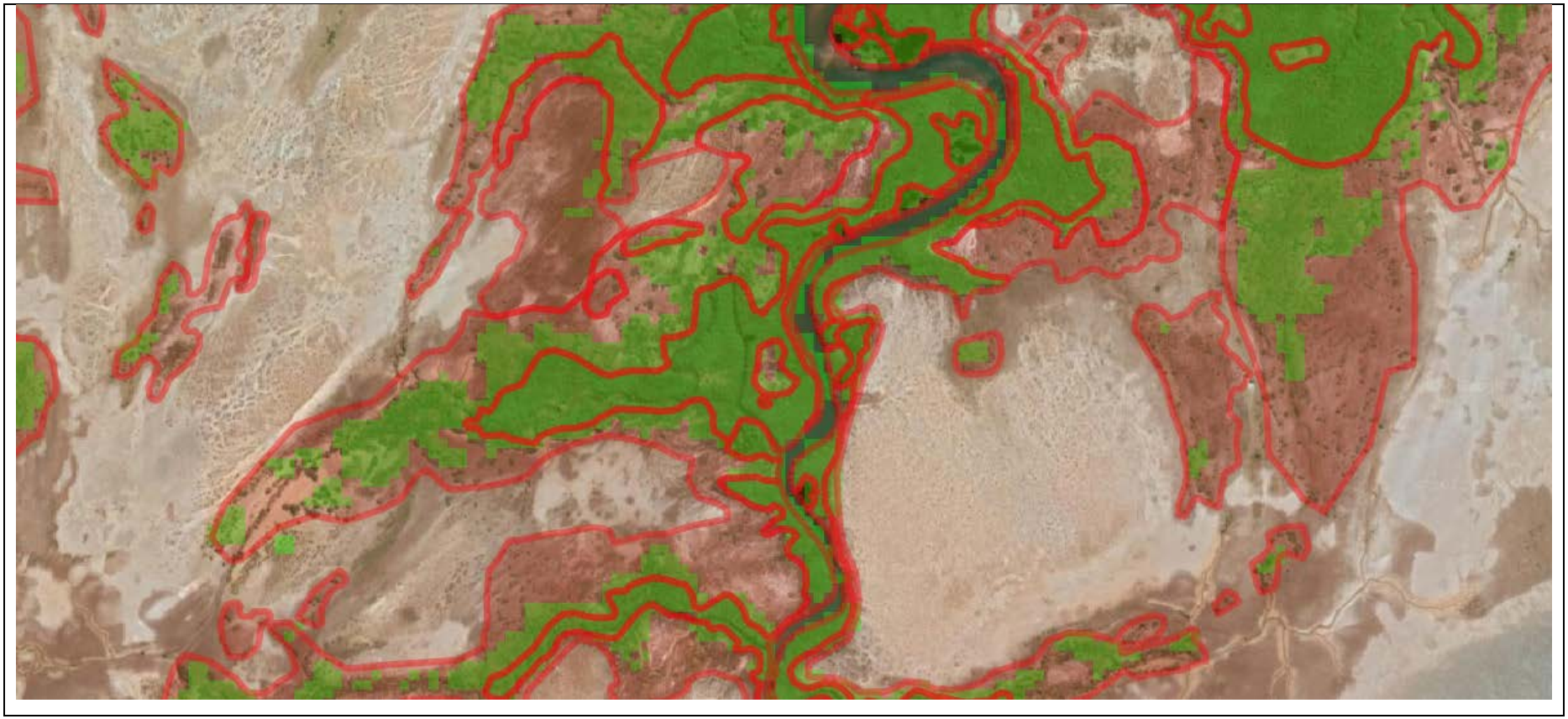

Figure 17. Google Earth Image. With O2Marine (2021) survey mangrove boundaries (red) and EnSTaR SVM mangrove extent for 2019 (green).

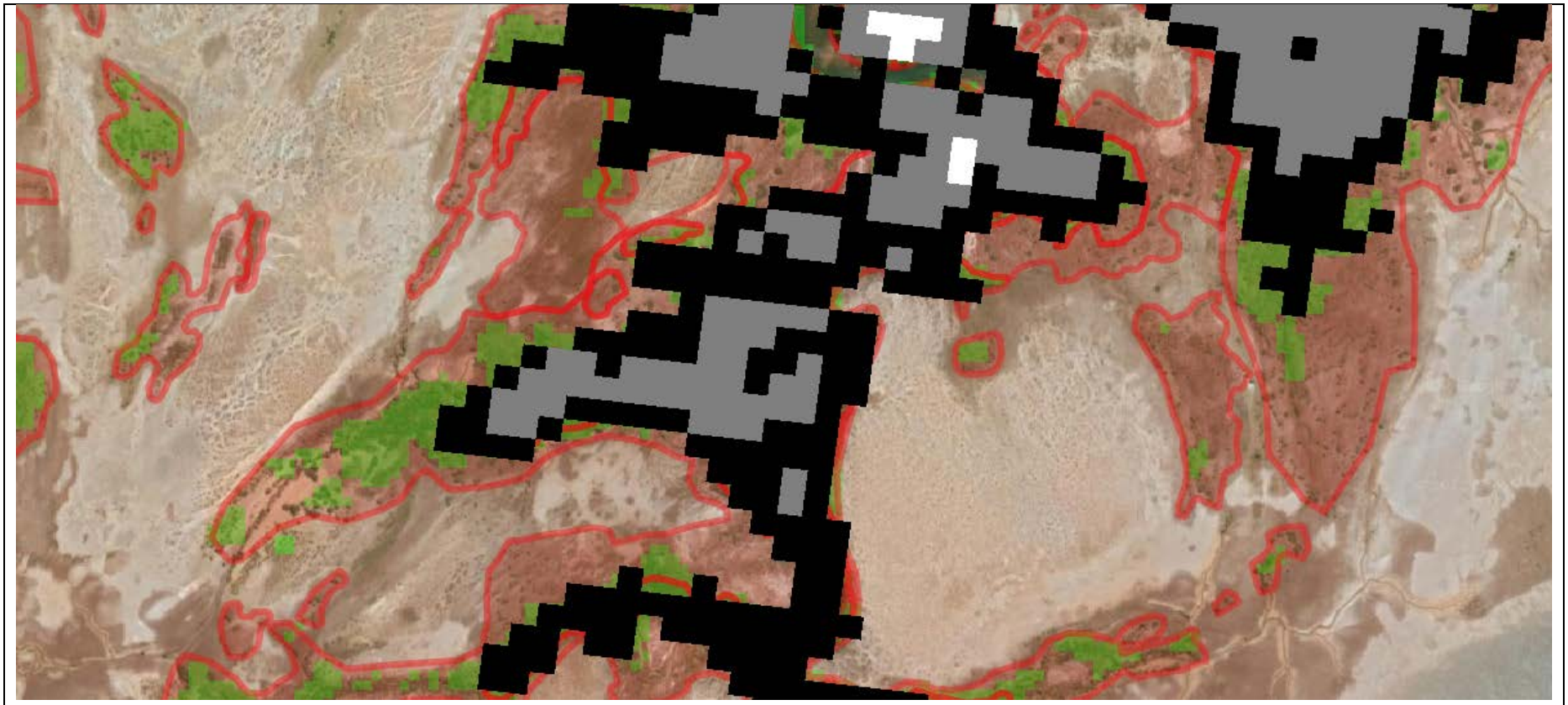

Figure 18. Google Earth Image. With O2Marine (2021) survey mangrove boundaries (red) with overlays of EnSTaR SVM mangrove extent for 2019 (green) and DEA 2019 data. Black/Grey/White represent mangrove density from low to high.

Figure 19 shows a Google Earth image from 2019 showing a detail of coastline where mangrove extent is easily discerned by visual inspection. Overlayed is the extent of the mangroves as defined by the O2Marine survey, indicated by the red boundaries. Figure 20 shows the same region as Figure 19 but with DEA mangrove density derived from 2020 Landsat data. Figure 21 shows the same region but with the SVM model-derived mangrove extent indicated by green. Note the DEA data are overlayed on the SVM data. The SVM data appears to align particularly well with the mangrove cover displayed in the underlying Google Earth image.

Figure 22 shows a 2019 Google Earth image displaying a larger extent of coastline with some sections of fringing mangrove. Figure 23 shows the same image with SVM-derived mangrove extent for 2020 highlighted in green. Figure 24 shows the same image with DEA mangrove density overlayed. Note the large extents of coastline where the Landsat-based DEA data files to detect mangrove.

Figure 19. Google Earth image showing detail of mangrove and O2Marine survey-derived mangrove extent in red.

Figure 20. Google Earth image showing detail of mangrove, O2Marine survey-derived mangrove extent and DEA mangrove cover. Black/Grey/White represent mangrove density from low to high.

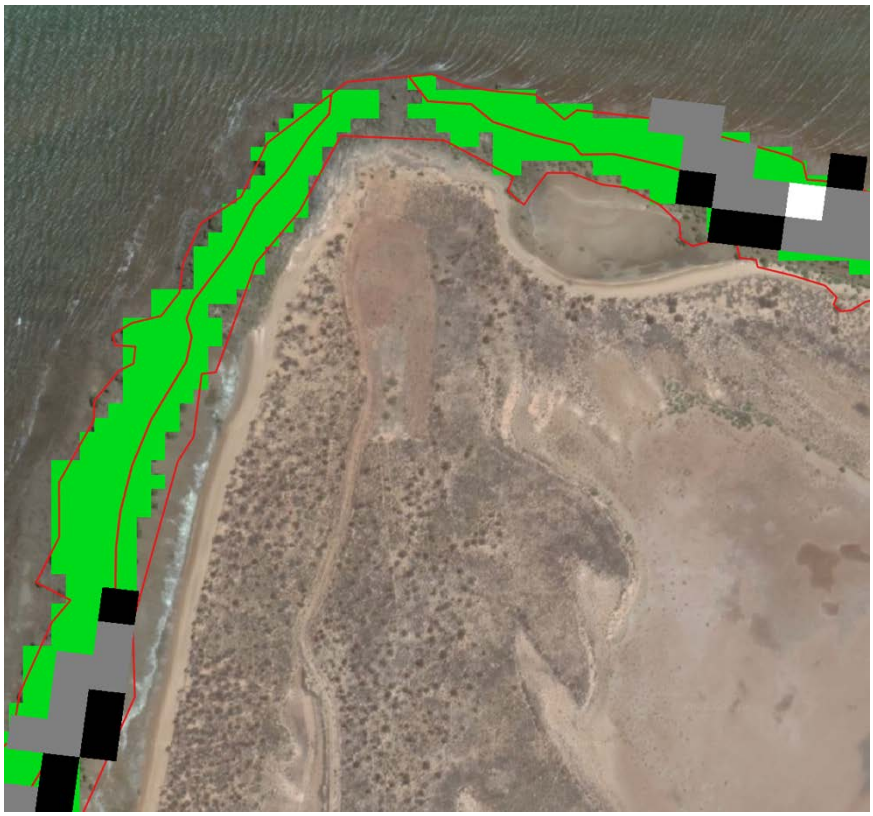

Figure 21. Google Earth image showing mangrove detail, O2Marine survey-derived mangrove extent (red boundary), DEA mangrove density and SVM derived mangrove map. DEA data black, grey and white represent mangrove density from low to high.

Figure 22. Google Earth image from 2019 showing a region of coastline with fringing mangroves.

Figure 23. Google Earth image from 2019 with SVM-drived mangrove extent for 2020 highlighted in green.

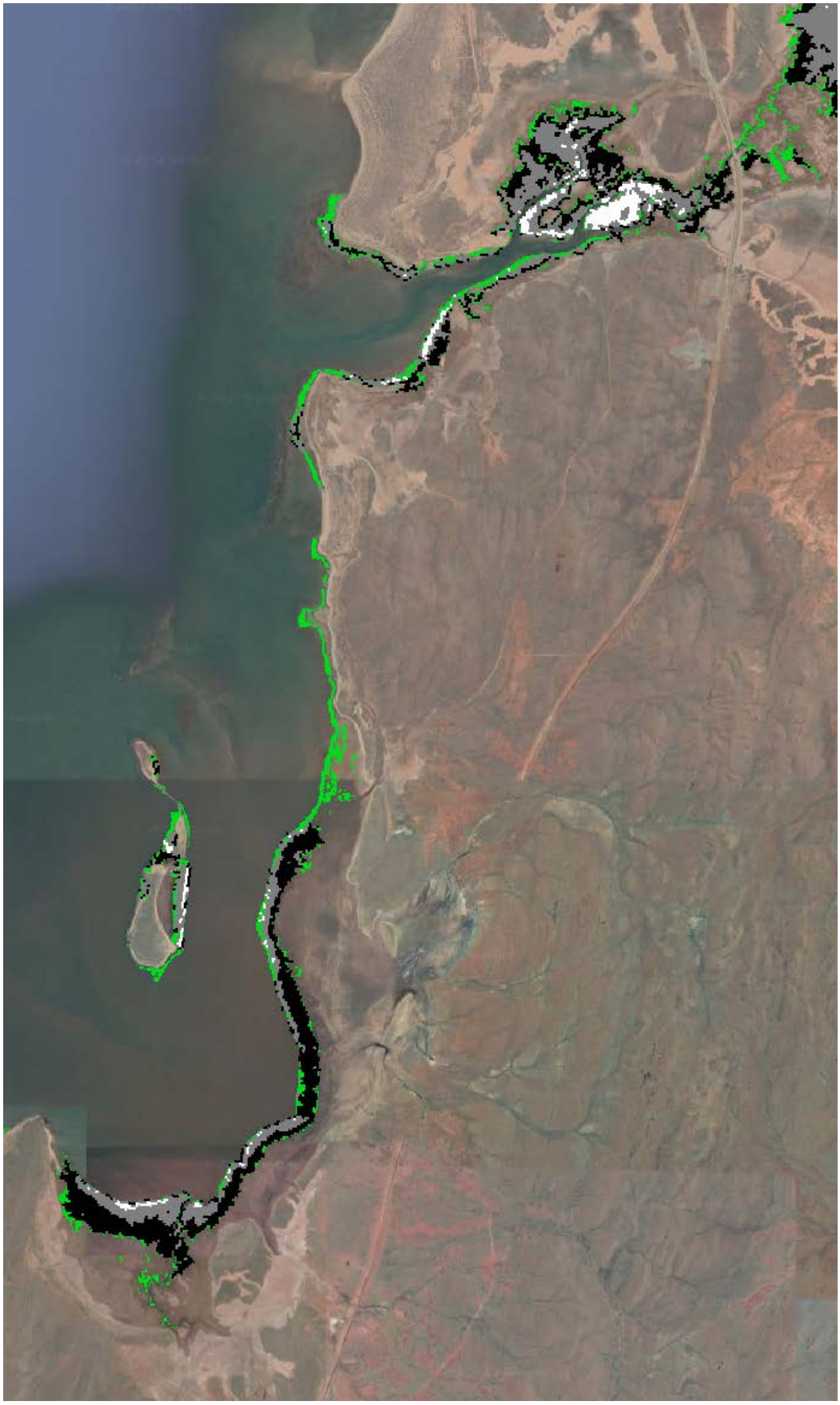

Figure 24. Google Earth image from 2019 with SVM-derived mangrove extent shown in green and DEA 2020 mangrove density shown in black, grey and white.

4.7 High and Low-density Mangrove Classification

The SVM model's performance over the low-density mangrove regions was relatively poor compared to performance over high density mangrove regions. To include the misclassified pixels over the low-density mangroves, additional post-SVM classification steps were developed to include pixels that were excluded by the SVM model. Pixels identified via this method are henceforth identified as low-density in this report.

The method to include pixels previously excluded by the SVM method is based on the following decision tree:

1. Select 3 x 3 neighbouring pixels for pixels identified as mangroves by the SVM model (for the first iteration) and then in subsequent iterations includes pixels identified as mangrove by this method.
2. If neighbouring pixels fulfill the following conditions, then each identified pixel is classified as a low-density mangrove pixel:
    a. NDVI >= 0.2492
    b. RSI >= 1.931 + 2 * 0.28 (standard deviation)
    c. S1-Backscatter >= -110.60
3. Method 1 and 2 were iteratively repeated until the difference between previous and current map versions were less than 5%.

NDVI, RSI and S1-Backscatter values are the mean values from the median NDVI, RSI and Sentinel-1 Backscatter values inside the low-density validation polygon presented in Table 1. The NDVI threshold of 0.2492 and S1-Backscatter are the mean values across low-density polygons. The mean RSI threshold of 1.931 was adjusted by 2 * 0.28 (standard deviation across low-density polygon pixels) because RSI tends to be high over low-density mangrove regions since low-density mangrove regions have more exposed bare ground, which usually translates to high RSI. The high and low-density mangrove classification maps over the validation layers are presented in Figure 14-17.

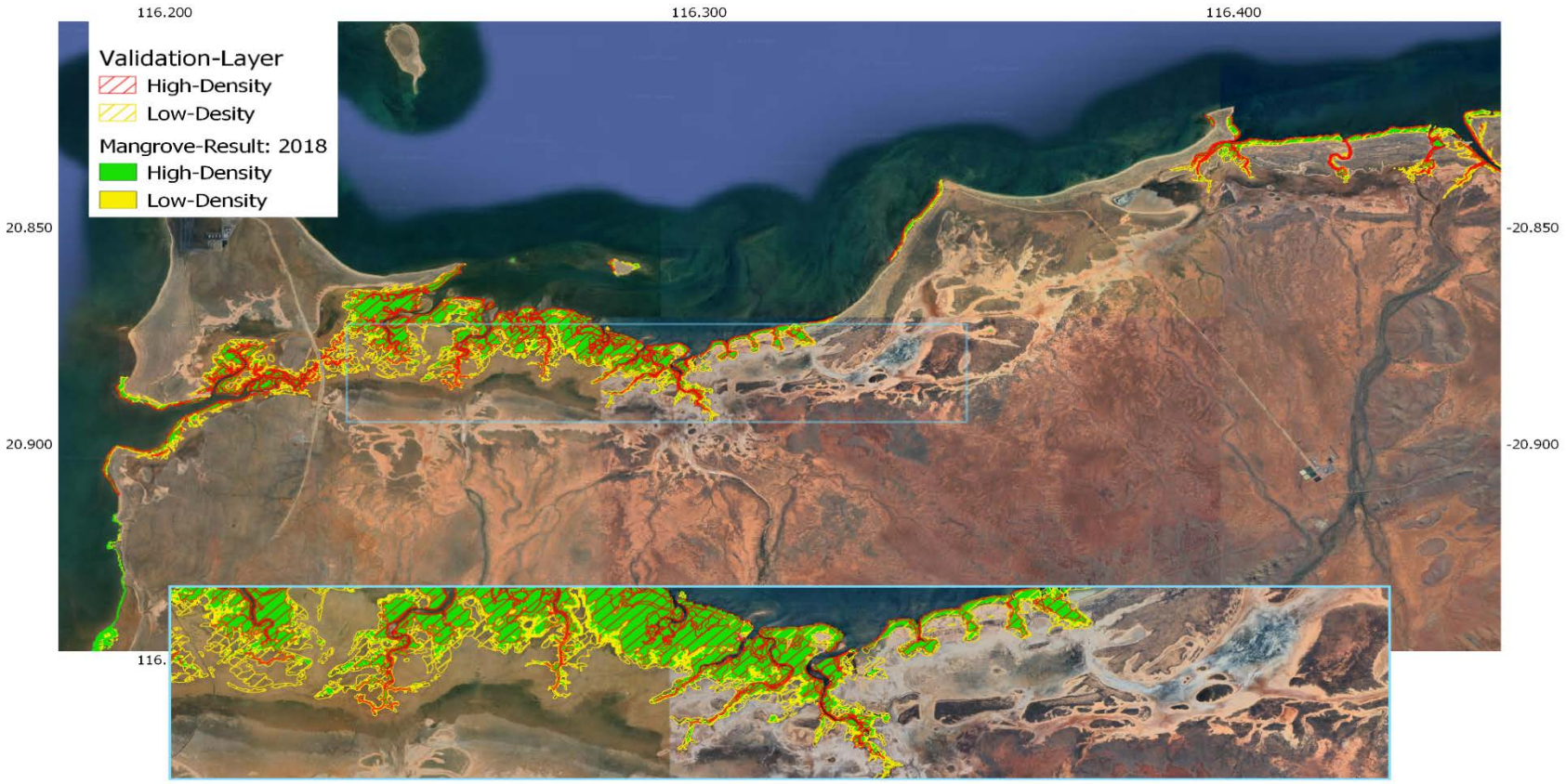

Figure 25. Low and High-Density Mangrove map for year 2018. The red shaded colour represents the high-density mangrove validation layer and filled green colour represents the high-density mangrove result. The yellow shaded colour represents the low-density mangrove validation layer and filled yellow colour represents the low-density mangrove result.

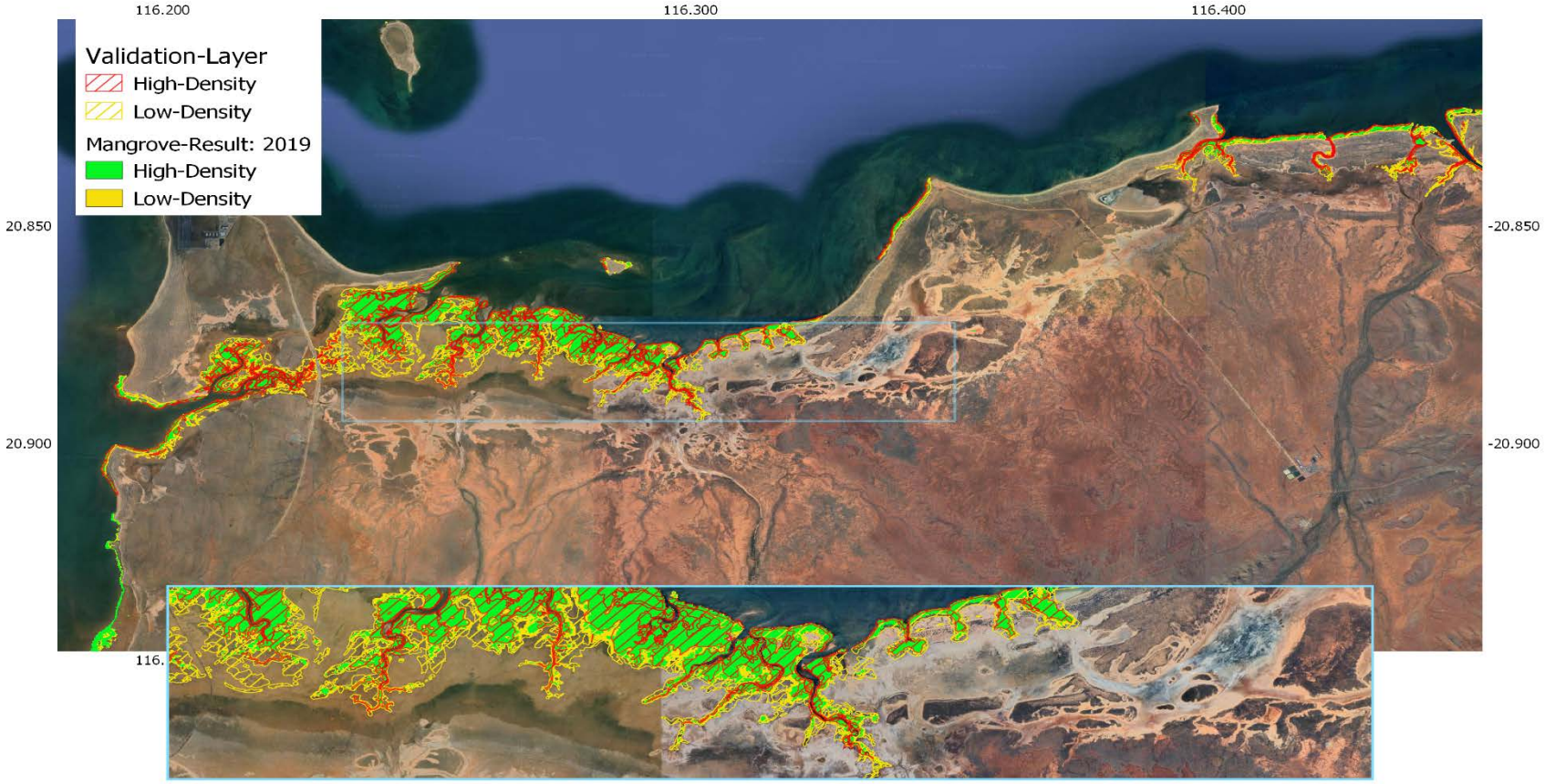

Figure 26. Low and High-Density Mangrove map for year 2019. The red shaded colour represents the high-density mangrove validation layer and filled green colour represents the high-density mangrove result. The yellow shaded colour represents the low-density mangrove validation layer and filled yellow colour represents the low-density mangrove result.

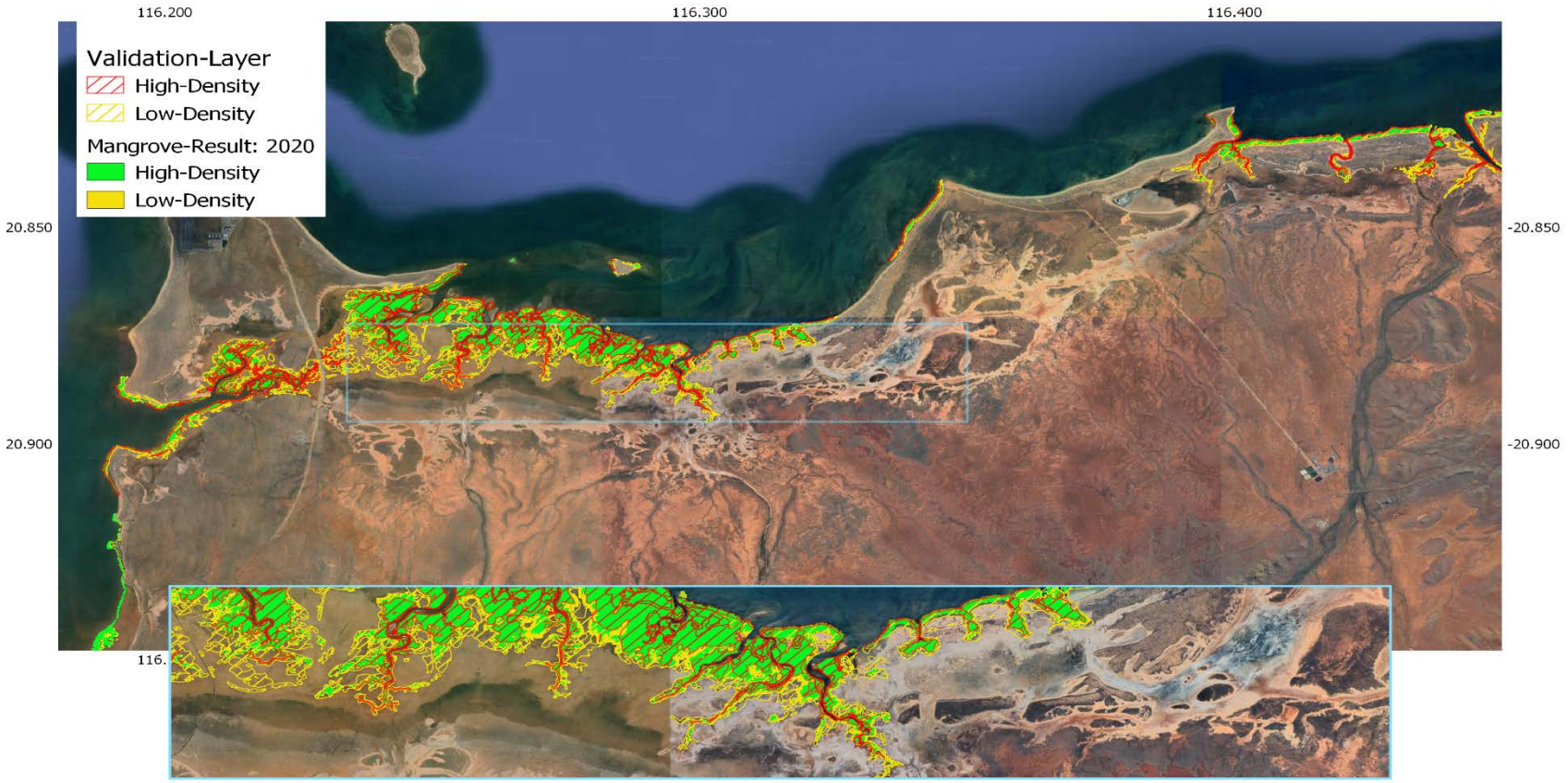

Figure 27. Low and High-Density Mangrove map for year 2020. The red shaded colour represents the high-density mangrove validation layer and filled green colour represents the high-density mangrove result. The yellow shaded colour represents the low-density mangrove validation layer and filled yellow colour represents the low-density mangrove result.

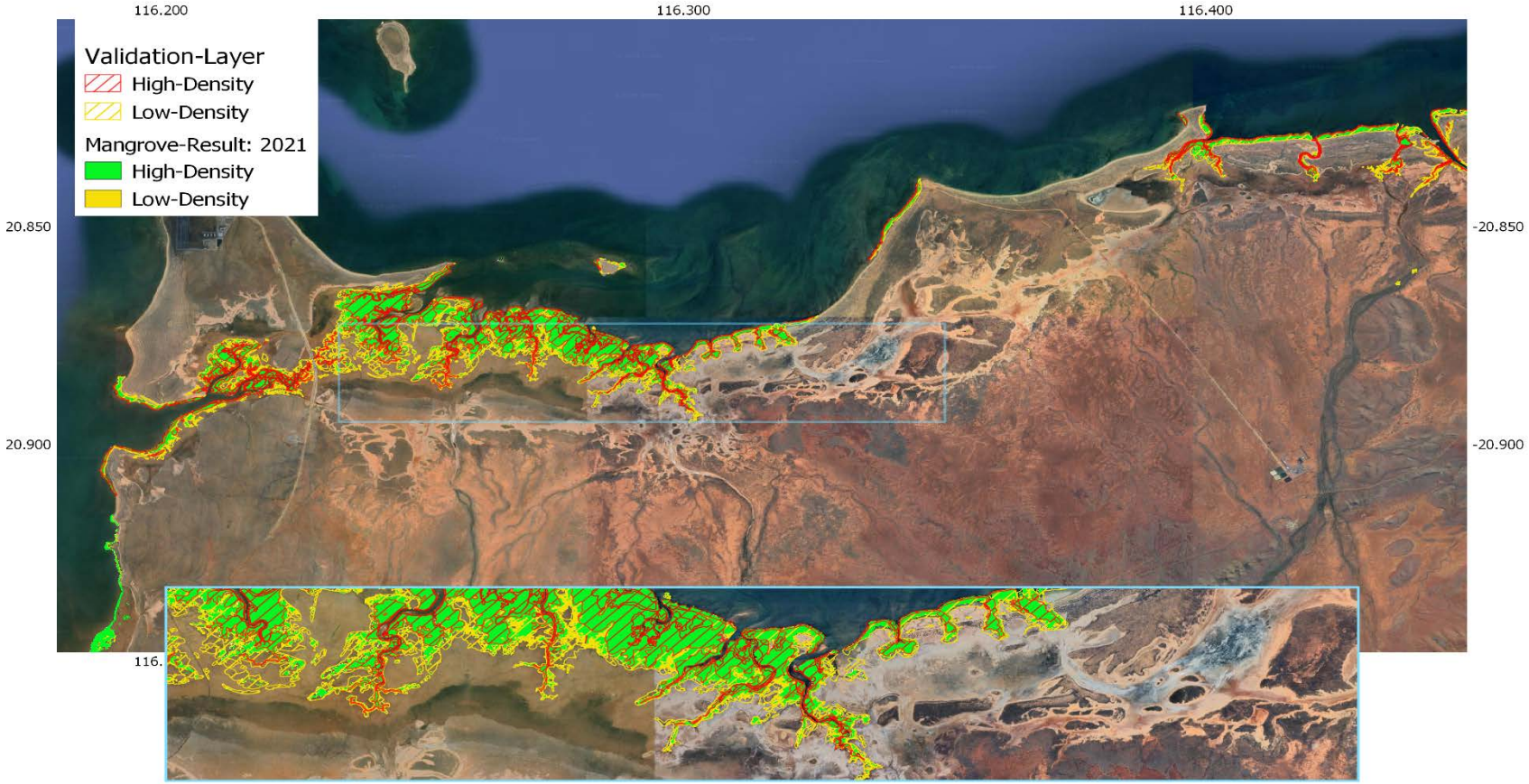

Figure 28. Low and High-Density Mangrove map for year 2021. The red shaded colour represents the high-density mangrove validation layer and filled green colour represents the high-density mangrove result. The yellow shaded colour represents the low-density mangrove validation layer and filled yellow colour represents the low-density mangrove result.

4.8 Low and High-density Classification Validation results

To undertake validation of high and low-density mangrove classification we extracted 689 and 818 pixels randomly from high and low-density validation layers respectively. A minimum of 100 metres separation was maintained between the extracted validation points. The year 2021 was used for the validation since the validation layers were created in 2021. The result of the validation is presented in Table 5. From the results, it is evident that that high-density mangrove is classified better in comparison to low-density mangrove. Low-density validation layers incorporate areas that are sparely covered by mangroves and includes bare-ground and other vegetations. This classification method is limited to identifying mangrove at pixel level so result for low-density mangrove is poorly performed.

Table 5. Validation results for Low and High-Density Mangrove classification result.

	Accuracy (%)	F1-Score (%)
Low-Density	30.53	46.78
High-Density	95.67	97.79

4.9 Low and high density processing extent

The processing of Sentinel data to grow the mapped extent of mangrove was undertaken for a region captured by 2 Sentinel tiles centred on the region of interest (See Figure 1 for the coverage of Sentinel tiles). The roughly 116 E to 116.55 E region process is shown in Figure 29. Note the high proportion of low density (white) identified in the SW corner. The total areas of high and low density mangrove are approximately 16.6 km^2 and 8.1 km^2. This shows the new method to identify low density mangrove has increased the mapped areas by approximately 33%.

Figure 29. Extent of updated low density(white) and high density(black) mangrove mapping.

5. Mapping sparse mangrove using Neo data

Pléiades Neo Imager is carried on board a constellation pair of commercial satellites launched in 2021. Neo provides very high spatial resolution multispectral data. Table 6 lists the spectral band information.

It is clear from the Sentinel results presented earlier that Sentinel sensors perform poorly at detecting very low density, or sparse, mangrove. For this work we aimed to assess the applicability of Neo data for detecting, mapping and quantifying the spatial coverage of sparse mangrove.

Table 6. Pléiades Neo spectral band information. All bands are 1.2 m resolution at nadir. Data are pansharpened to 0.3.

	wavelength	Spatial resolution
Panchromatic	450 - 800	0.3
Band 1 – Red	619 - 690	1.2
Band 2 – Green	533 - 591	1.2
Band 3 – Blue	446 - 520	1.2
Band 4 – NIR	768 - 888	1.2
Band 5 – Red edge	697 - 750	1.2
Band 6 – Deep blue	416 - 457	1.2

A sample of Neo data was obtained, with capture date 21st Jan 2022. Figure 30 shows the location of the Neo data overlayed on a Google Maps image. The spatial extents of the data are 116.2028E to 116.2969E and 20.8577S to 20.8951S. The data were divided into 1 km^2 regions for processing, shown in Figure 31.

Figure 30. Neo data overlayed on Google map image.

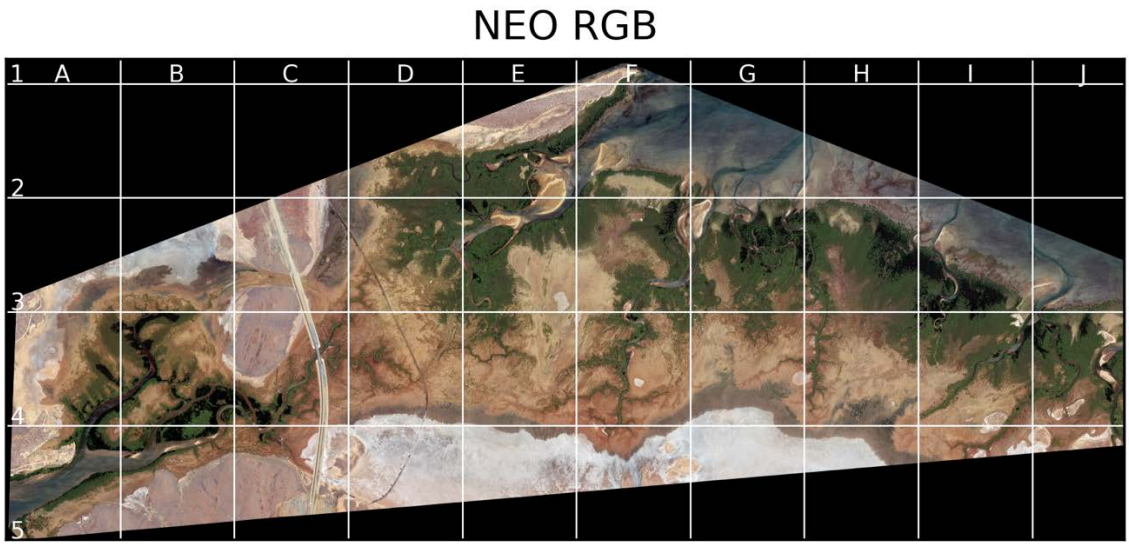

Figure 31. Neo data true colour image showing the 1 km^2 processing regions.

Spectral bands 1 and 4 were used to calculate NDVI, then a threshold of 0.35 was used to identify mangrove. Figures 32 to 35 show an example of mangrove mapping for region C4. Figure 32 shows a true colour image based on NEO bands 1-3. Figure 33 shows the same true colour image with results of Sentinel-based mangrove mapping. Each Sentinel pixel is 10 m x 10 m. The black pixels represent dense mangrove, and the grey pixels represent low density mangrove identified by the methods explained in Section 4.7. It is clear by visual inspection that some sparse mangroves are not identified by Sentinel, as well as some "fringing mangroves" along the river edge not being identified. Figure 34 shows the Neo true colour

image with pixels identified using the NDVI threshold, coloured white. Figure 35 shows the Sentinel mapping results combined with the Neo mapping results. Calculations of classified pixel areas show dense mangrove 165,799 m^2, low density mangrove 75,831 m^2, and sparse mangrove 17,783 m^2. The total image area is 1 km^2, thus the proportions of mangrove classes are 16.6%, 7.6% and 1.6% respectively.

Figure 32. New true colour image for region C4.

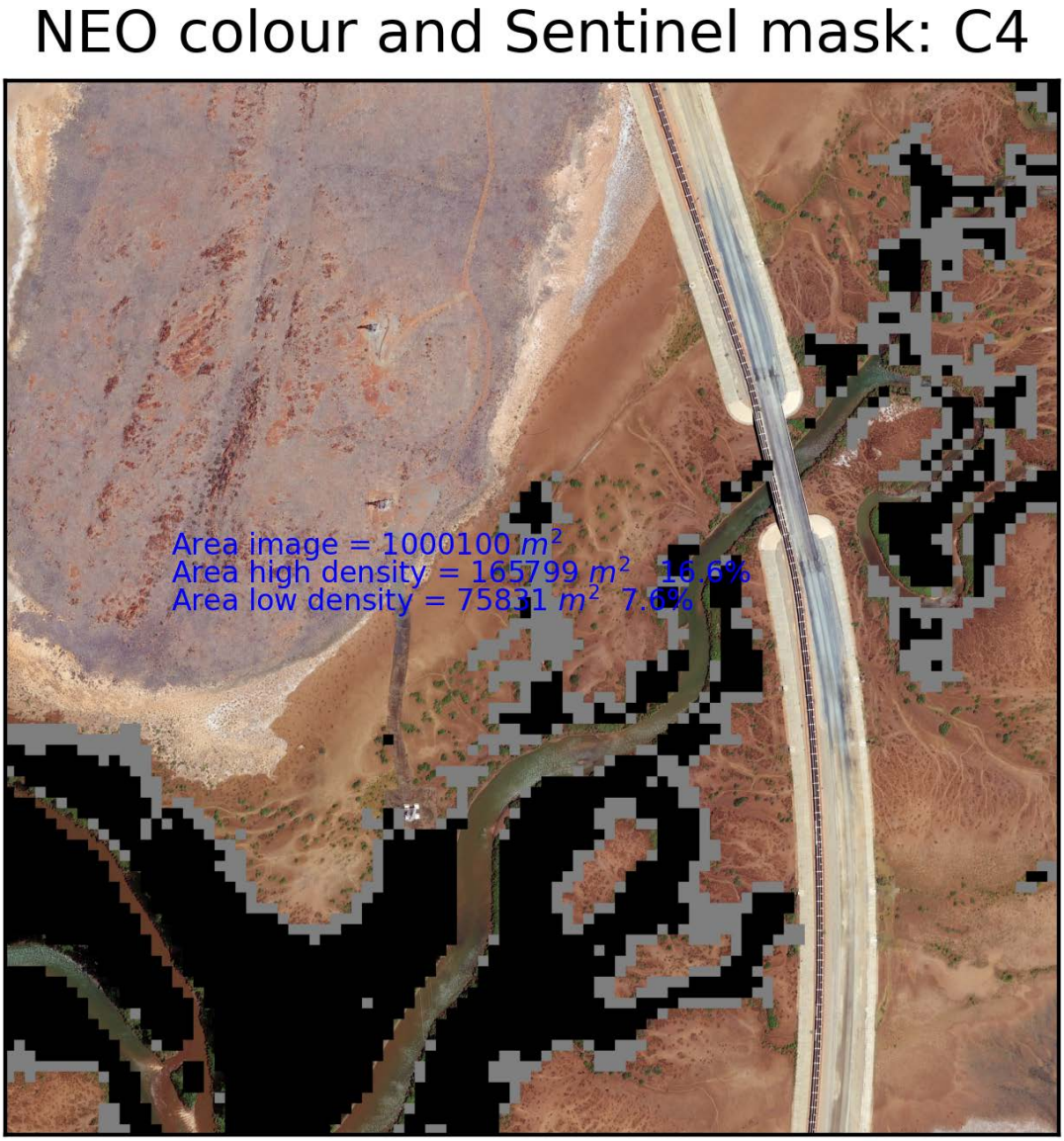

Figure 33. Neo true colour image with Sentinel dense (black) and "less dense" (grey) mangrove.

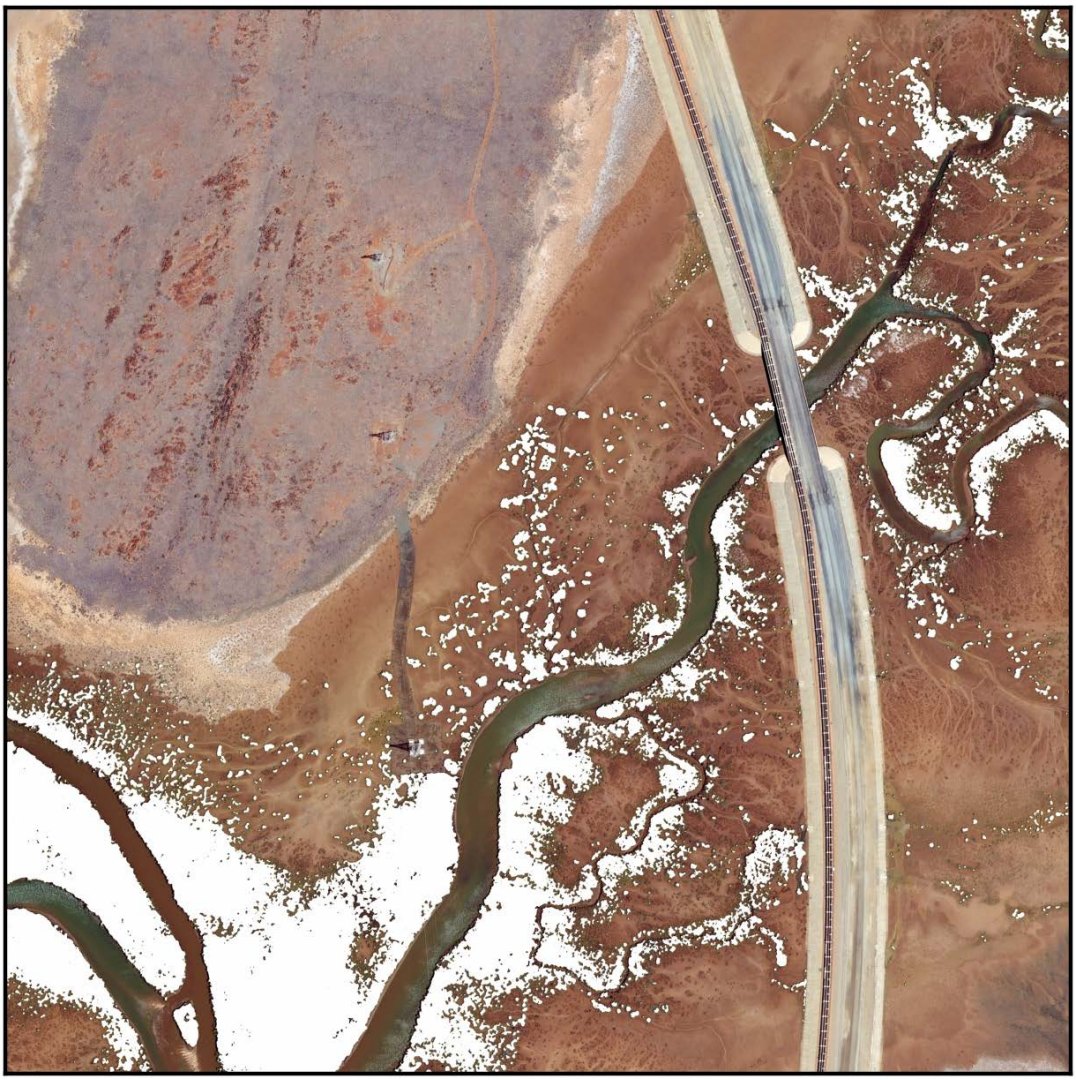

Figure 34. Neo True colour image with Neo-NDVI regions (white).

Figure 35. Neo true colour image with Sentinel dense (black), "less dense" (grey) and Neo-NDVI sparse mangrove (white).

Appendix 1 contains true colour images for all the regions shown in Figure 30, as well as figures akin to Figure 34, showing overlayed Sentinel and Neo NDVI mangrove classes. Calculations of areas for each region labelled in Figure 31, and shown in Appendix 1, show the total area of Neo data is approximately 27.4 km^2. For this region, the proportion of dense mangrove identified by Sentinel is 26.7% and low density identified as 5.1%. The proportion of sparse mangrove identified by Neo is 0.8%.

6. Discussion

The mapping of mangrove using the SVM model was carried out over the north western region of Western Australia for the years 2018 to 2021 using a combination of optical remote sensing data from Sentinel-2 A/B, DEM, and Synthetic Aperture Radar data from Sentinel-1 A/B. The validation of the results shows that the SVM model performed well in mapping the high-density mangrove types but performed less well in identifying low-density mangrove. The lower validation percentage of the SVM model in the low-density mangrove area might be because the SVM model is developed to identify mangrove at per-pixel level, while the ground-truth contained the features polygonised irrespective of the presence of pixels from other land types. Better quantified validation data, at per-pixel levels, needs to be used to improve the validation of the results in a more robust manner.

The SVM model was particularly developed for the study site and the implication of applying the model to other regions needs to be studied. Further, the SVM model was trained to identify pixels with only two features, mangrove and not-mangrove, thus this limits the identification of pixels that might contain mixed surface types in a pixel. Essentially, we may interpret the classification of a pixel as “mangrove” to be a “pixel dominated by mangrove”, and a pixel classed as “not mangrove” as a “pixel not dominated by mangrove”. The results of this work suggest strongly a need for the community to improve the description or classification of “ground type” with a more considered approach to density of cover and mangrove extent.

To overcome the poor performance of Sentinel in identifying low density mangrove, we developed a method to search for pixels adjacent to previously identified mangrove pixels. Based on thresholds of NDVI, PSI and S1-backscatter, we were able to “grow” the mangrove regions to identify low density regions. The region selected for application of the low density identification encompassed the extent of 2 Sentinel pixels, centred on the region of interest and the location of validation data. This method identified approximately a further 33% of mangrove extent. It is to be noted that the SW region appeared to show a high proportion of low density mangrove. Visual inspection of results suggests mangroves were poorly identified by the first step, identification of high density, but well identified by the second low density identification step.

Although the identification of low density mangrove using Sentinel data was improved, there were clearly some regions of very sparse mangrove that were not identified. We acquired a sample of Pléiades Neo data and developed an NDVI approach to identifying mangrove at 30 cm spatial resolution. The results suggest a high confidence, based on visual assessment of true colour images compared to the map results. We do not have ground truth data at the

accuracy or spatial resolution required to undertake a rigorous assessment of Neo mapping accuracy. For the sample region (~ 27.4 km^2), Sentinel identified approximately 7.3 km^2 high density and 1.4 km^2 low density. Neo identified approximately 0.2 km^2. The Sentinel low density method identified approximately 13% extra mangrove extent than the high density mapping.

It is important to be aware of the spatial scale of raster-based mapping. The Sentinel data is at 10 m resolution and the Neo data is at 0.3 m resolution. We have not attempted to downscale the Neo results to a 10 m representation, thus a direct comparison of "total cover" or "extent" mapped by Neo should not be undertaken without careful consideration of the required mapping or monitoring aims. Nonetheless, we have shown the great potential of Neo data for mapping mangrove to a very high spatial resolution and for regions of sparse cover that are typically not identified by moderate resolution sensors.

The Sentinel 2 satellites were launched in 2015 and 2017, therefore there is a large and growing archive of global satellite data that can be used to study baseline metrics and temporal variability of mangrove ecosystems. The Pléiades Neo Imagers were launched in 2021 and they do not capture the whole globe routinely, thus the archive of historical data is sparse.

References

Bauer-Marschallinger, B., Cao, S., Navacchi, C. *et al.* The normalised Sentinel-1 Global Backscatter Model, mapping Earth's land surface with C-band microwaves. *Sci Data* **8,** 277 (2021). https://doi.org/10.1038/s41597-021-01059-7

Bunting P., Rosenqvist A., Lucas R., Rebelo L-M., Hilarides L., Thomas N., Hardy A., Itoh T., Shimada M. and Finlayson C.M. (2018). The Global Mangrove Watch – a New 2010 Global Baseline of Mangrove Extent. *Remote Sensing* 10(10): 1669. doi: 10.3390/rs1010669.

Dennis, C.D., Steven, E.F. and Monique, G.D. (2012) A comparison of pixel-based and object-based image analysis with selected machine learning algorithms for the classification of agricultural landscapes using SPOT-5 HRG imagery. *Remote Sens. Environ*., 118, 259–272.

Diniz, C, Cortinhas, L, Nerino, G, Rodrigues, J, Sadeck, L, Adami, M and Souza-Filho, PWM (2019), 'Brazilian Mangrove Status: Three Decades of Satellite Data Analysis', *Remote Sensing*, vol. 11, pp.808

Gao, Bo-Cai (1996). NDWI—A normalized difference water index for remote sensing of vegetation liquid water from space. *Remote Sensing of Environment*. **58** (3): 257–266

Huete, A., Didan, K., Miura, T., Rodriguez, E.P., Gao, X. and Ferreira, L.G. (2002) Overview of the radiometric and biophysical performance of the MODIS vegetation indices. *Remote Sens. Environ.*, *83*, 195–213

Jiang, Y., Zhang, L., Yan, M., Qi, J., Fu, T., Fan, S. and Chen, B. (2021) High-Resolution Mangrove Forests Classification with Machine Learning Using Worldview and UAV Hyperspectral Data. *Remote Sens*., 13, 1529

Li, F., Jupp, D. L. B., Reddy, S., Lymburner, L., Mueller, N., Tan, P. and Islam, A. (2010). An evaluation of the use of atmospheric and brdf correction to standardize landsat data. *IEEE Journal of Selected Topics in Applied Earth Observations and Remote Sensing*, *3*(3), 257–270. https://doi.org/10.1109/JSTARS.2010.2042281

Lien, T.H.P. and Lars, B. (2017) Monitoring mangrove biomass change in Vietnam using SPOT images and an object-based approach combined with machine learning algorithms. *ISPRS J. Photogramm*., 128, 86–97.

Lucas R., Rebelo L.-M., Fatoyinbo L., Rosenqvist A., Itoh T., Shimada M., Simard M., Souza-Filho P. W., Thomas N, Trettin C., Accad A., Carreiras J. and Hilarides L (2014) Contribution of L-band SAR to systematic global mangrove monitoring. *Marine and Freshwater Research* **65**, 589-603. doi.org/10.1071/MF13177

Lymburner, L., Bunting, P., Lucas, R., Scarth, P., Alam, I., Phillips, C., Ticehurst, C. and Held, A. (2020) Mapping the multi-decadal mangrove dynamics of the Australian coastline, Remote Sensing of Environment, Volume 238, 2020, 111185, ISSN 0034-4257, doi.org/10.1016/j.rse.2019.05.004.

O2Marine (2022), Eramurra Solar Salt Project, Intertidal Benthic Communities and Habitat Report, 19WAU-0027/R200304, WA Marine PTY LTD, 19th September 2022

Payne, A. L., and Tille, P. J. (1992), An inventory and condition survey of the Roebourne Plains

and surrounds, Western Australia. Department of Primary Industries and Regional Development, Western Australia, Perth. Technical Bulletin 83.

Wang, M., Cao, W., Guan, Q., Wu, G., Jiang, C., Yan, Y. and Su, X. (2018) Potential of texture metrics derived from high-resolution PLEIADES satellite data for quantifying aboveground carbon of Kandelia candel mangrove forests in Southeast China. *Wetl. Ecol. Manag*., 26, 789–803

Zhu, Z. and Woodcock, C.E. (2012). Object-based cloud and cloud shadow detection in Landsat imagery Remote Sensing of Environment 118 (2012) 83-94.

Zhu, Z., Wang, S. and Woodcock, C.E. (2015). Improvement and expansion of the Fmask algorithm: cloud, cloud shadow, and snow detection for Landsats 4-7, 8, and Sentinel 2 images *Remote Sensing of Environment* 159 (2015) 269-277

Appendix 1

Neo images showing true colour and combined Sentinel and Neo-mapped mangroves.
Sentinel results at 10 m resolution, Neo results at 0.3 m resolution.
Sentinel results. Black = dense mangrove, grey = low density mangrove.
Neo results. White = sparse
The tables show the areas of mangrove for each image region.

TOTALS m^2	27415397	7331788	1393353	213232
TOTALS km^2	27.415397	7.331788	1.393353	0.213232
%	100.00%	26.74%	5.08%	0.78%
	image	high	low	sparse
A1	-			
A2	-			
A3	267936	3731	2029	446
A4	930823	274350	36235	3954
A5	927993	202322	37832	11762
B1	-			
B2	-			
B3	665764	30080	36950	2344
B4	1000100	536033	100920	14210
B5	881058	150563	26861	8107
C1	-			
C2	78438	0	0	0
C3	974878	1708	1836	1213
C4	1000100	165799	75831	17783
C5	794381	23923	24644	5516
D1	-			
D2	439050	243094	27921	2820
D3	1000100	508627	90459	7925
D4	1000100	73048	74405	13355
D5	711498	0	0	0
E1	-			
E2	825866	312253	22076	7557
E3	1000100	512832	32510	10421
E4	1000100	161588	72301	12507
E5	626167	0	0	0

	image	high	low	sparse
F1	88771	5617	695	227
F2	998412	177123	22692	3357
F3	1000100	536391	103153	7251
F4	1000100	249582	89581	17202
F5	540862	3199	3309	1046
G1	-			
G2	764217	12477	478	191
G3	1000100	704693	73710	8401
G4	1000100	91574	56661	5506
G5	455495	0	0	422
H1	-			
H2	365795	0	0	8
H3	1000100	735409	87712	5616
H4	1000100	202858	99118	7794
H5	370023	0	0	0
I1	-			
I2	34799	0	0	0
I3	932568	313718	6738	5023
I4	1000100	523950	78900	12242
I5	284846	21012	13227	1619
J1	-			
J2	-			
J3	485980	43052	3581	228
J4	801494	492158	79403	14062
J5	166983	19024	11585	3117

NEO RGB

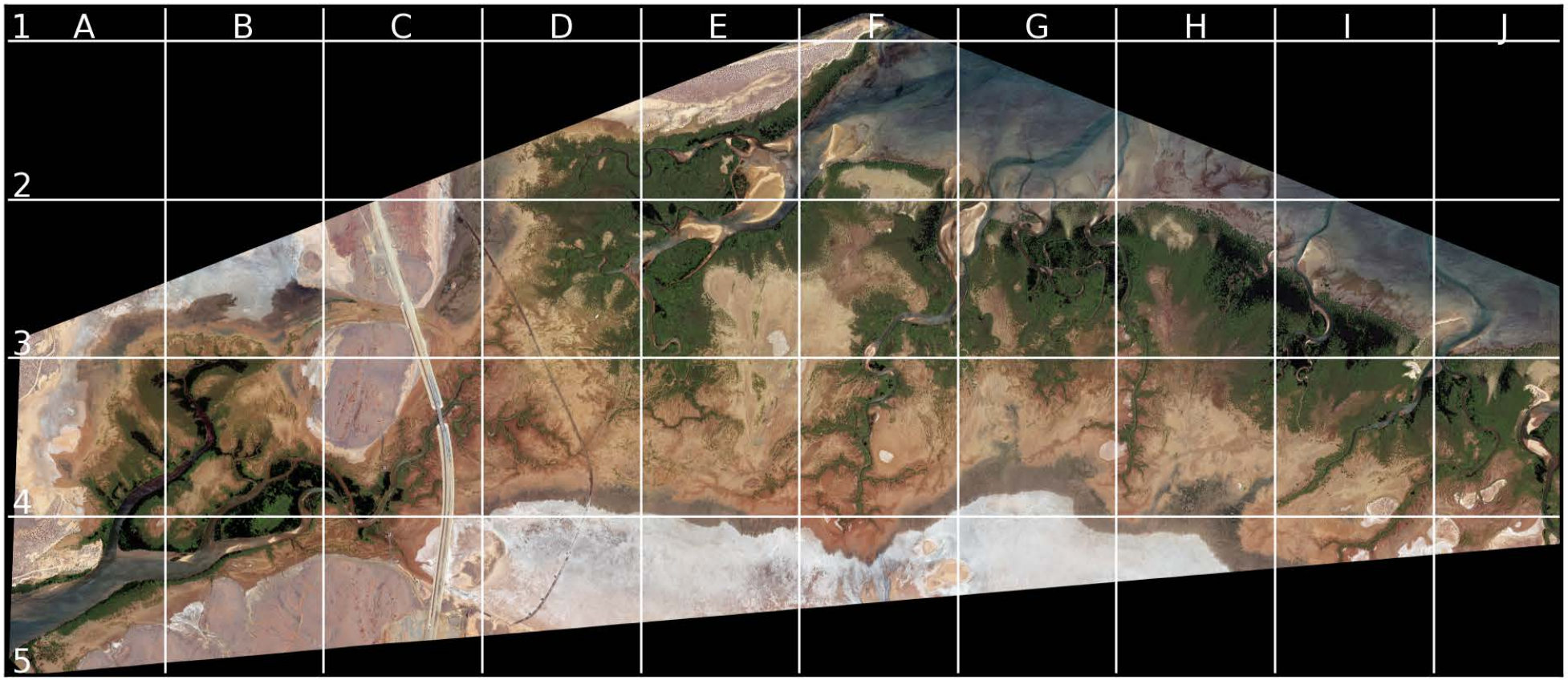

NEO true colour: A3

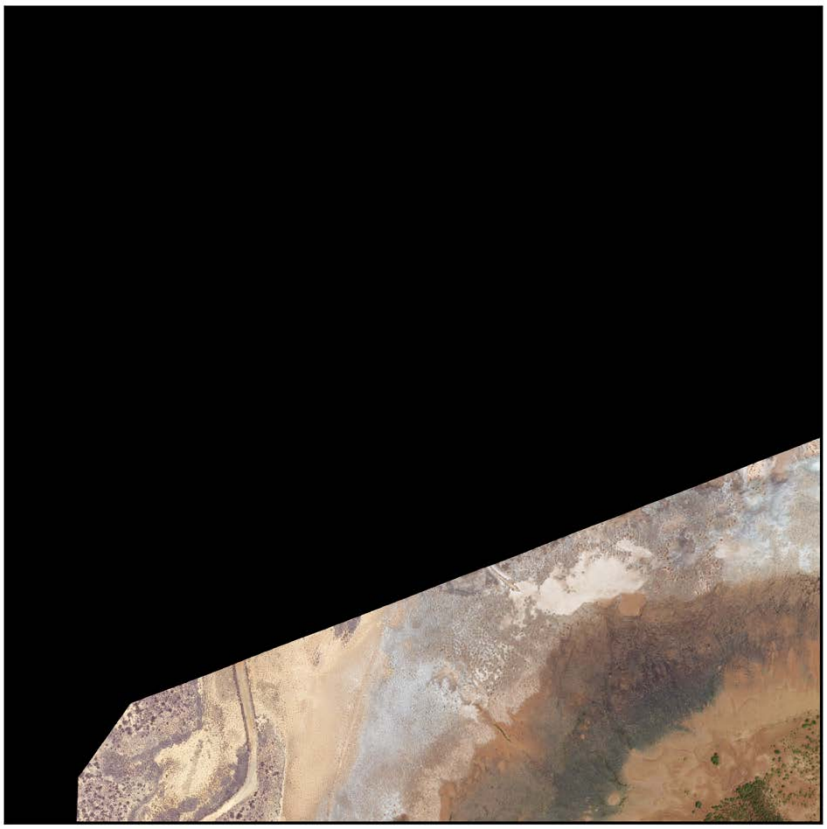

Mangrove. NEO & Sentinel: A3

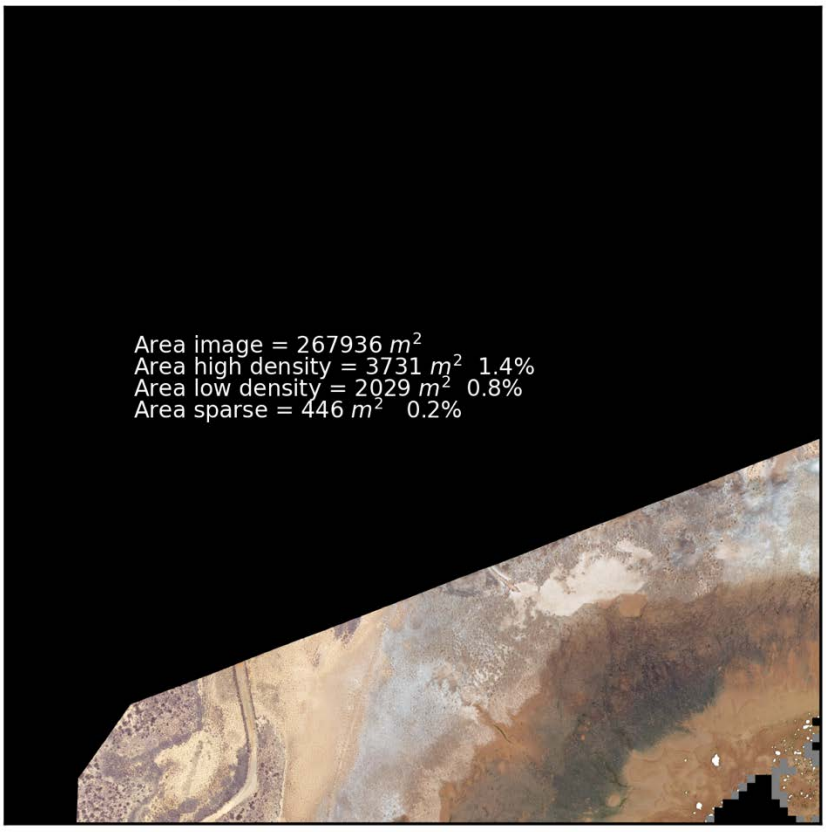

NEO true colour: A4

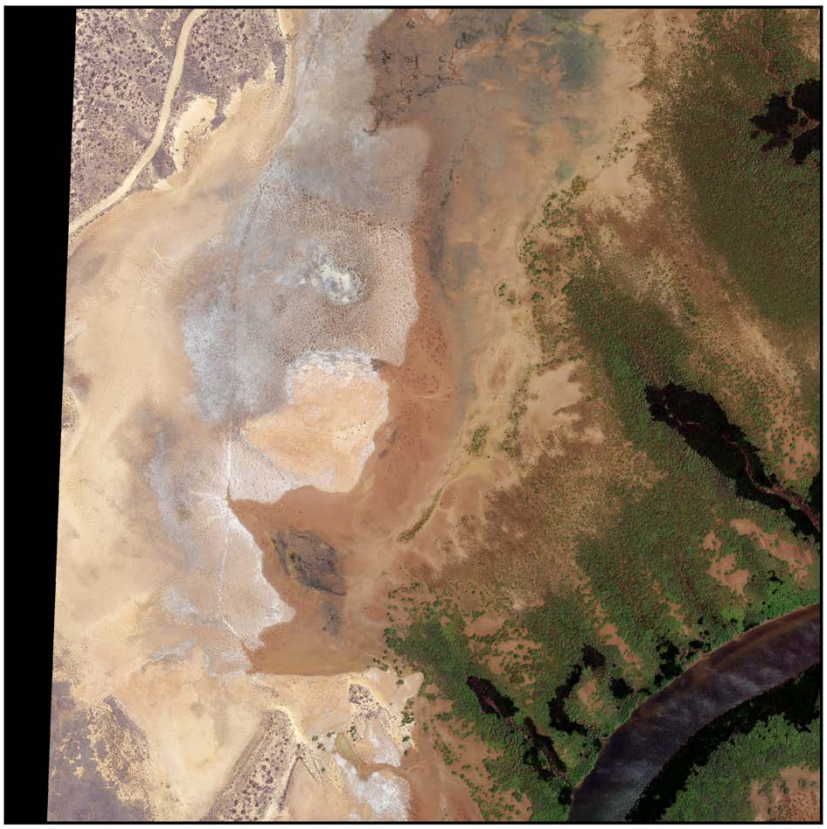

Mangrove. NEO & Sentinel: A4

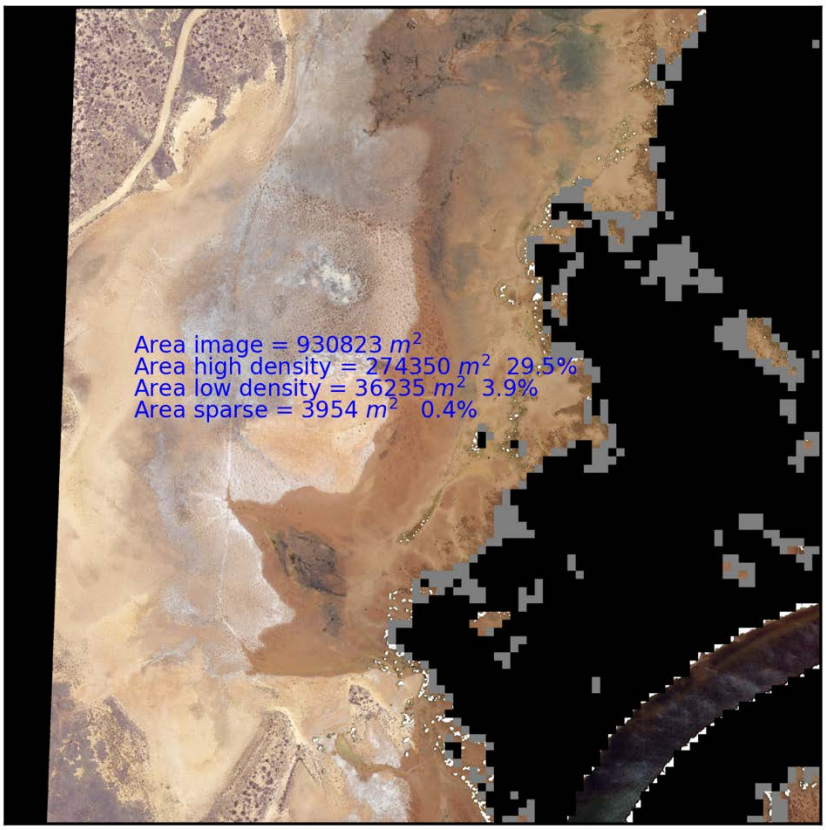

NEO true colour: A5

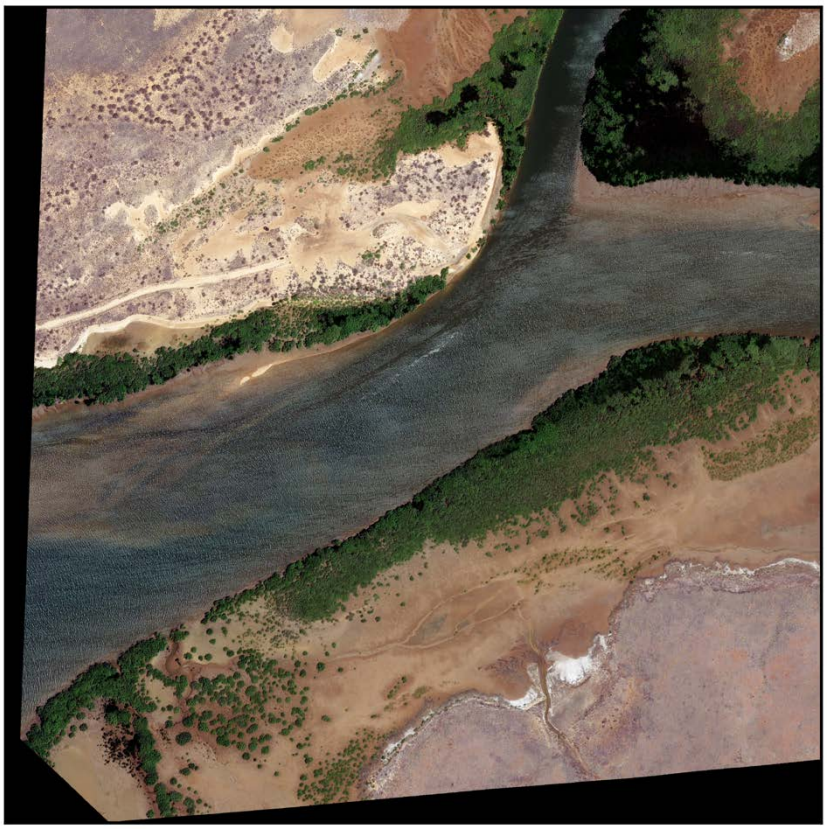

Mangrove. NEO & Sentinel: A5

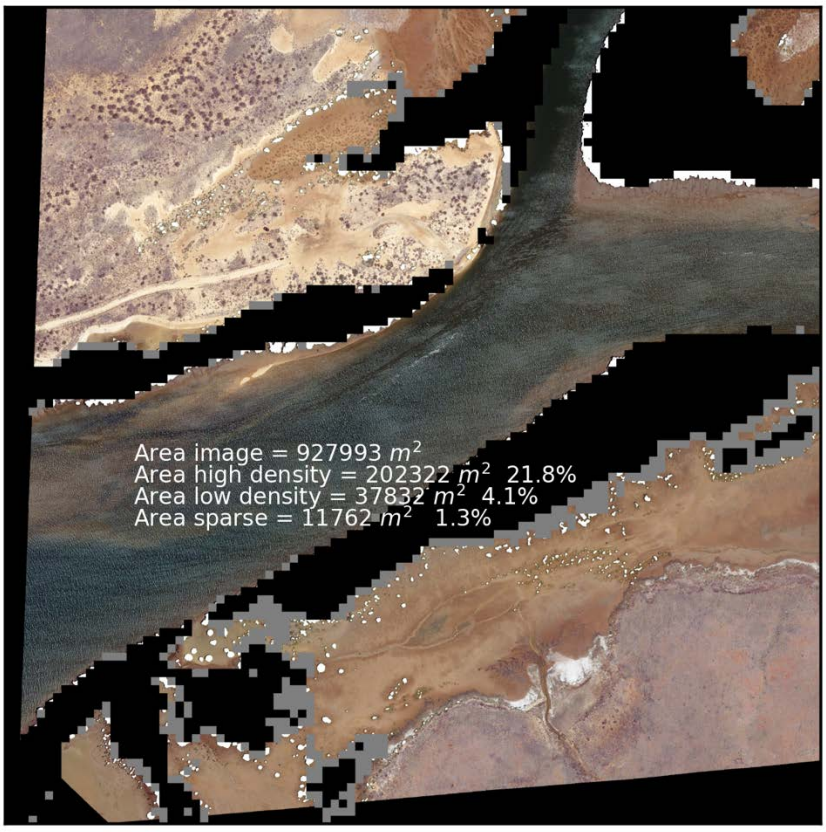

NEO true colour: B3

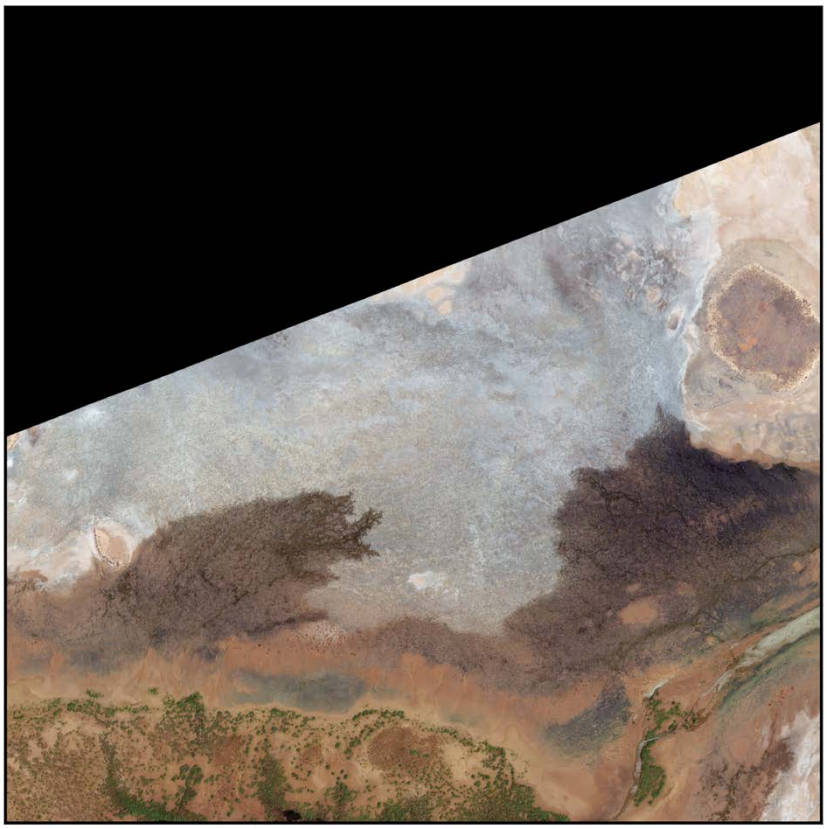

Mangrove. NEO & Sentinel: B3

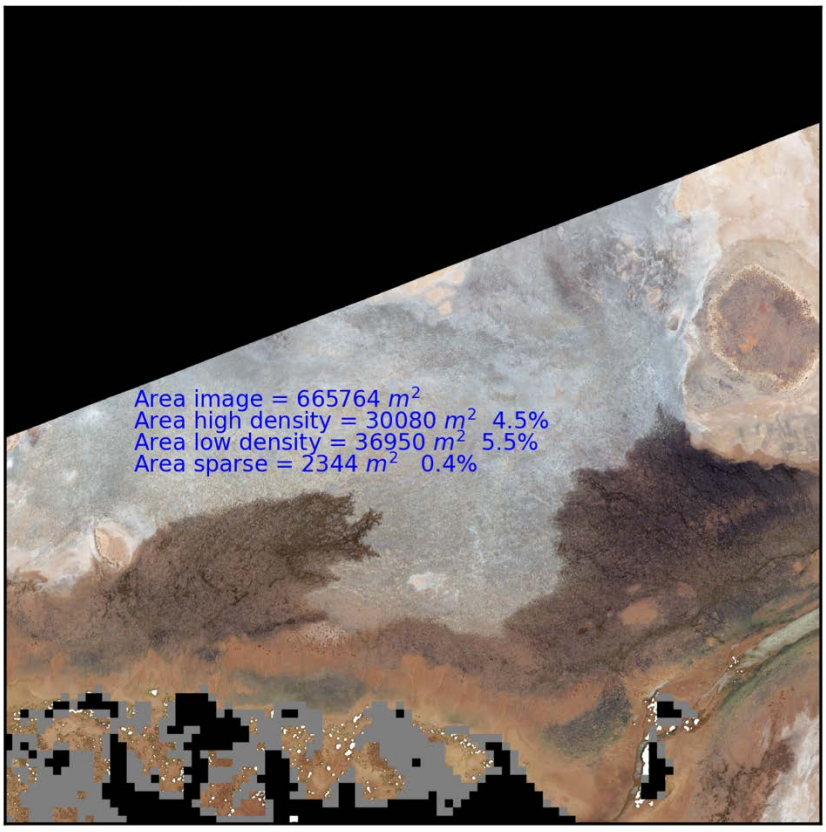

NEO true colour: B4

Mangrove. NEO & Sentinel: B4

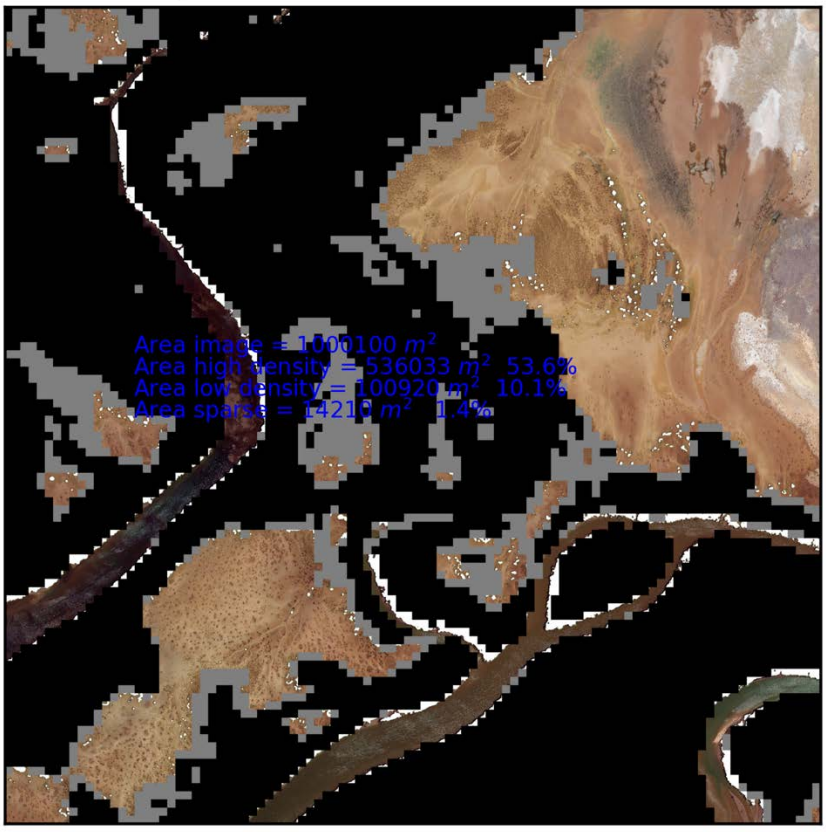

NEO true colour: B5

Mangrove. NEO & Sentinel: B5

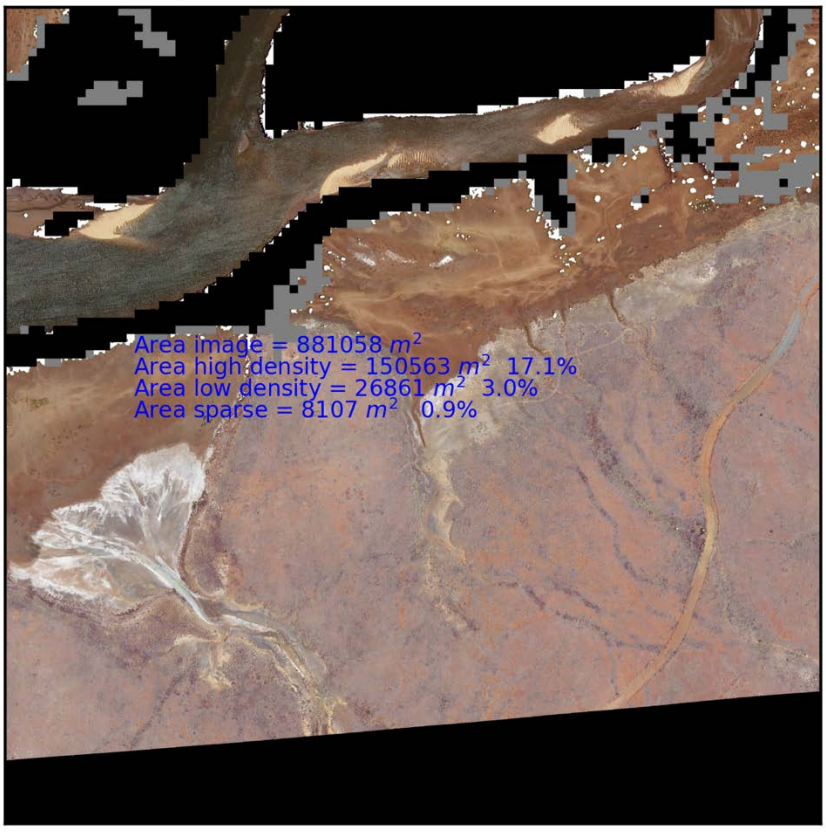

NEO true colour: C2

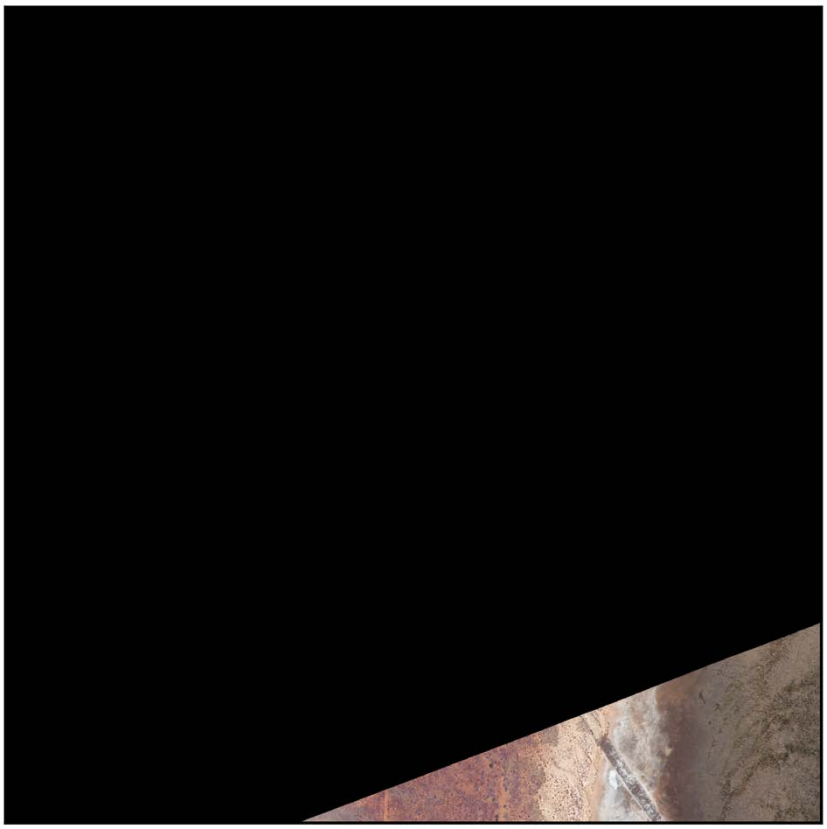

Mangrove. NEO & Sentinel: C2

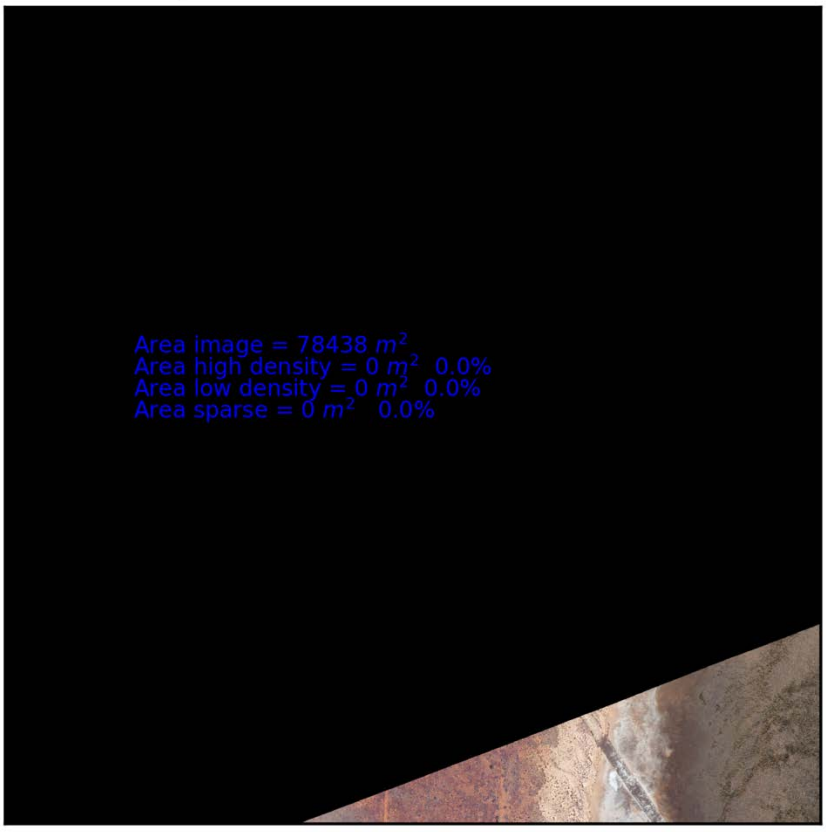

NEO true colour: C3

Mangrove. NEO & Sentinel: C3

NEO true colour: C4

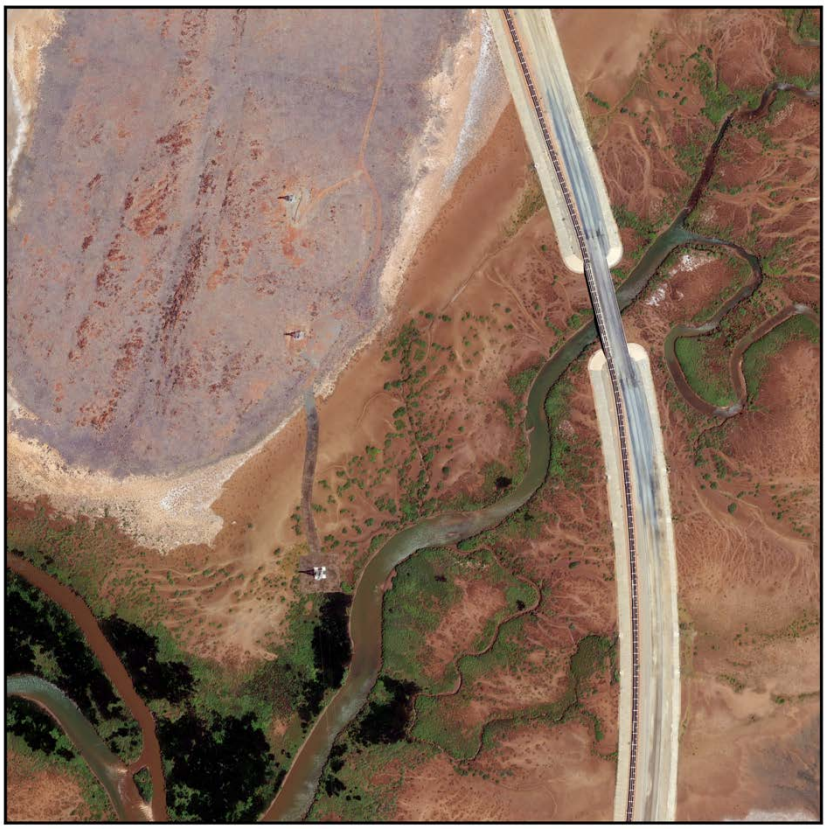

Mangrove. NEO & Sentinel: C4

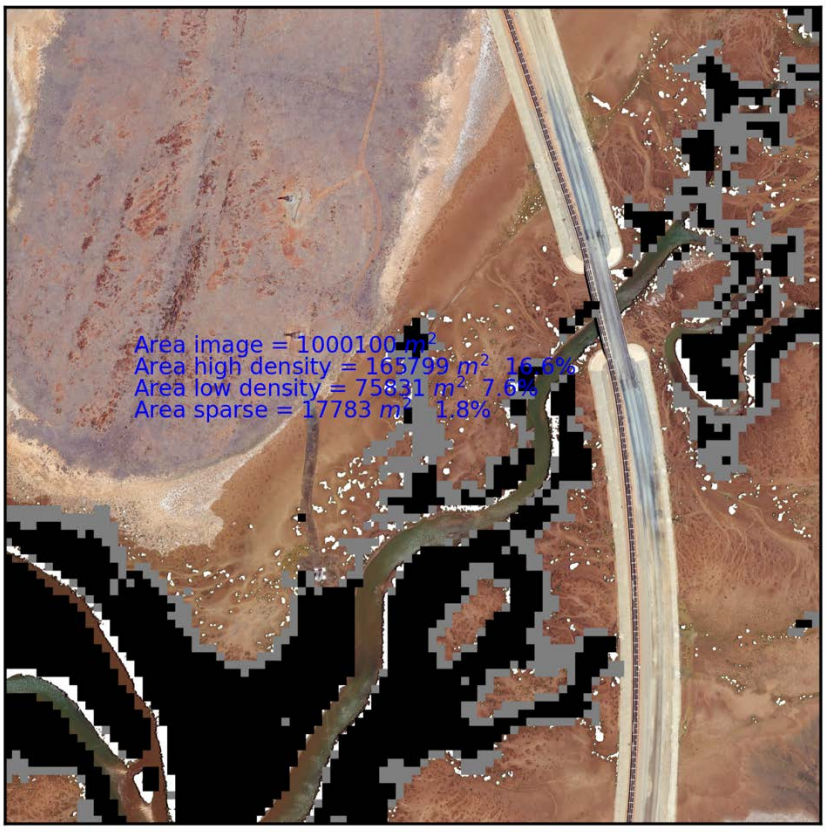

NEO true colour: C5

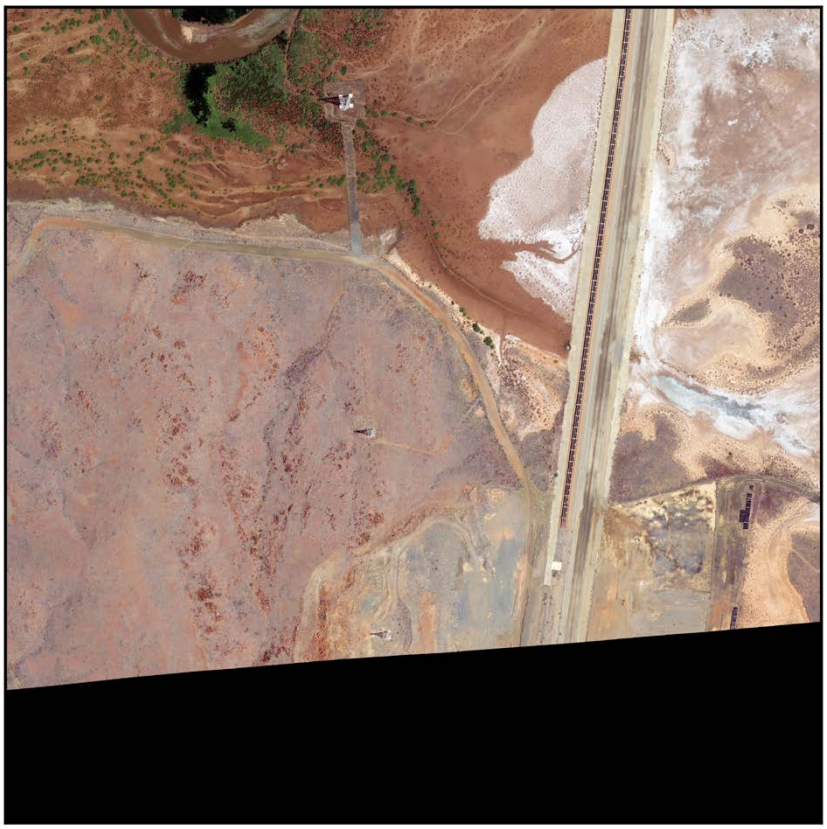

Mangrove. NEO & Sentinel: C5

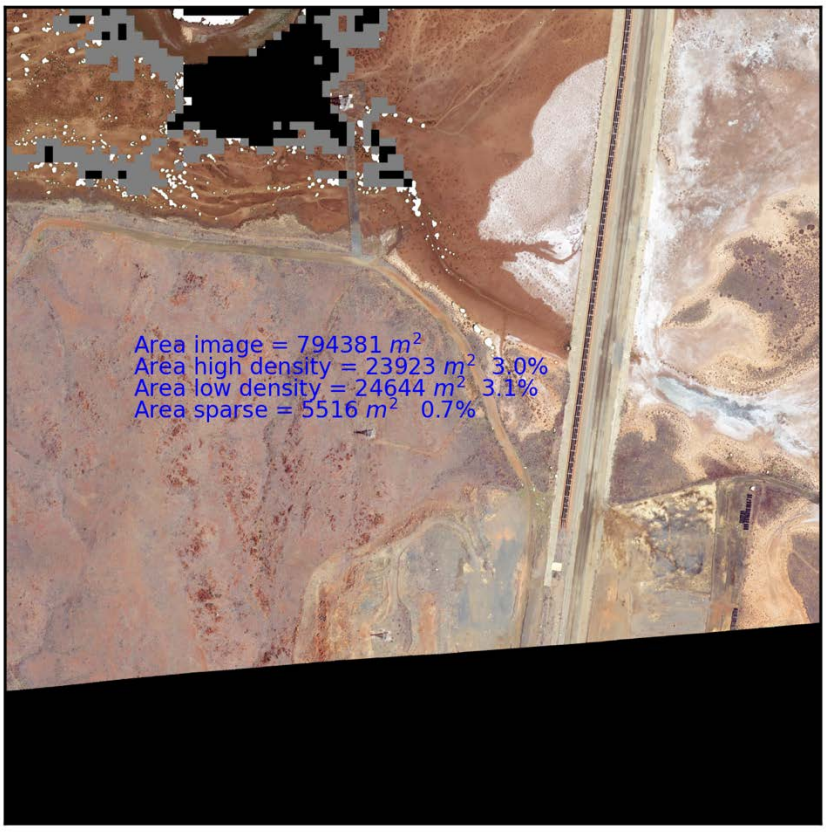

NEO true colour: D2

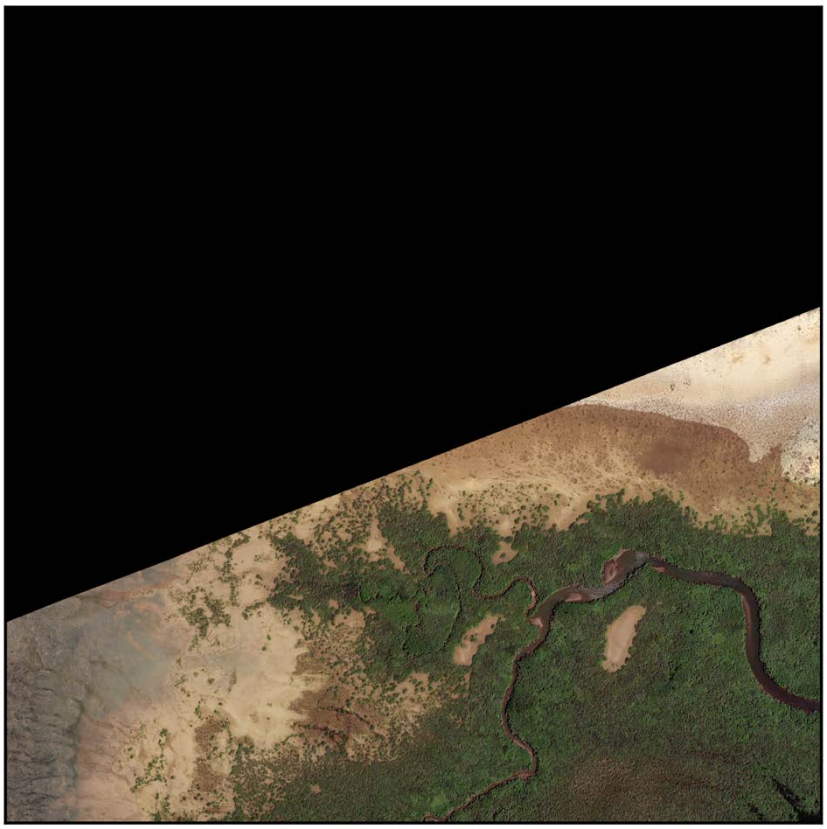

Mangrove. NEO & Sentinel: D2

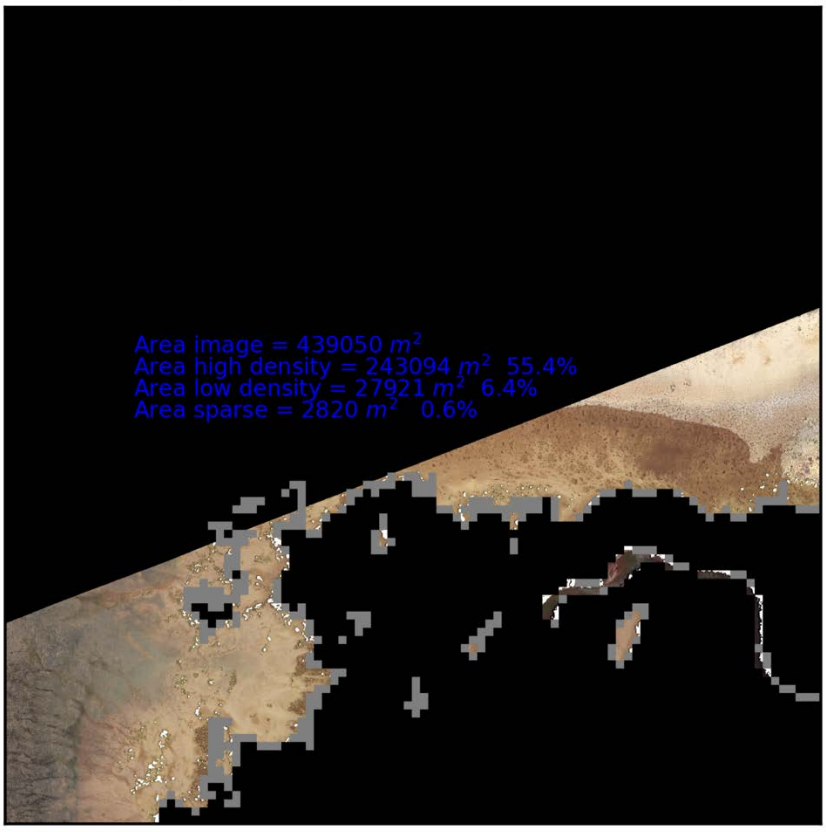

NEO true colour: D3

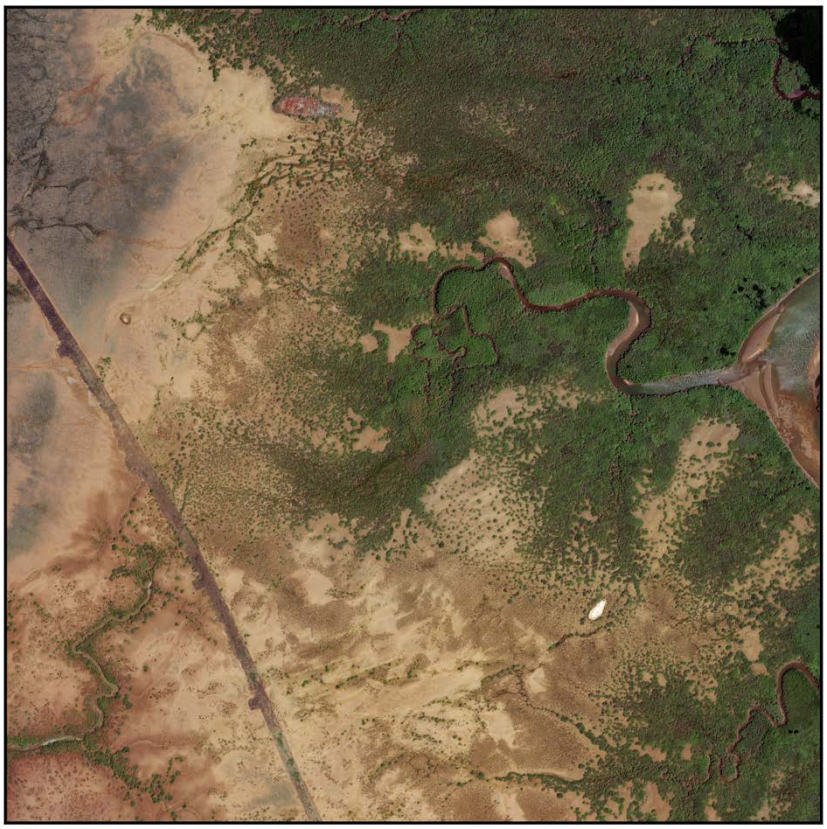

Mangrove. NEO & Sentinel: D3

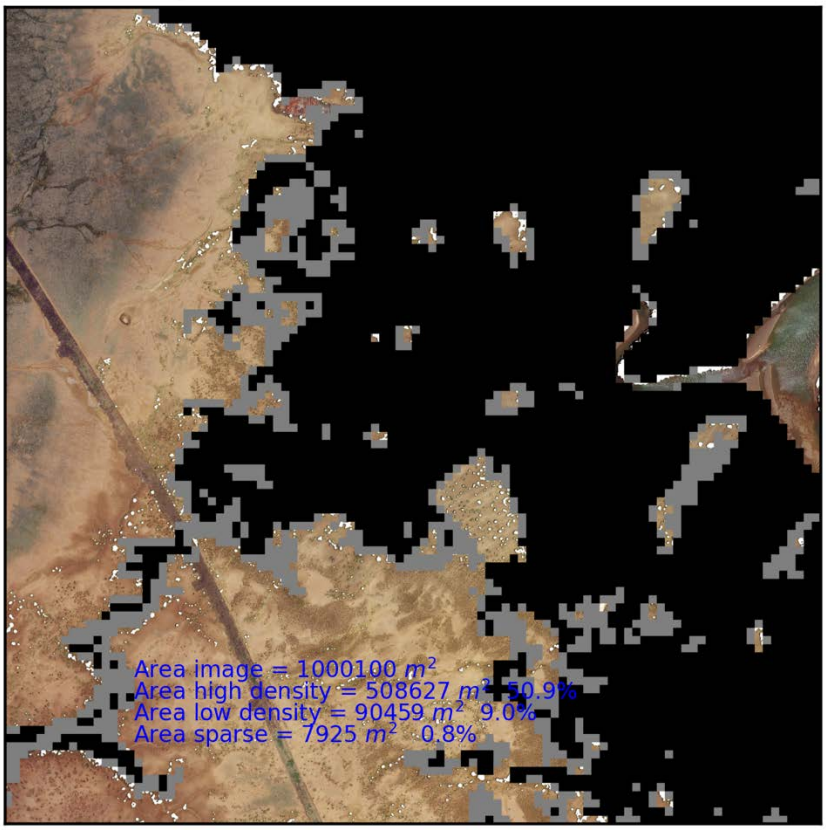

NEO true colour: D4

Mangrove. NEO & Sentinel: D4

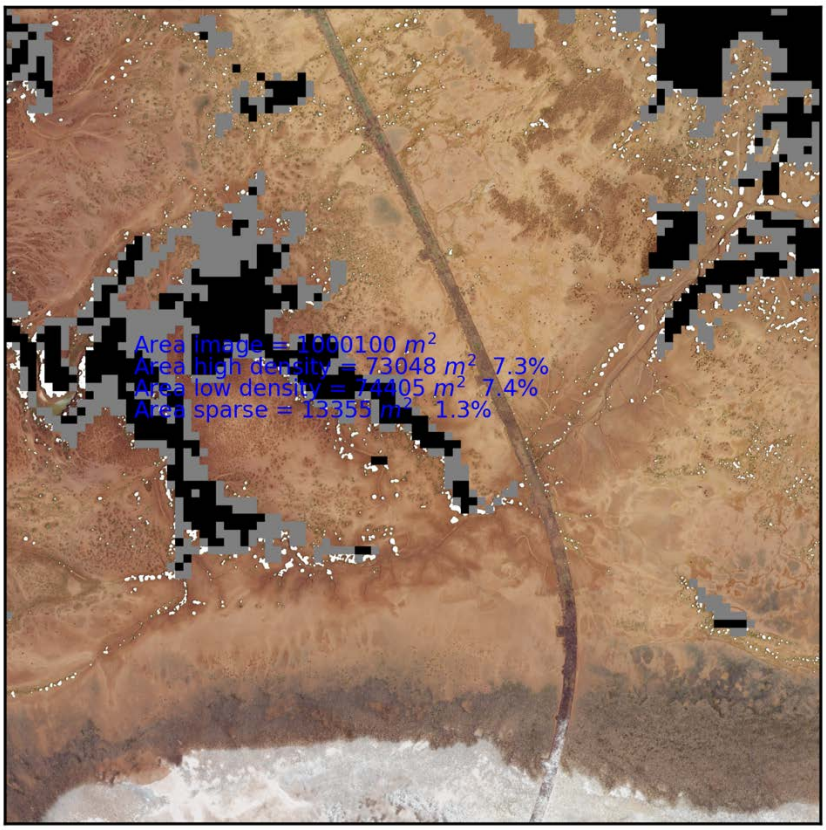

NEO true colour: D5

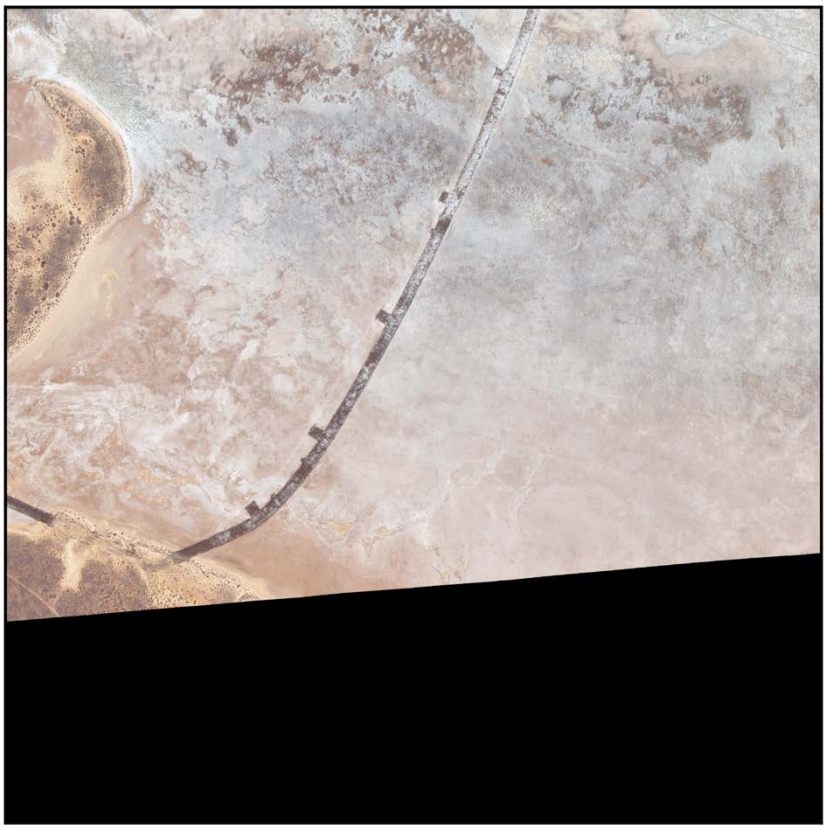

Mangrove. NEO & Sentinel: D5

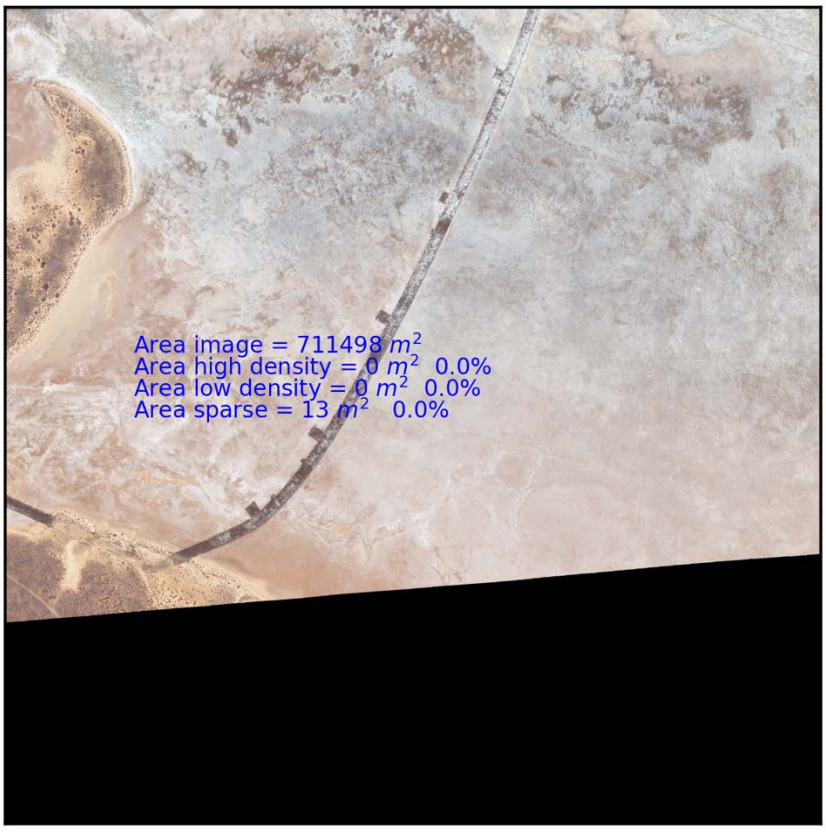

NEO true colour: E2

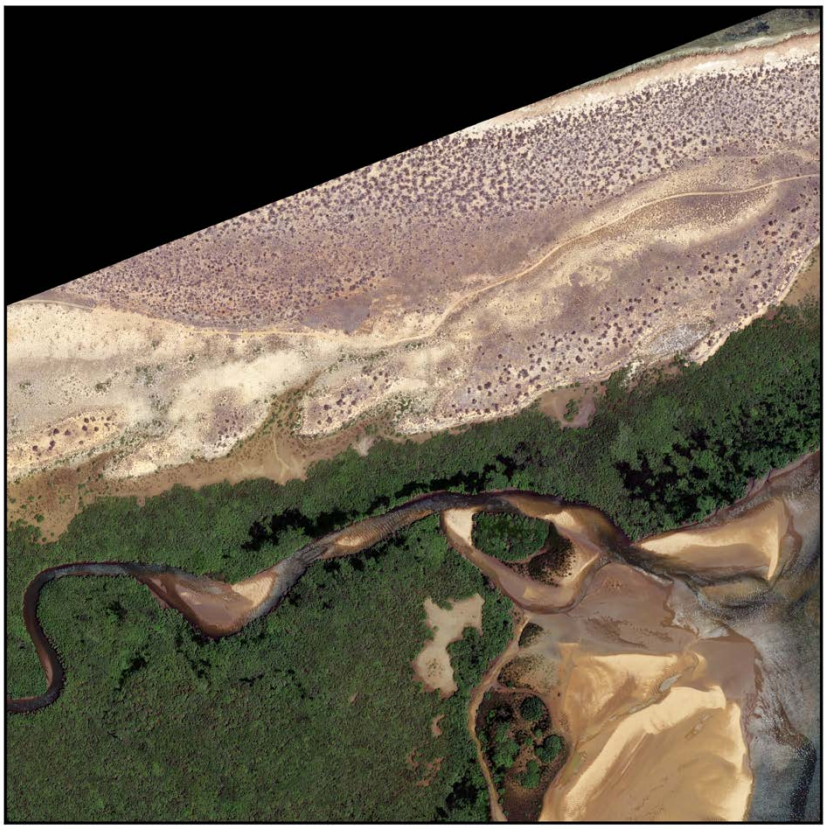

Mangrove. NEO & Sentinel: E2

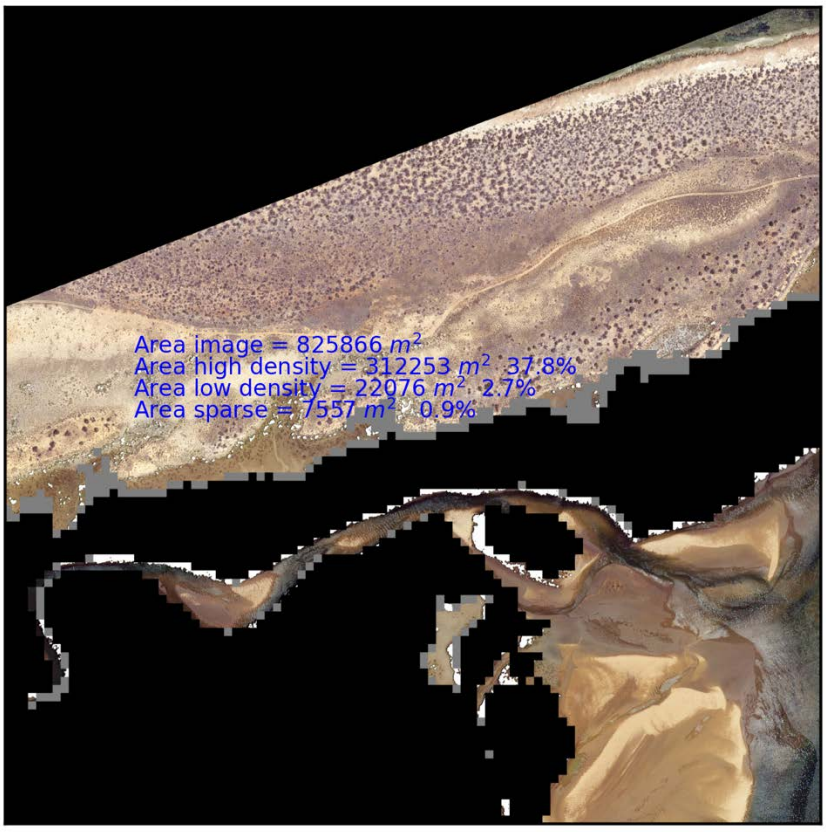

NEO true colour: E3

Mangrove. NEO & Sentinel: E3

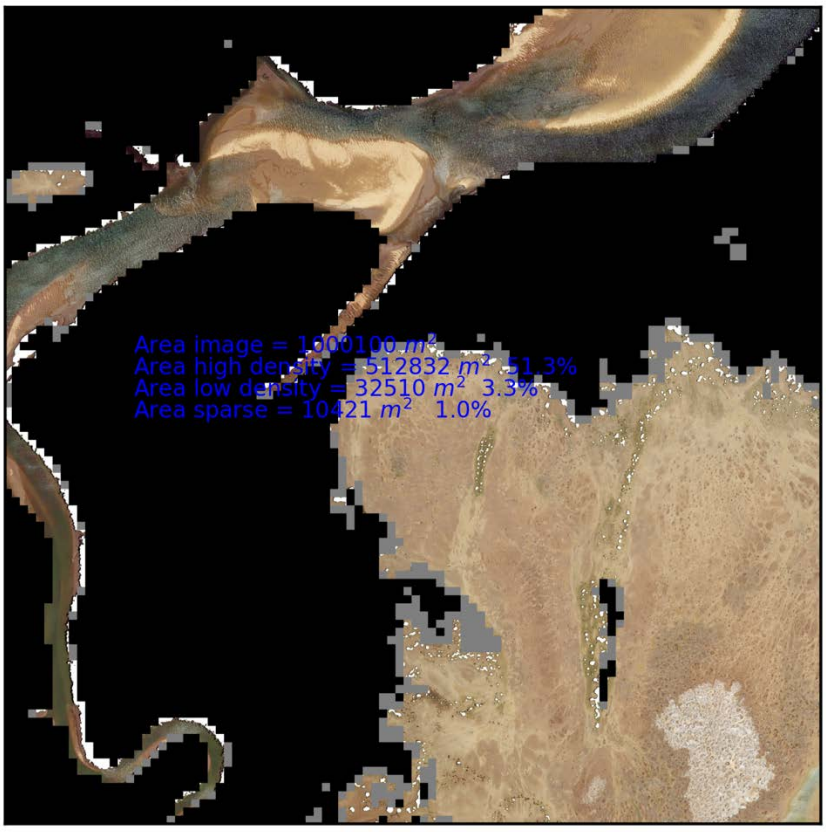

NEO true colour: E4

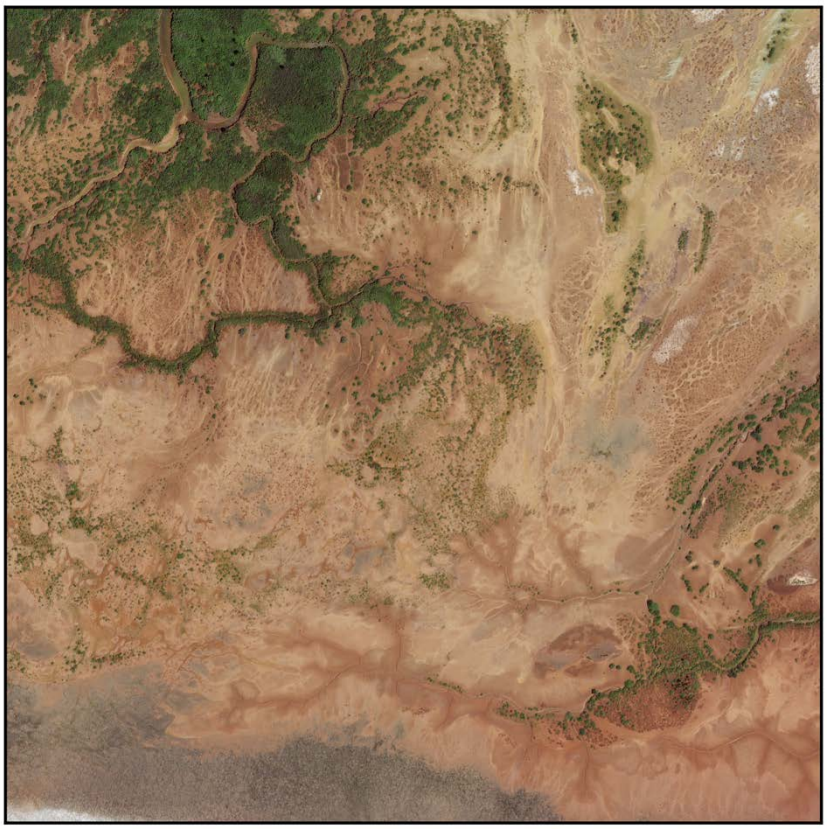

Mangrove. NEO & Sentinel: E4

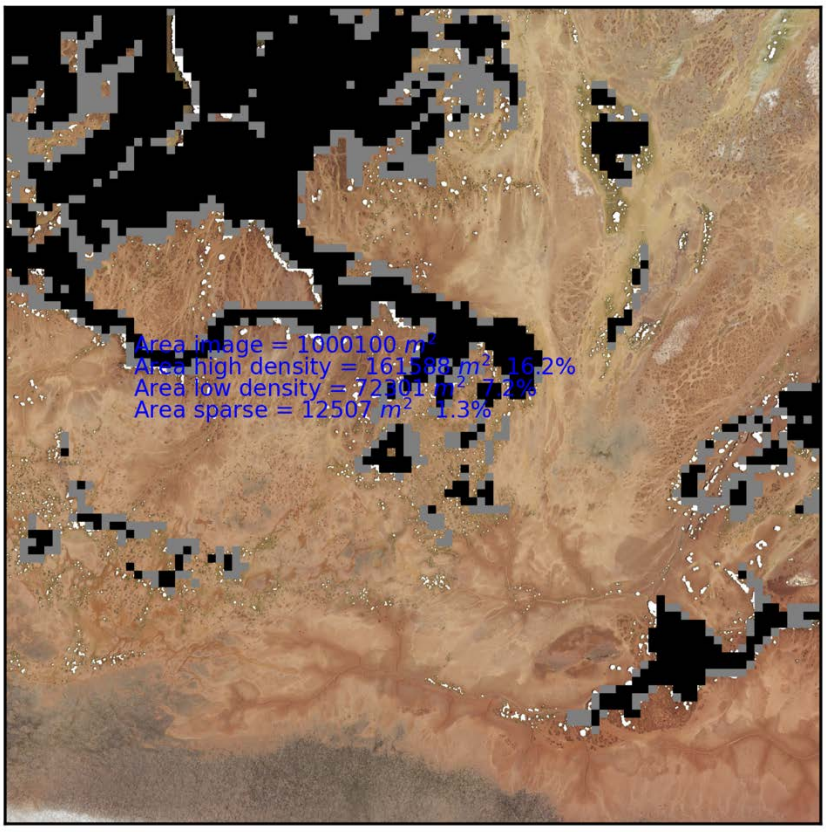

NEO true colour: E5

Mangrove. NEO & Sentinel: E5

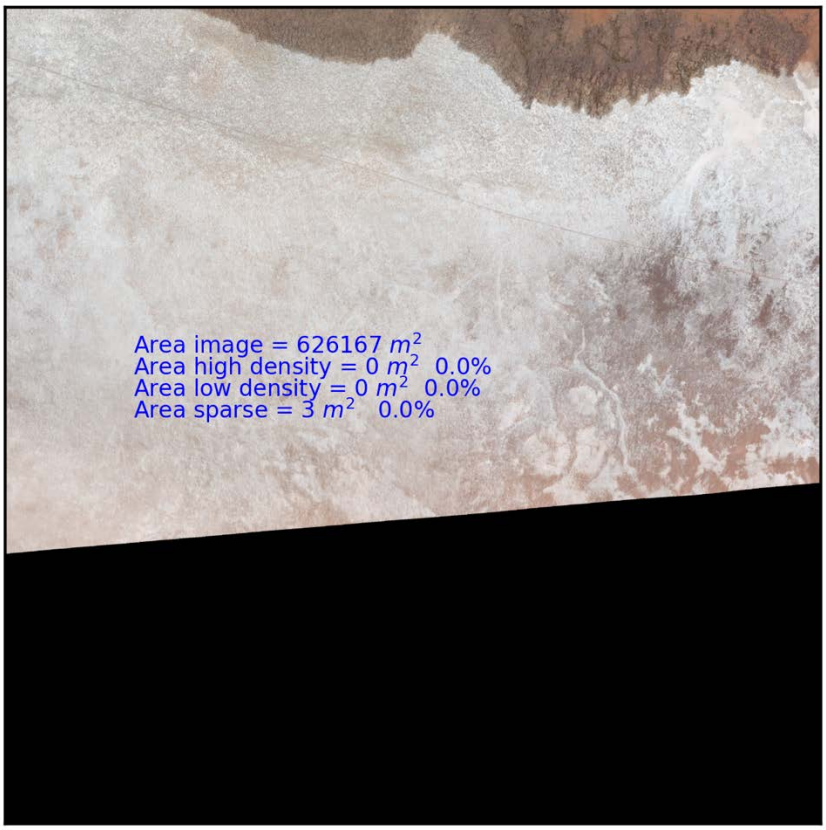

NEO true colour: F1

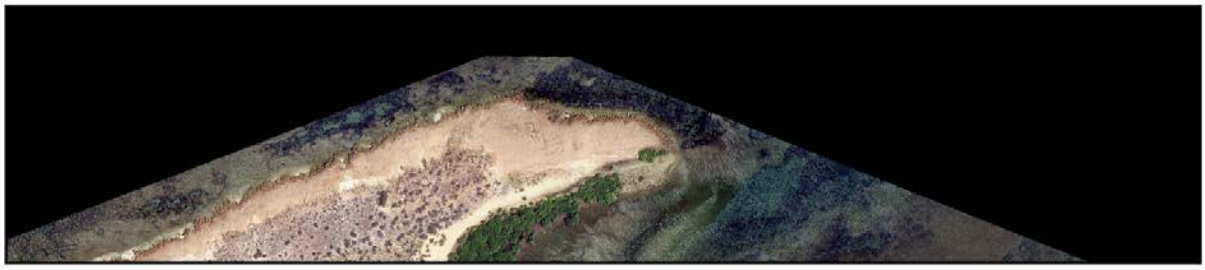

Mangrove. NEO & Sentinel: F1

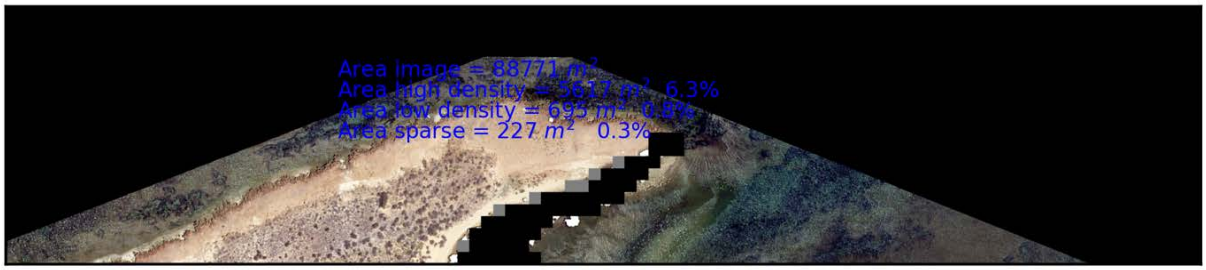

NEO true colour: F2

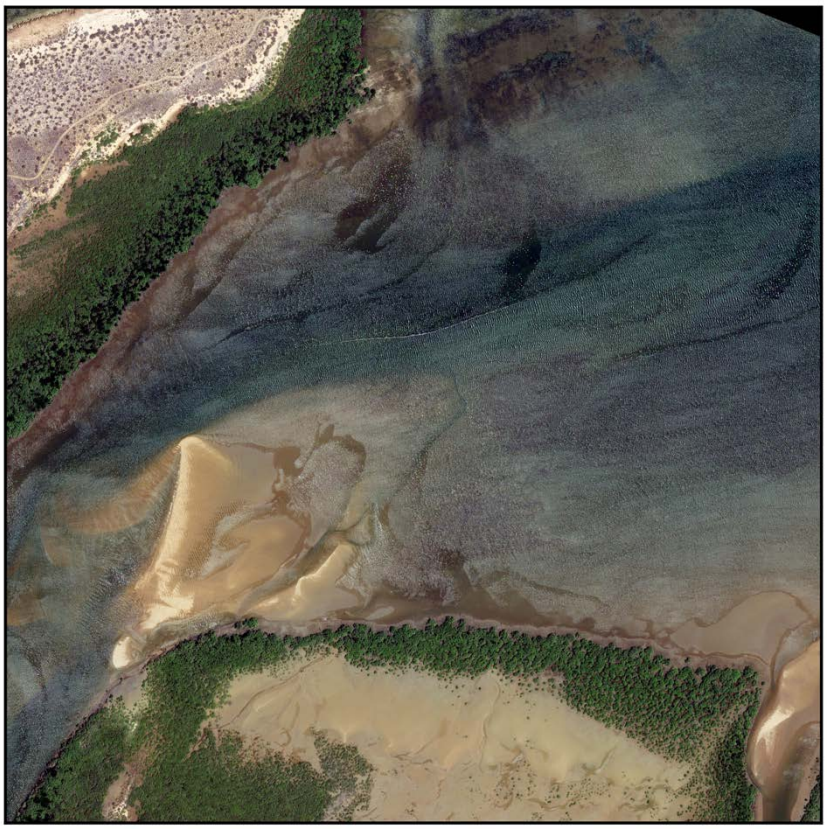

Mangrove. NEO & Sentinel: F2

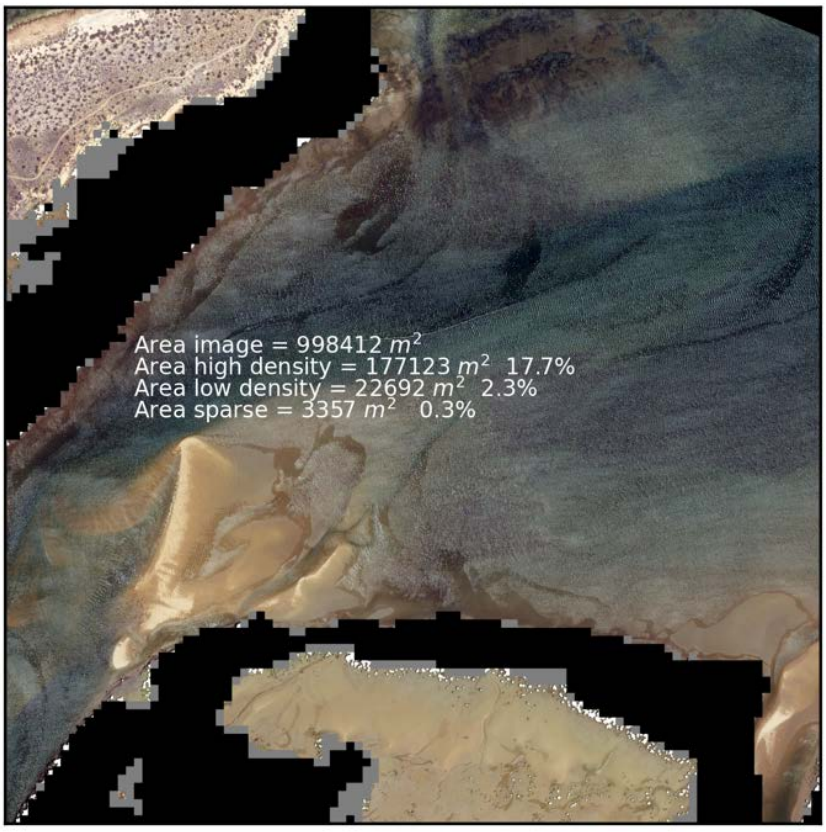

NEO true colour: F3

Mangrove. NEO & Sentinel: F3

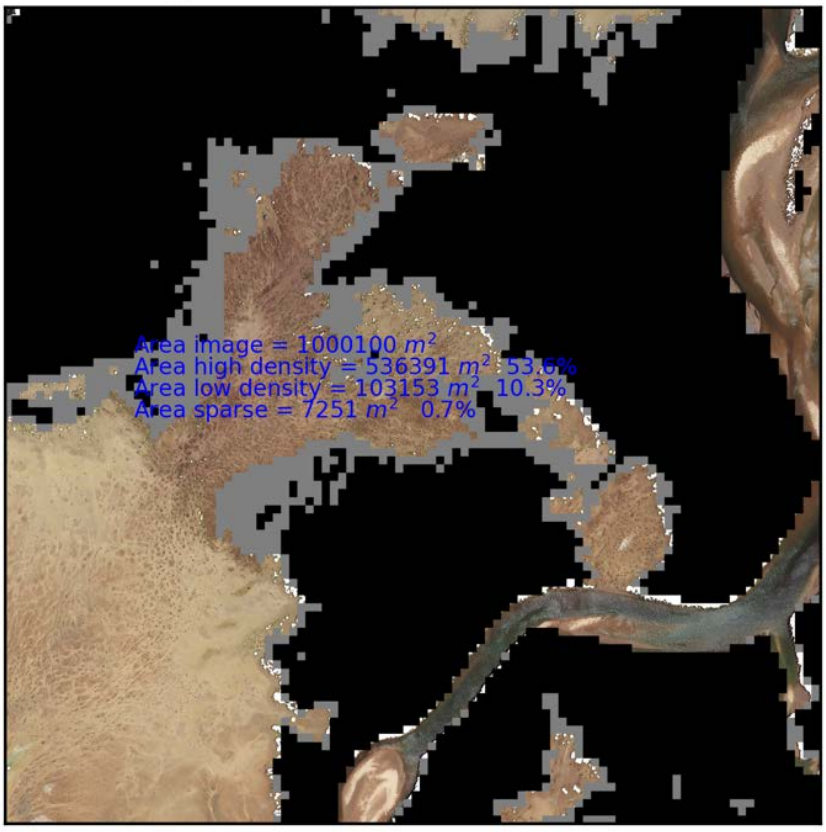

NEO true colour: F4

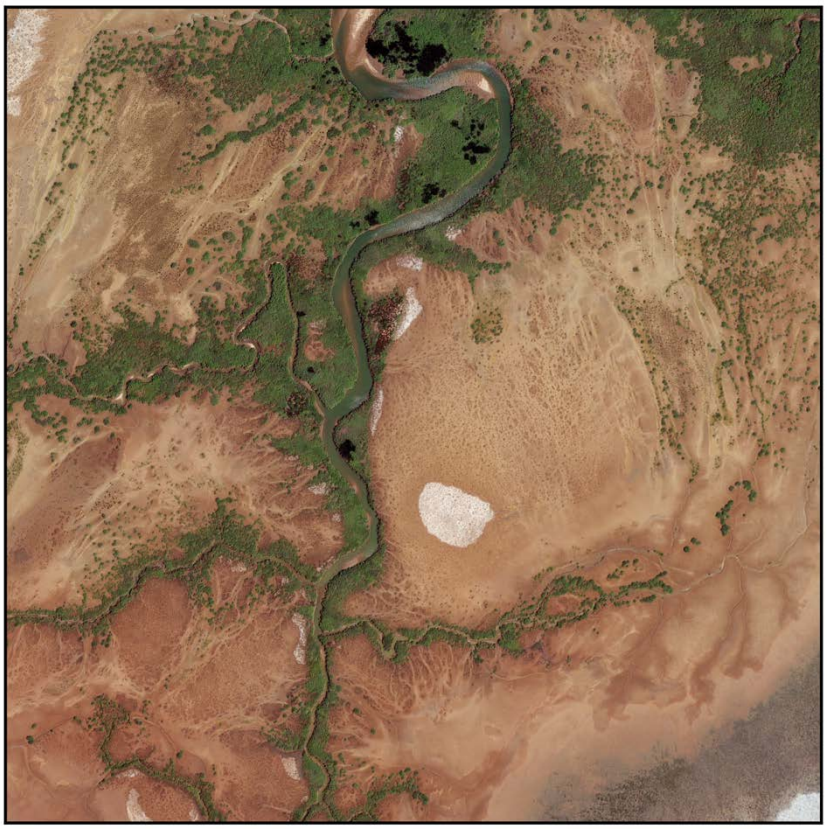

Mangrove. NEO & Sentinel: F4

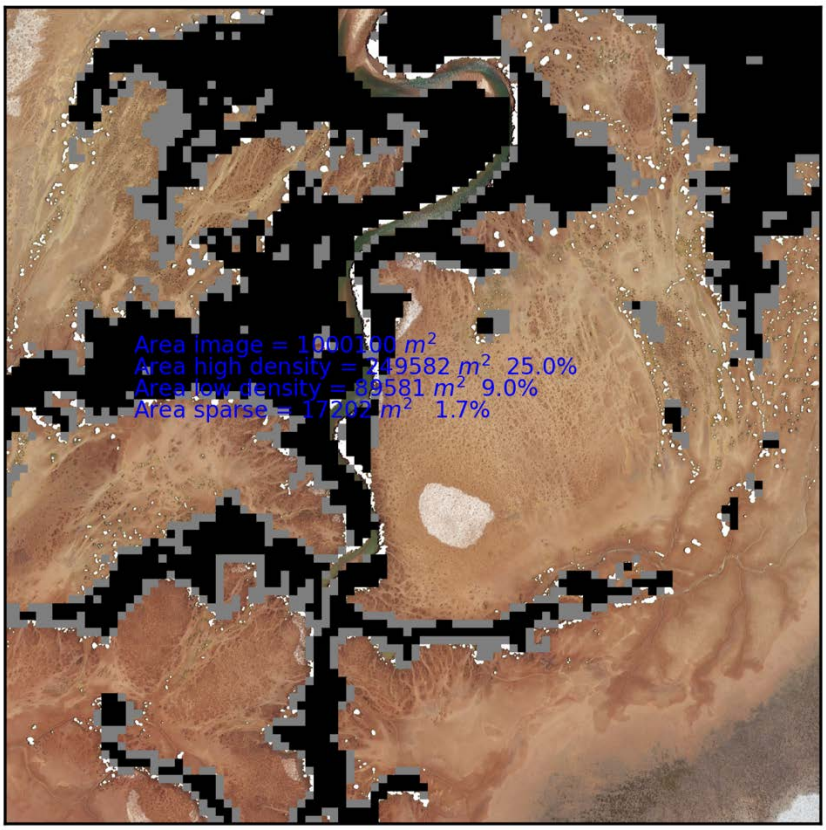

NEO true colour: F5

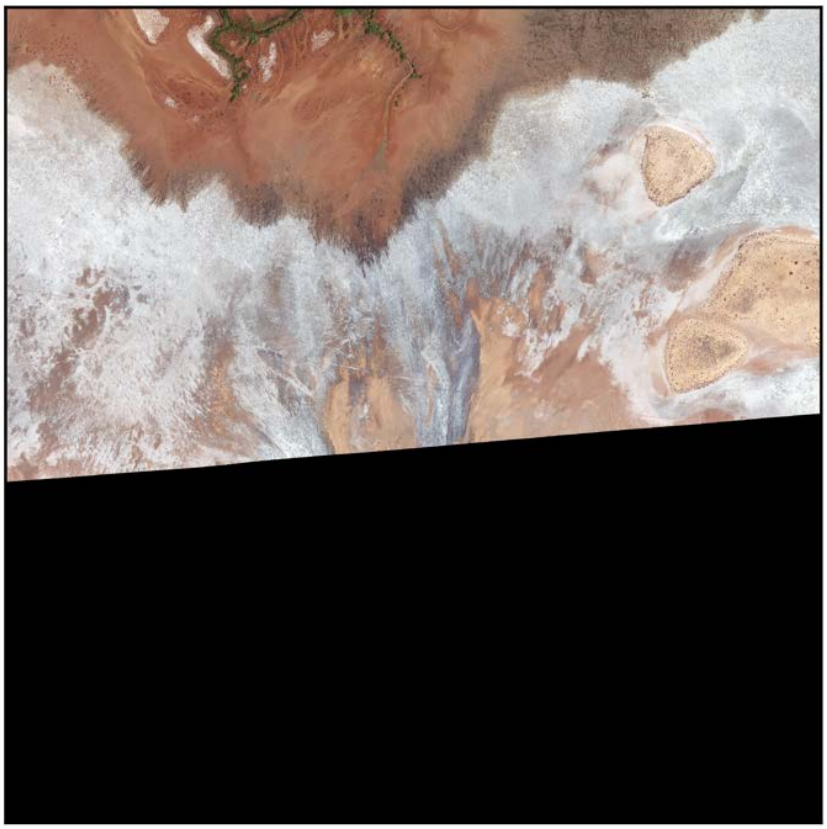

Mangrove. NEO & Sentinel: F5

NEO true colour: G2

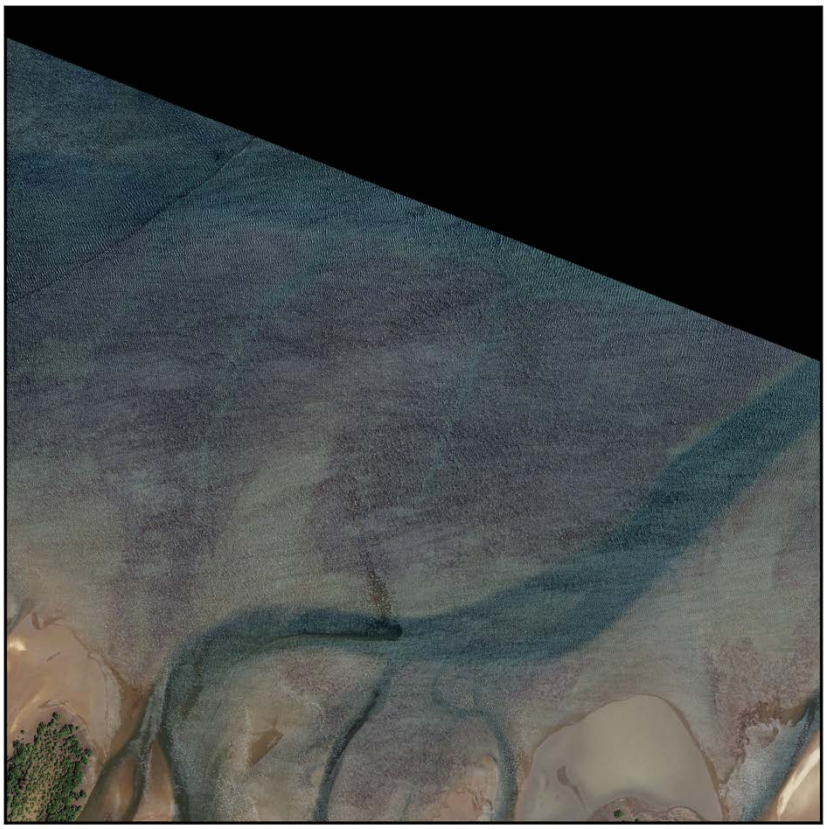

Mangrove. NEO & Sentinel: G2

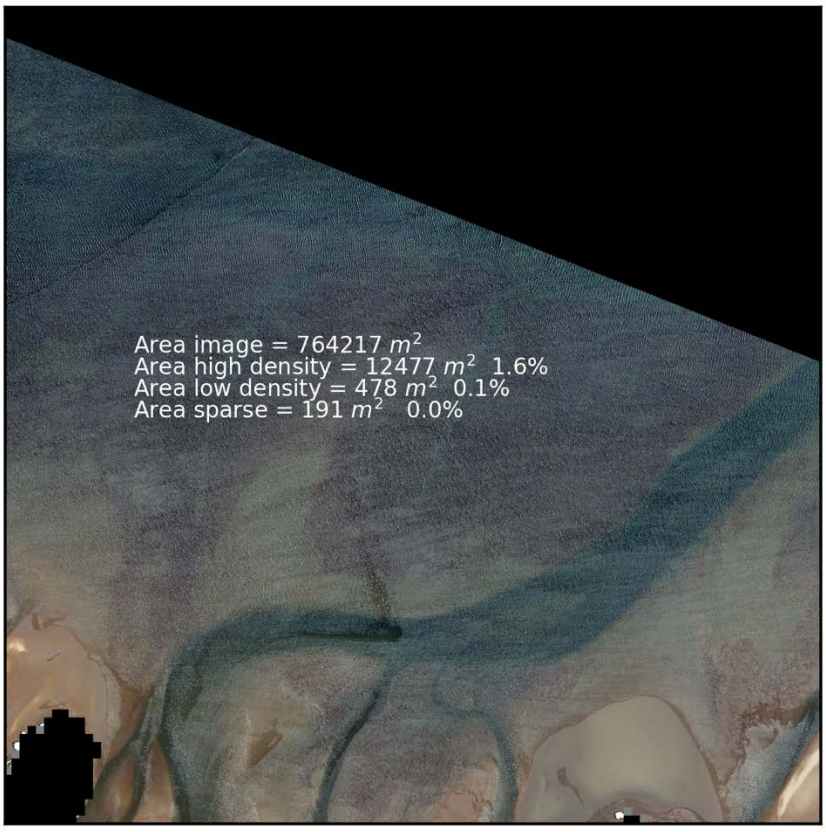

NEO true colour: G3

Mangrove. NEO & Sentinel: G3

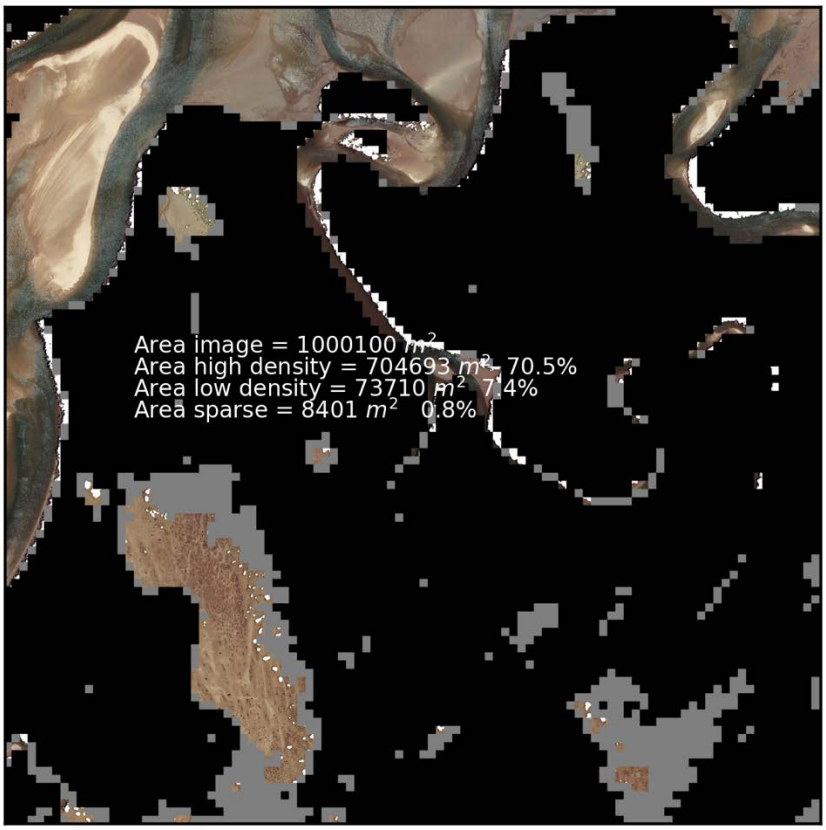

NEO true colour: G4

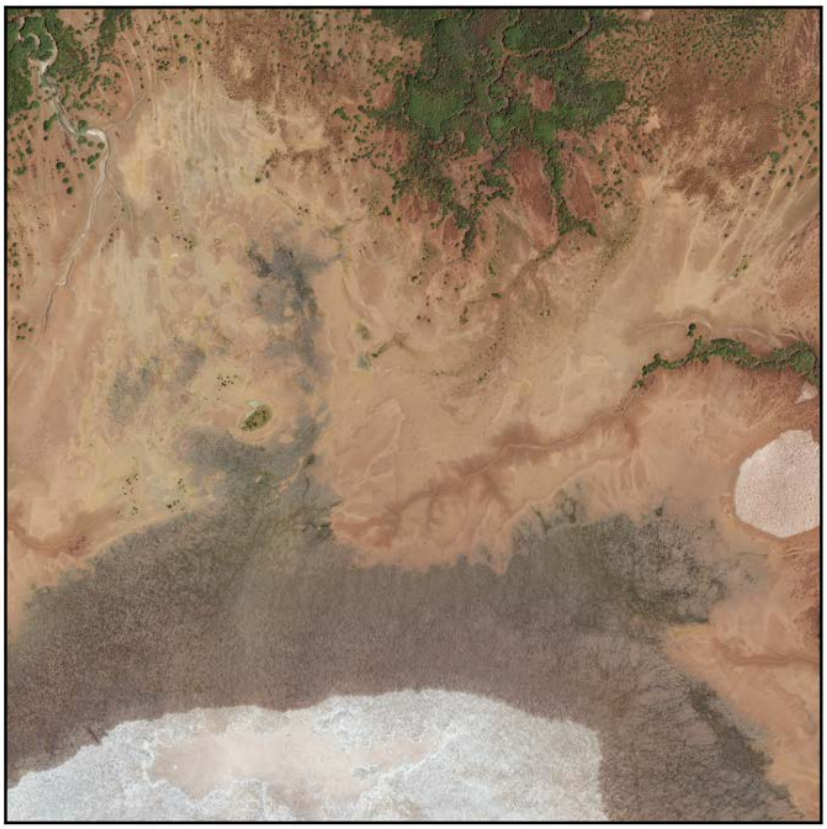

Mangrove. NEO & Sentinel: G4

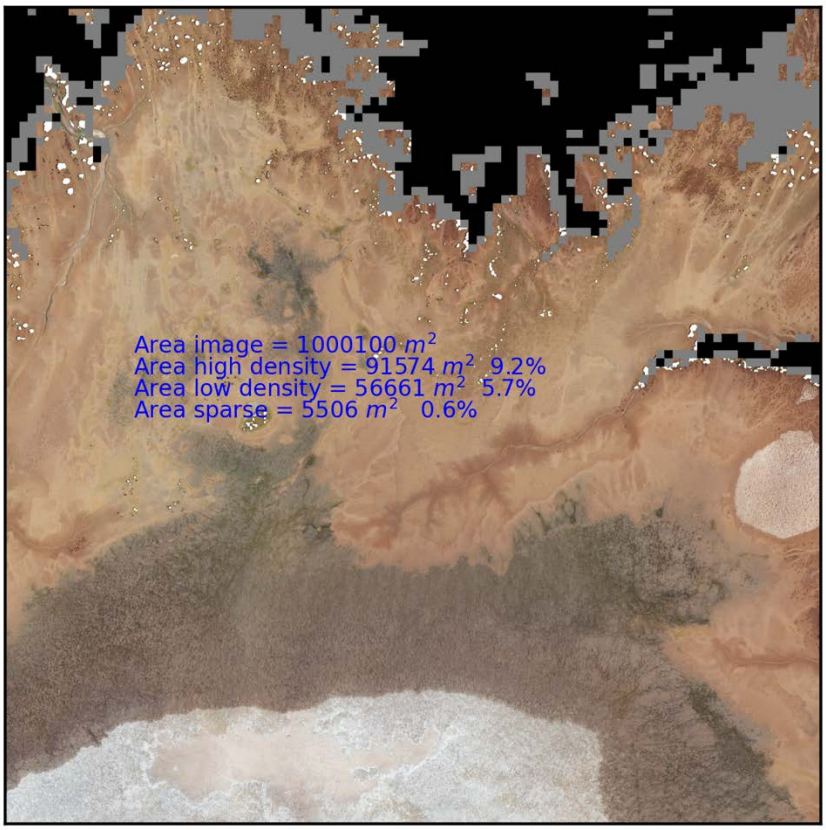

NEO true colour: G5

Mangrove. NEO & Sentinel: G5

NEO true colour: H2

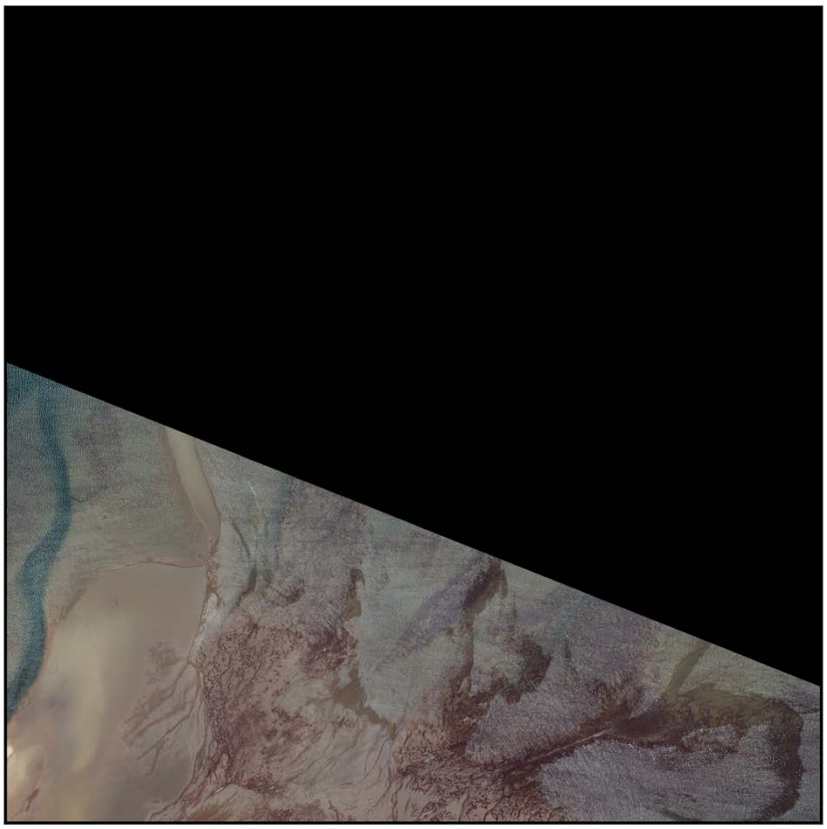

Mangrove. NEO & Sentinel: H2

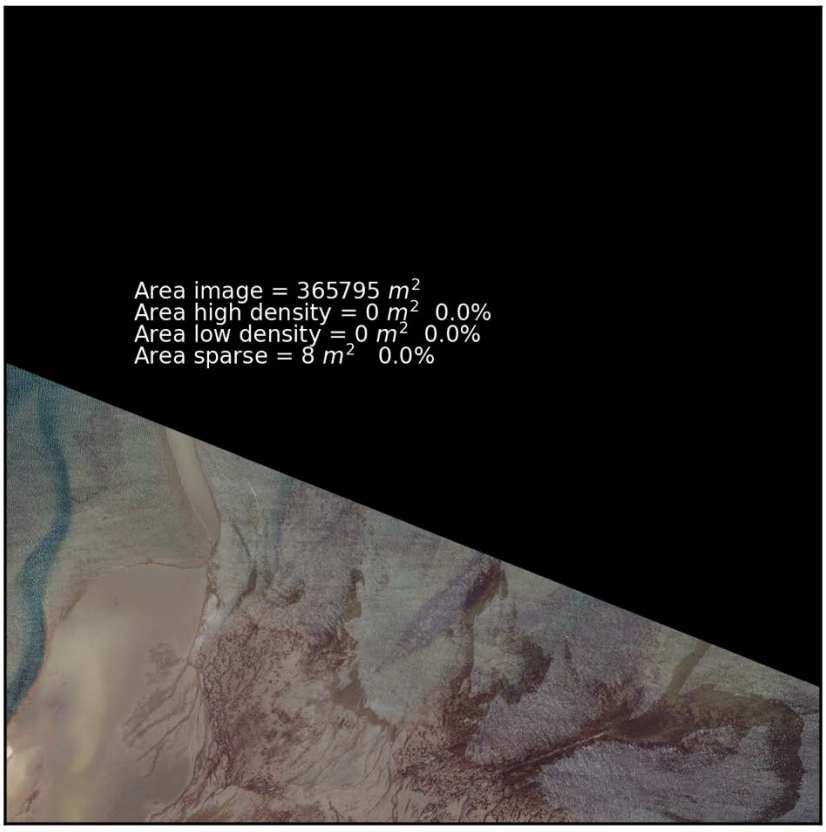

NEO true colour: H3

Mangrove. NEO & Sentinel: H3

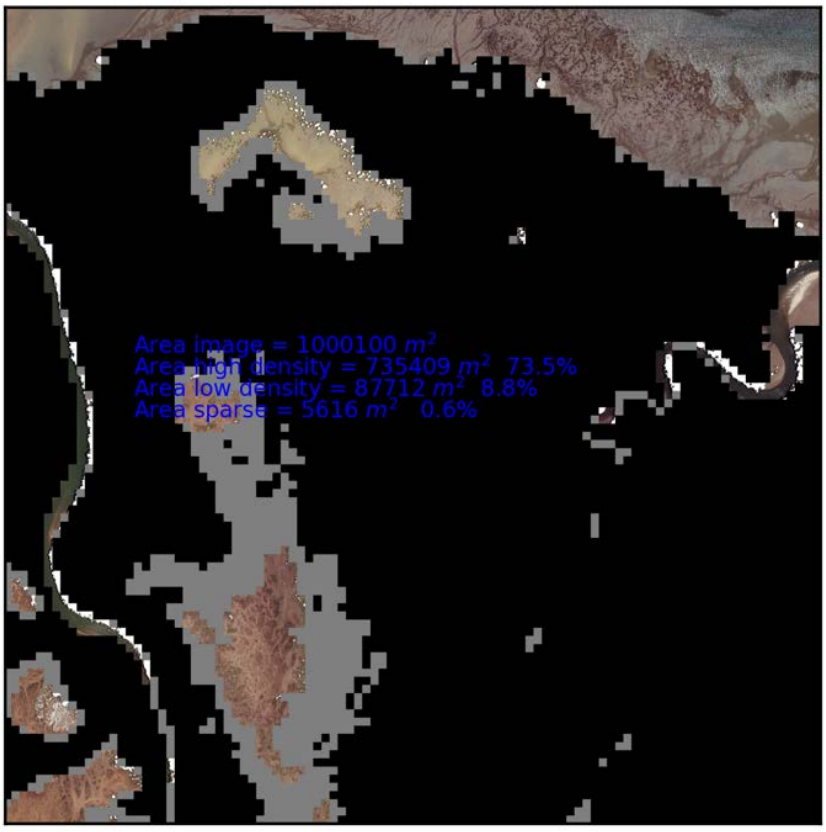

NEO true colour: H4

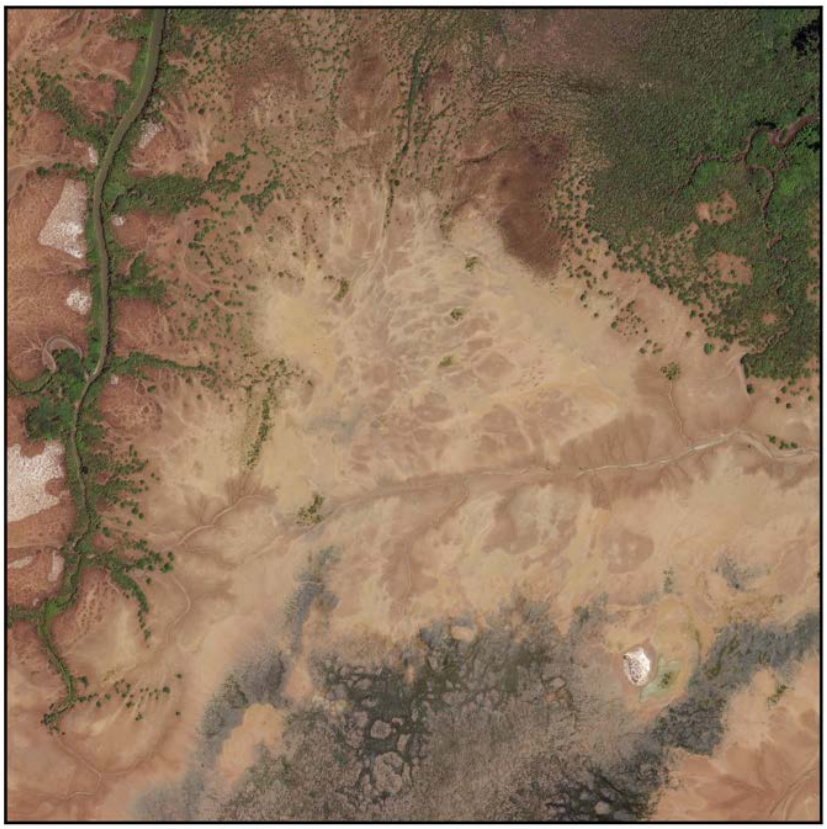

Mangrove. NEO & Sentinel: H4

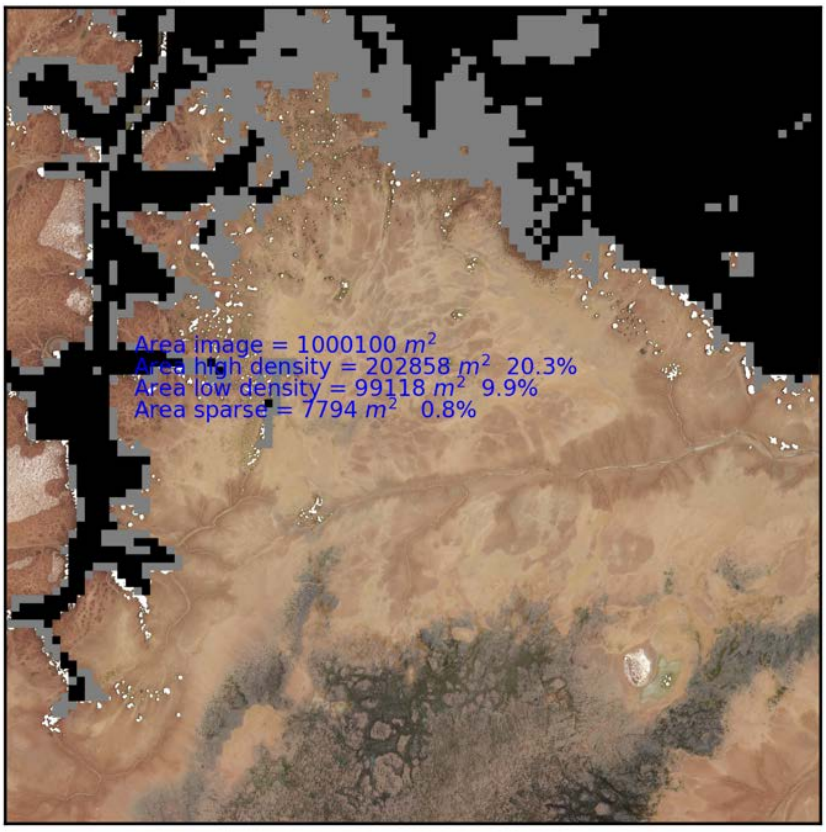

NEO true colour: H5

Mangrove. NEO & Sentinel: H5

NEO true colour: I2

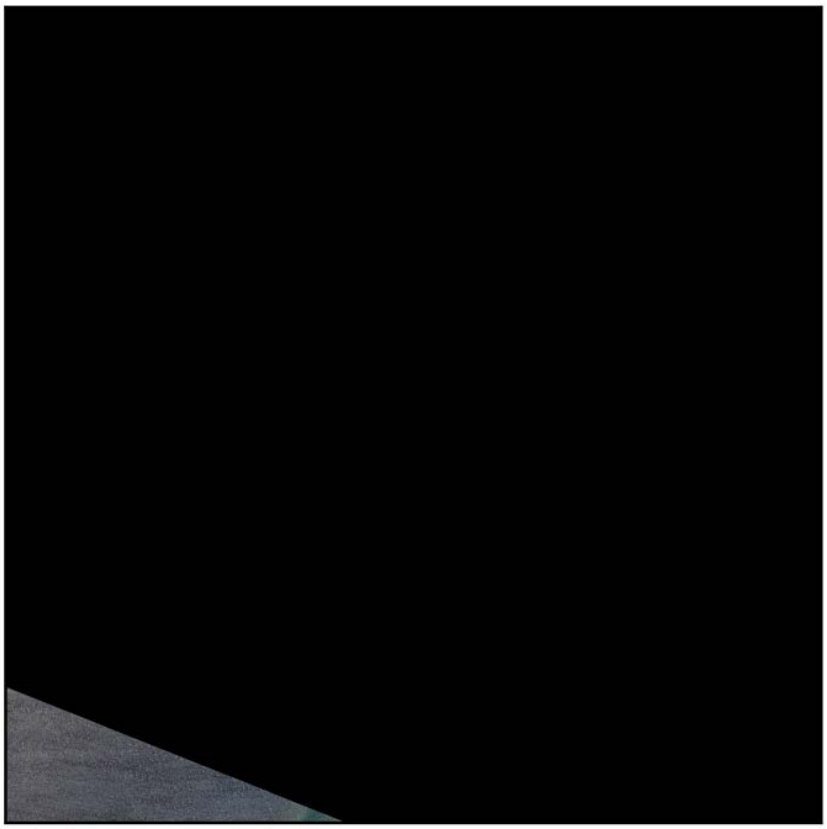

Mangrove. NEO & Sentinel: I2

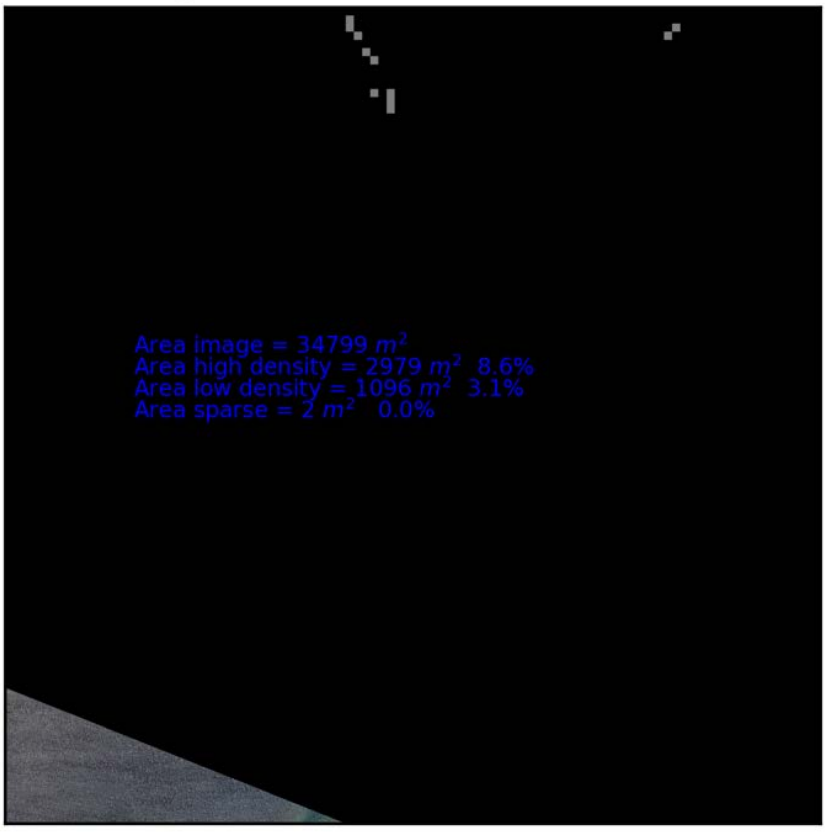

NEO true colour: I3

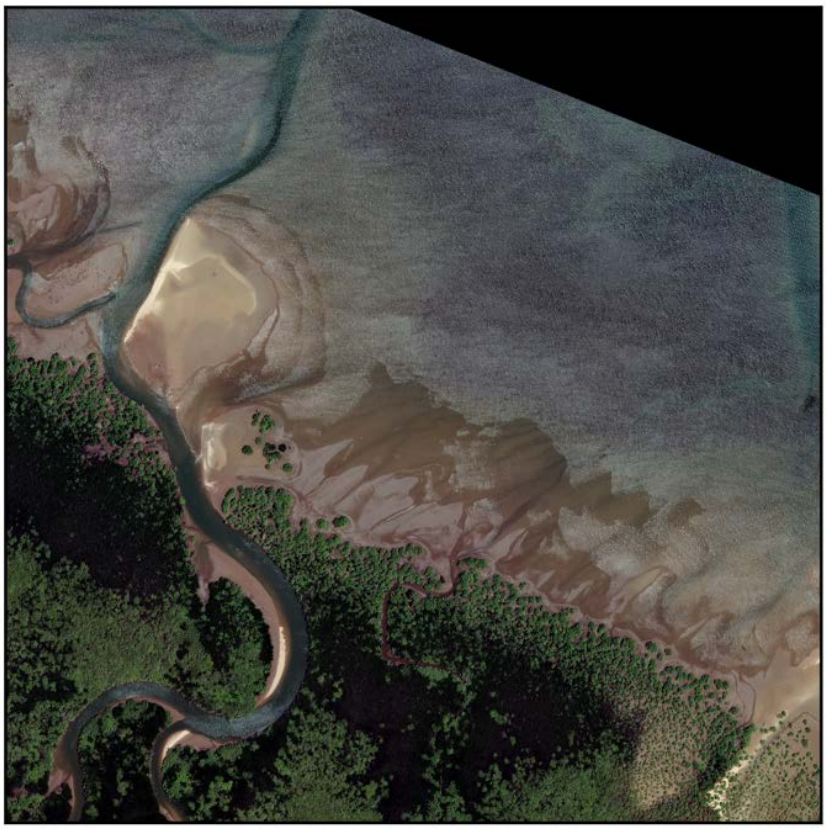

Mangrove. NEO & Sentinel: I3

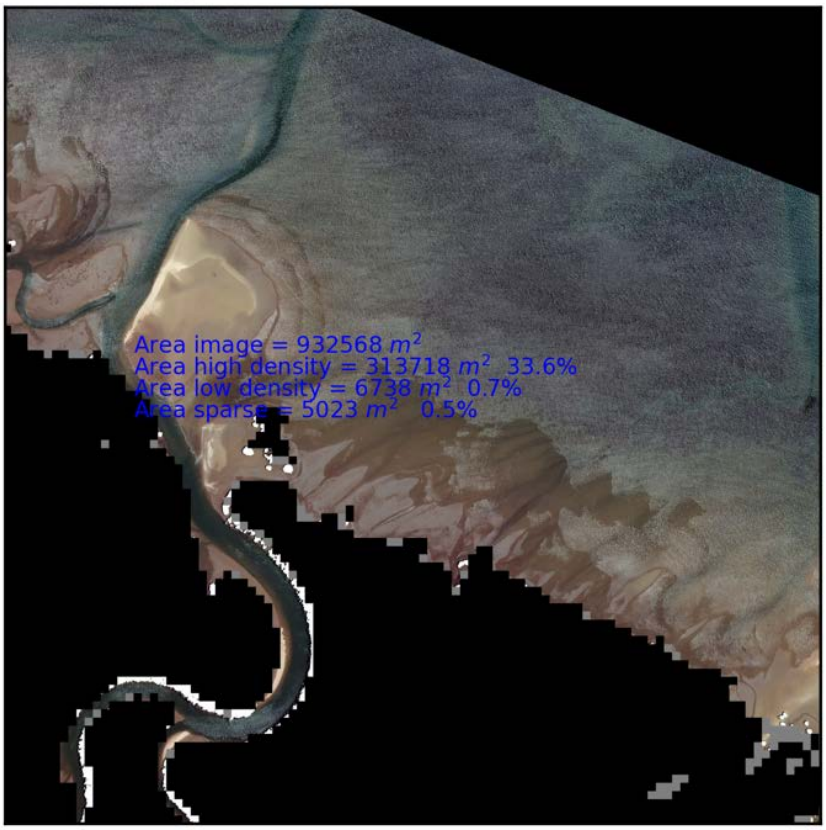

NEO true colour: I4

Mangrove. NEO & Sentinel: I4

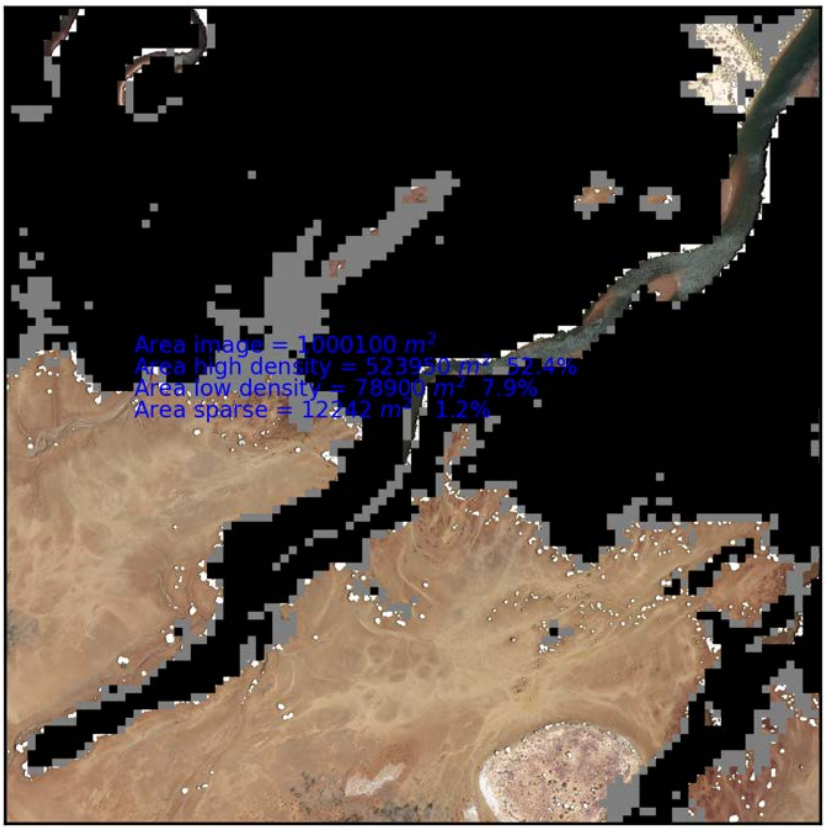

NEO true colour: I5

Mangrove. NEO & Sentinel: I5

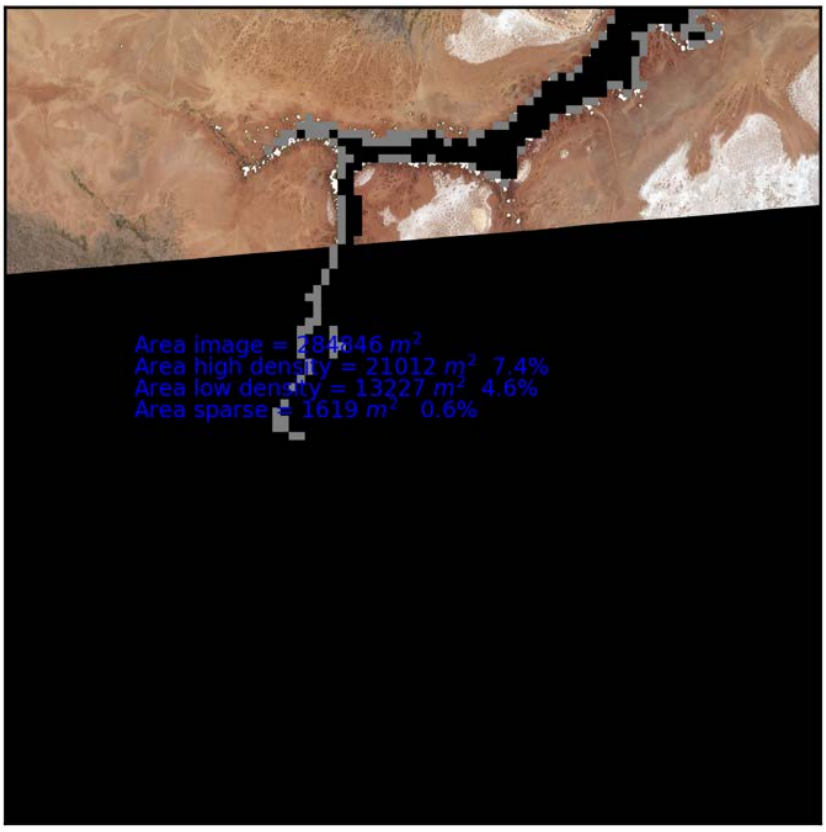

NEO true colour: J3

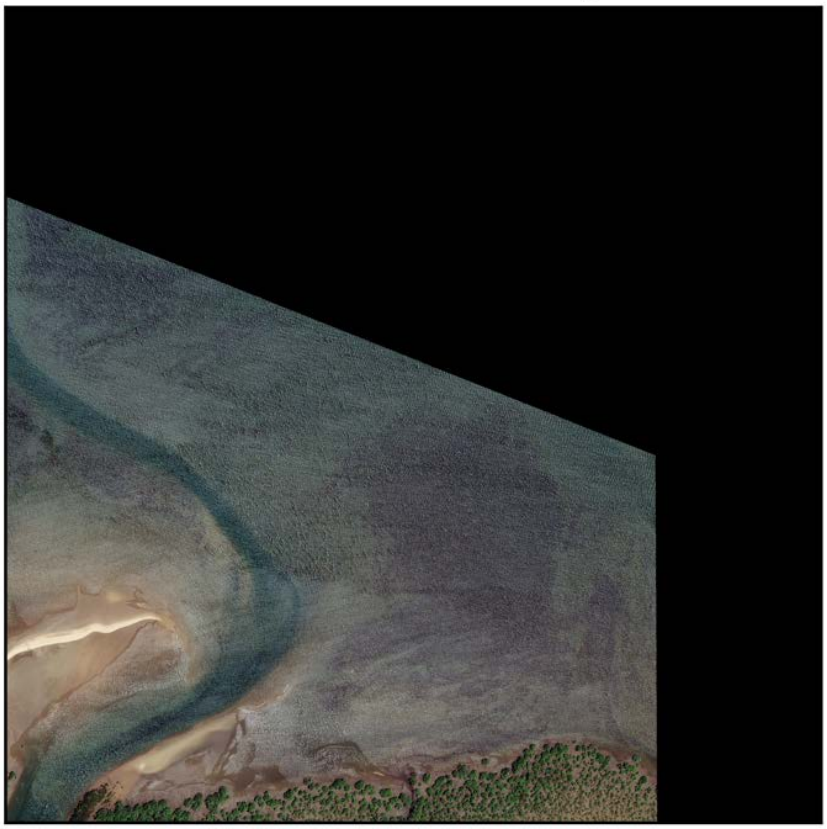

Mangrove. NEO & Sentinel: J3

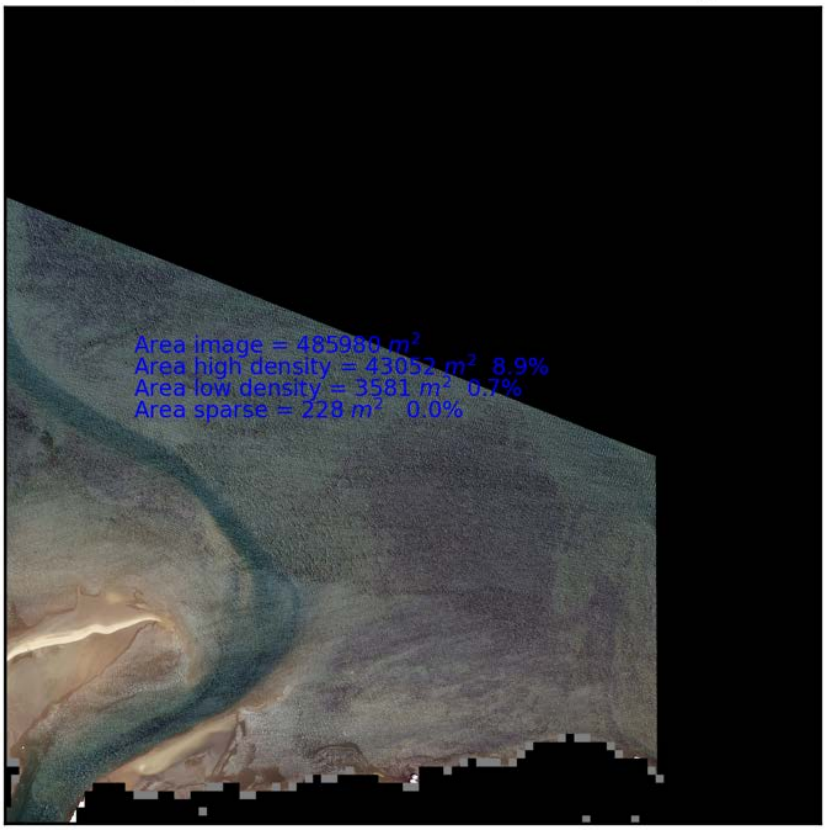

NEO true colour: J4

Mangrove. NEO & Sentinel: J4

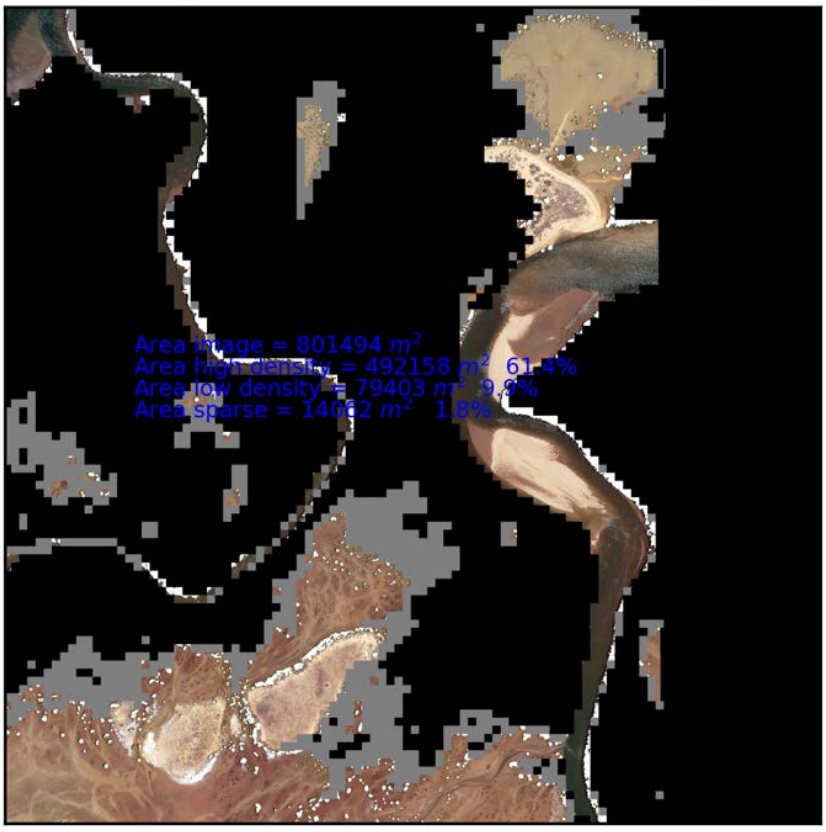

NEO true colour: J5

Mangrove. NEO & Sentinel: J5